NAVAL POSTGRADUATE SCHOOL
Monterey, California

THESIS

IMPULSIVELY-STARTED FLOW ABOUT
RECTANGULAR CYLINDERS

by

Clyde J. Ihrig

September 1983

Thesis Advisor: T. Sarpkaya

Approved for public release; distribution unlimited.

SECURITY CLASSIFICATION OF THIS PAGE (When Data Entered)

REPORT DOCUMENTATION PAGE

READ INSTRUCTIONS BEFORE COMPLETING FORM

1. REPORT NUMBER	2. GOVT ACCESSION NO. / 3. RECIPIENT'S CATALOG NUMBER
4. TITLE (and Subtitle): Impulsively-Started Flow About Rectangular Cylinders	5. TYPE OF REPORT & PERIOD COVERED: Master's Thesis; September 1983
	6. PERFORMING ORG. REPORT NUMBER
7. AUTHOR(s): Clyde J. Ihrig	8. CONTRACT OR GRANT NUMBER(s)
9. PERFORMING ORGANIZATION NAME AND ADDRESS: Naval Postgraduate School, Monterey, California 93943	10. PROGRAM ELEMENT, PROJECT, TASK AREA & WORK UNIT NUMBERS
11. CONTROLLING OFFICE NAME AND ADDRESS: Naval Postgraduate School, Monterey, California 93943	12. REPORT DATE: September 1983
	13. NUMBER OF PAGES: 116
14. MONITORING AGENCY NAME & ADDRESS (if different from Controlling Office)	15. SECURITY CLASS. (of this report)
	15a. DECLASSIFICATION/DOWNGRADING SCHEDULE

16. DISTRIBUTION STATEMENT (of this Report)

Approved for public release; distribution unlimited.

17. DISTRIBUTION STATEMENT (of the abstract entered in Block 20, if different from Report)

18. SUPPLEMENTARY NOTES

19. KEY WORDS (Continue on reverse side if necessary and identify by block number)

Impulsive Flow
Rectangular Cylinder
Bluff Body
Lift and Drag

20. ABSTRACT (Continue on reverse side if necessary and identify by block number)

Impulsively-started flow about sharp-edged rectangular cylinders has been investigated experimentally. The forces acting on the bodies have been determined, as a function of the relative displacement of the fluid at a subcritical Reynolds number, for various angles of attack.

DD FORM 1 JAN 73 1473 EDITION OF 1 NOV 65 IS OBSOLETE
S/N 0102-LF-014-6601

SECURITY CLASSIFICATION OF THIS PAGE (When Data Entered)

The results have shown that the shedding of the first two or three vortices and the manner in which they are generated have profound effects on all the characteristics of resistance. The results have also shown that the drag force in the transient state is always larger than that in the asymptotic steady state, pointing out the importance of the understanding of impulsively-started flow about bluff bodies. The data presented here are expected to form the basis of future numerical analyses of similar time-dependent flows. At present, accurate analytical and numerical data, for comparison with those presented herein, do not exist, save for the later stages of motion where the behavior of flow becomes nearly identical to that of steady flow.

Impulsively-Started Flow About Rectangular Cylinders

by

Clyde J. Ihrig
Lieutenant Commander, United States Navy
B.S., United States Naval Academy, 1970

Submitted in partial fulfillment of the
requirements for the degree of

MASTER OF SCIENCE IN MECHANICAL ENGINEERING

from the

NAVAL POSTGRADUATE SCHOOL
September 1983

ABSTRACT

Impulsively-started flow about sharp-edged rectangular cylinders has been investigated experimentally. The forces acting on the bodies have been determined, as a function of the relative displacement of the fluid at a subcritical Reynolds number, for various angles of attack.

The results have shown that the shedding of the first two or three vortices and the manner in which they are generated have profound effects on all the characteristics of resistance. The results have also shown that the drag force in the transient state is always larger than that in the asymptotic steady state, pointing out the importance of the understanding of impulsively-started flow about bluff bodies. The data presented here are expected to form the basis of future numerical analyses of similar time-dependent flows. At present, accurate analytical and numerical data, for comparison with those presented herein, do not exist, save for the later stages of motion where the behavior of flow becomes nearly identical to that of steady flow.

TABLE OF CONTENTS

LIST OF TABLES

LIST OF FIGURES

TABLE OF SYMBOLS AND ABBREVIATIONS

b	Vortex Lateral Spacing
B	Width of Test Section (Vertical Tunnel)
Cd	Drag Coefficient
Cl	Lift Coefficient
Cpb	Base Pressure Coefficient
d	Test Body Depth
f_v	Vortex-Shedding Frequency
k	Base Pressure Parameter
L	Test Body Length
Re	Reynolds Number
S	Fluid Displacement
St	Strouhal Number
t	Time
T	Time
U	Velocity
U(t)	Time Dependent Velocity
w	Test Body Width
α	Angle of Incidence (Angle of Attack)
ε	Turbulence Intensity
λ	Turbulence Scale
ρ	Fluid Density
ν	Fluid Kinematic Viscosity

ACKNOWLEDGEMENT

The author is most grateful for the comprehensive support of Distinguished Professor Turgut Sarpkaya, whose patient guidance and astute perception of all facets of the problem at hand have made this research a very meaningful and rewarding experience. A significant note of thanks is extended to Mr. Jack McKay, of the Naval Postgraduate School technical staff, for his skillful and industrious efforts which were essential to the experimental process described herein. The author also is especially appreciative for the love, understanding and support that has been provided by his wife, Jennifer.

I. INTRODUCTION

An extensive literature search and the perusal of the most relevant contributions have shown that the existing analytical or numerical methods are not yet in a position to describe the behavior of the large scale fluid motion in the wake of bluff bodies subjected to impulsively started flow. Solutions based on the Navier-Stokes equations are limited to extremely small Reynolds numbers and to relatively small fluid displacements. Solutions based on the discrete vortex method, or on its variations, suffer from the problems associated with the introduction of the nascent vortices, vortex excursions, shear-layer instabilities, inaccurate representation of viscous and turbulent dissipation of vorticity, and numerous instabilities. The assumption of an inviscid fluid imposes an unrealistically large number of conditions on the simulation of the behavior of a viscous flow. It does not, therefore, appear that the numerical methods applied either directly or indirectly (through the use of one or more conformal transformations) are in a position to predict the force and vortex-shedding characteristics of bluff bodies in time-dependent flows even for the most manageable impulsively-started flow. Experiments must be carried out to delineate the most important features of such flows partly for practical and partly, and perhaps more importantly, for the purpose of providing a physical insight toward the development of analytical methods.

Experimental investigations of the behavior of drag and lift forces and vortex shedding frequency and their dependence on specific parameters for bluff bodies have been confined to steady flows. Very little experimental data for impulsively-started flow at sufficiently high Reynolds numbers (greater than 10,000) exists.

The purpose of this study was to determine experimentally the evolution of the drag and lift forces and the vortex shedding frequency and their dependence on several key parameters for five rectangular cylinders in impulsively-started flow at a Reynolds number of about 20,000.

II. PREVIOUS INVESTIGATIONS

Architectural design and construction of buildings and structures in the past few decades have shifted to the use of more economical and light weight materials. The new materials do not have the structural-damping characteristics of the heavier construction materials used in older structures. This has required wind engineering design to prevent damage to cladding, mullions, windows and other architectural features. According to Lee [Ref. 1], "while the fluctuating forces and the associated vortex shedding from a circular cylinder have been the subject of considerable research, comparatively little attention has been paid to other bluff body shapes. Little information is available on... vortex shedding from sharp edged bluff structures, although this is a problem of considerable practical significance."

Several recent investigations have studied drag force, lift force, pressure distribution and vortex shedding frequency for steady flows about rectangular cylinders. The drag and lift forces shown in Figure 1 are a function of several parameters given by the expression

$$\text{Force}_{(\text{Drag or Lift})} = f(w,d,U,dU/dt,\rho,\nu,\varepsilon,\lambda,L,\alpha,B,t) \qquad (1)$$

where w represents the width normal to the flow; d, the depth of the cylinder; U, the velocity of the ambient flow; dU/dt, the flow acceleration; ρ, the density of the fluid; ν, the kinematic viscosity of the fluid; ε, the turbulence intensity of the flow; λ, the turbulence scale of the flow; L, the length of the cylinder; α, the angle of incidence (angle of attack) of the flow; B, the width of the test section and t, time. Dimensional analysis yields the drag coefficient (Cd) and the lift coefficient (Cl) as

$$Cd = \frac{\text{Drag Force}}{1/2\rho w U^2 L} = f(Ut/w, d/w, Uw/\nu, \alpha, \varepsilon, \lambda/w, L/w, w/B, wdU/dt/U^2) \quad (2)$$

$$Cl = \frac{\text{Lift Force}}{1/2\rho d U^2 L} = f(Ut/w, d/w, Uw/\nu, \alpha, \varepsilon, \lambda/w, L/w, w/B, wdU/dt/U^2) \quad (3)$$

where Ut/w represents the relative displacement; d/w, the configuration of the rectangular cylinder; Uw/ν, the Reynolds number (Re); α, the angle of incidence; ε, the turbulence intensity; λ/w, the turbulence scale; L/w, the aspect ratio; w/B, the blockage ratio, and w/dU/dt/U^2, the acceleration parameter.

The pressure distribution on the rear (base) face of a rectangular cylinder is related to the drag force. Base pressure varies inversely with the drag, hence a large negative base pressure corresponds to an increased drag force. The dimensionless coefficient of base pressure (Cpb) is defined as

$$Cpb = \frac{p_b - p_o}{1/2\ U^2} \tag{4}$$

where p_b represents the base pressure p_o, the ambient pressure.

Dimensional analysis of the vortex shedding frequency, (f_v), yields the Strouhal number (St) as

$$St = \frac{f_v\ w}{U} = f(d/w, Uw/\nu, \alpha, \varepsilon, \lambda/w, L/w, w/B) \tag{5}$$

The time dependence is omitted in Equation (5) because the Strouhal number is only defined for the later stages of fluid motion.

The recent experimental and numerical studies of steady flow about rectangular cylinders did not need to consider the relative displacement or acceleration parameters. The majority of the investigations were conducted at moderate Reynolds numbers (Re = 100,000) and have revealed the dependence of the flow characteristics and the force coefficients on the remaining parameters discussed above.

As uniform notation was not used in the previous works, all results have been transformed or recalculated as necessary to conform to the notation presented herein.

Nakaguchi, Hashimoto and Muto [Ref. 2] in 1968 found considerable variation in Cd with d/w and especially noted that a critical value of d/w = 2/3 yielded a maximum drag coefficient nearly equal to 3. Additionally, they noted that the maximum Cd decreased as d/w was increased, as shown in Figure 2.

The maximum Cd noted was significantly greater than the expected value of 2 which was previously known to be valid for square prisms. In 1972, Bearman and Trueman [Ref. 3] and Bostock and Mair [Ref. 4] confirmed the earlier findings. Furthermore, it was noted in the above mentioned investigations that the Strouhal number was nearly constant at 0.13 for d/w = 0 to 1 and then slowly decreased until multiple Strouhal numbers as high as 0.16 were measured at d/w = 2.8 as shown in Figure 3. Flow visualization employed by Nakaguchi et al. [Ref. 2] showed that for d/w = 2.8, the wake width decreased due to reattachment which caused the vortex longitudinal spacing to decrease and hence the Strouhal number to rise. The variation of the drag coefficient with d/w was explained by the proximity of the vortex formation to the rear face (base) of the body. Again through flow visualization, it was shown by Bearman and Trueman that for d/w = 2/3 the growing vorticies were closest to the base face. These vorticies have entrained fluid from the base region which reduced the base pressure and increased the drag coefficient. For d/w > 2/3 the vorticies formed further downstream which allowed the base pressure to increase and reduce the drag coefficient.

Bearman and Trueman [Ref. 3] demonstrated a definite trend of higher Cd with increasing Reynolds number, particularly for d/w = 0.5 to 1.0. They also showed that Strouhal number was basically independent of the Reynolds number in the range of 10,000. Knauss [Ref. 5] in 1974 also concluded that Strouhal

number was independent of Reynolds number in the lower range of Re = 500 to 1400. Courchesne and Laneville [Ref. 6] and Obasaju [Ref. 7] in 1978 demonstrated that the dependence of Cd on Reynolds number vanished for Re > 50,000. In 1982, Davis and Moore [Ref. 8], in an extensive numerical study of the flow at relatively low Reynolds numbers (100 to 1000), found that Cd increased with Re. They further noted that Strouhal number peaked at a value of 0.17 for Re = 300 then decreased to a nearly constant value of 0.13 as Reynolds number reached 1000. The behavior of St predicted by Davis and Moore is supported by the data of Bearman and Trueman and Knauss.

In 1966, Vickery [Ref. 9] showed that the fluctuating lift forces on a square prism were nearly four times greater than those measured earlier on circular cylinders and also reported that the angle of incidence dramatically affected Cpb, Cd and Cl. He showed that Cpb reached a minimum for α = 15 to 20 degrees. Vickery's experiments also showed only a slight variation of Strouhal number with the angle of incidence but noted a peak in St for α = 15 to 20 degrees as shown in Figure 4. Results of Knauss [Ref. 5] at low Re were in agreement with those of Vickery. Vickery concluded that a significant change in bluffness occurred for α > 15 degrees resulting in "a sudden widening of the wake due to flow detachment...(and) a corresponding sudden reduction in (vortex) shedding frequency." Lee [Ref. 1] in 1975 observed that Cpb reached a maximum value and that Cd and Cl reached minimum values on a square prism for

α = 15 to 20 degrees with a corresponding peak in Strouhal number as shown in Figures 5, 6 and 7. Lee reasoned that the impingement of the shear layers on the side walls and their subsequent deflection force vortex formation to occur further away from the base region and resulted in a lower Cd. He further suggested that "the increase in Strouhal number to a maximum at the angle at which the flow re-attaches to the side face, can be explained on the basis of the variation of the mean drag (Cd) with angle of incidence (α). The maximum value (of St)... is thought to be associated with a minimum wake width and hence with minimum longitudinal vortex spacing. If a constant ratio of vortex spacing to width is presumed (Von Karman) this would lead to an increase in the Strouhal number." Rockwell [Ref. 10] in 1977 and Obasaju [Ref. 7] in 1978 confirmed the findings of Vickery and Lee. The numerical model of Davis and Moore [Ref. 8] predicted a higher Cd at α = 15 degrees than for α = 0 degrees in marked contrast to Lee's findings. This may indicate either a weakness in the numerical model or an as yet unexplained effect of relatively small Reynolds numbers (100 to 1000).

Vickery [Ref. 9] in 1966 demonstrated the strong influence of ambient turbulence on Cd and Cl on a square cross-section. He found a nearly 50 percent reduction in the force transfer coefficients for a turbulent flow with intensity of 10 percent and scale of 1.33 as compared to the case of smooth flow. Vickery stated that the effect of turbulence was most notable

at low angles of incidence (α < 20 degrees) probably due to the intermittent reattachment of the separated flow. Finally, he noted that Strouhal number appeared to be independent of turbulence. In 1974, Lee [Ref. 1] determined that the increased turbulence intensity gave rise to higher base pressure and resulted in a reduction of the drag coefficient as shown in Figures 8 and 9. He suggested that the turbulence thickened the shear layers which caused them to be deflected further out at the trailing edges of the body causing vortex formation to move further from the base region. Subsequently, Lee [Ref. 11] showed that the variation of Cd with turbulence scale exhibited a distinct maximum at $\lambda/w = 1$ and that Cd increased with increasing λ/w. Nakamura and Tomonari [Ref. 12] in 1976 found that with increasing turbulence intensity the peak Cd became lower and occurred at d/w values smaller than that in smooth flow as shown in Figure 10. Nakamura et al. reasoned that "an increase in the mixing rate of the shear layers due to the turbulence can make the shear layers thicker and closer to the sides, resulting, evidently, in an earlier re-attachment to the sides for much thicker prisms, "i.e., large d/w. Courchesne and Laneville [Ref. 13] in 1982 confirmed earlier findings and stated that Cd is principally influenced by the intensity of the turbulence and that the turbulence scale had only a minor effect. Nakamura et al. concurred with the conclusions of Courchesne and Laneville.

Aspect ratio has a significant effect on the two-dimensionality of the experiments used to measure the fluctuating forces on rectangular prisms. In 1968, Graham [Ref. 14] determined that if the aspect ratio was large (L/w = 30) and if the end plates were not used, the correlation of vortex shedding behind the body in the spanwise direction was very poor. According to Vickery [Ref. 9], if the aspect ratio was quite small, the two-dimensionality of the experiment was suspect and the magnitude of the force fluctuations decreased. Lee [Ref. 15] has suggested that the end plates are not required or useful on sharp-edged models since the separation points are fixed and the end effects are restricted to end regions only as thick as the upstream wall boundary layer. Lee's conclusions have been disputed by Obasaju [Ref. 7] who determined that the end plates are required particularly for tests involving flow at incidence. Obasaju's conclusions were based solely on base pressure measurements on a single face of a square model and hence did not deal with the integrated effects such as lift and drag.

All closed tunnel experiments on bluff bodies have incurred blockage effects due to the confinement of the walls on the wakes. Courchesne and Laneville [Ref. 6] in 1978 experimentally evaluated the wall blockage effects on the drag coefficient of two-dimensional rectangular cylinders in smooth flow. They have concluded that for $d/w < 1.2$ and $w/B = 5$ to 13 percent Maskell's blockage correction, given by

$$\frac{Cd}{Cd\ corr.} = \frac{k^2}{k^2 corr.} = 1 + \frac{Cd}{k^2 corr - 1} \left[\frac{w}{B}\right] \left[\frac{L}{B}\right] \qquad (6)$$

where $k^2 = 1 - Cpb$, was best suited. Courchesne et al. further found that for larger d/w alternate empirical formulae given by

$$\frac{Cd\ corr.}{Cd} = \left(1 - \frac{w}{B}\,\frac{L}{B}\right)^N \qquad (N = 1.305) \qquad (7)$$

$$\frac{Cd\ corr.}{Cd} = 1 - \zeta\,\frac{w}{B}\,\frac{L}{B} \qquad (\zeta = 1.171) \qquad (8)$$

should be utilized for wall blockage corrections.

Very little information has been found on the behavior of impulsively-started flows about rectangular cylinders. Davis and Moore [Ref. 8] presented a numerical study of vortex shedding from rectangles at low Reynolds numbers. In this study they have predicted fluctuating Cl and Cd after steady state has been reached for an impulsively-started flow. Their results correctly predicted that drag coefficient, as a function of relative displacement, oscillates at twice the vortex shedding frequency. Davis and Moore further demonstrated the pure sinusoidal response of Cd and Cl, as a function of Ut/w, for a square prism at low Reynolds number and at normal incidence. In contrast, for d/w = 1.7 the behavior of Cd and Cl, as a function of Ut/w, was a violent initial oscillation followed by pure sinusoidal response. Finally, Davis and Moore found that for α = 15 degrees a non-zero average coefficient of lift

and a regular pattern of Cd oscillations were prevalent. No experimental data could be found to compare with the results of Davis and Moore's numerical predictions.

In a majority of the previous investigations cited, a definite inverse relationship between Cd and Strouhal number was noted. Bearman and Trueman [Ref. 3] correlated the product of Cd and St with k. Bearman extended this correlation and proposed a universal Strouhal number (S_B), based on vortex spacing parameters b and h, given by

$$S_B = St \frac{1}{k} \frac{b}{w} \tag{9}$$

where b represents lateral vortex spacing. He provided detailed observations revealing $S_B = 0.181$ over a wide range of k and α. Bearman's findings were subsequently confirmed by Lee [Ref. 1] as shown in Figure 11. Awbi [Ref. 16] in 1981 disputed the applicability of the universal Strouhal number for $d/w > 2$. In 1974 Knauss [Ref. 5] proposed that drag coefficient could be predicted based on Strouhal number using the correlation given by

$$St = \frac{.208}{Cd^{2/3}} \tag{10}$$

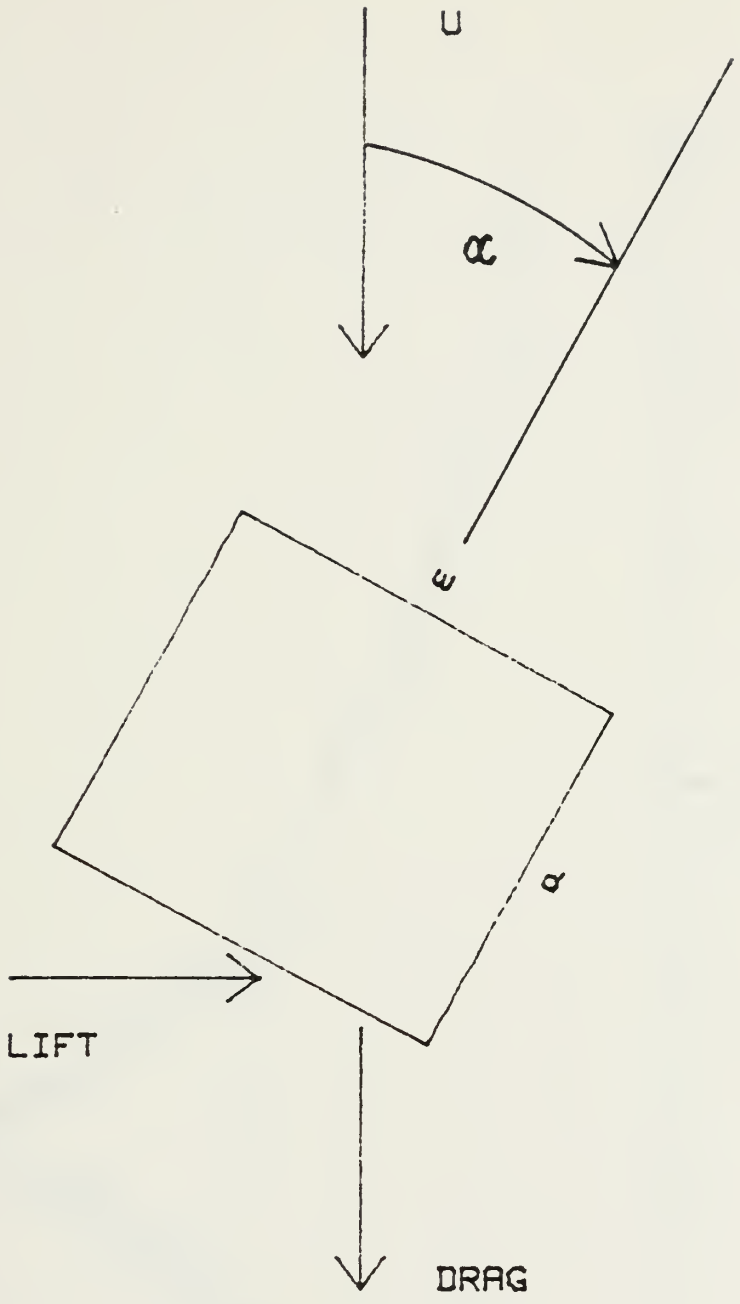

Figure 1. Definition Sketch for the Forces.

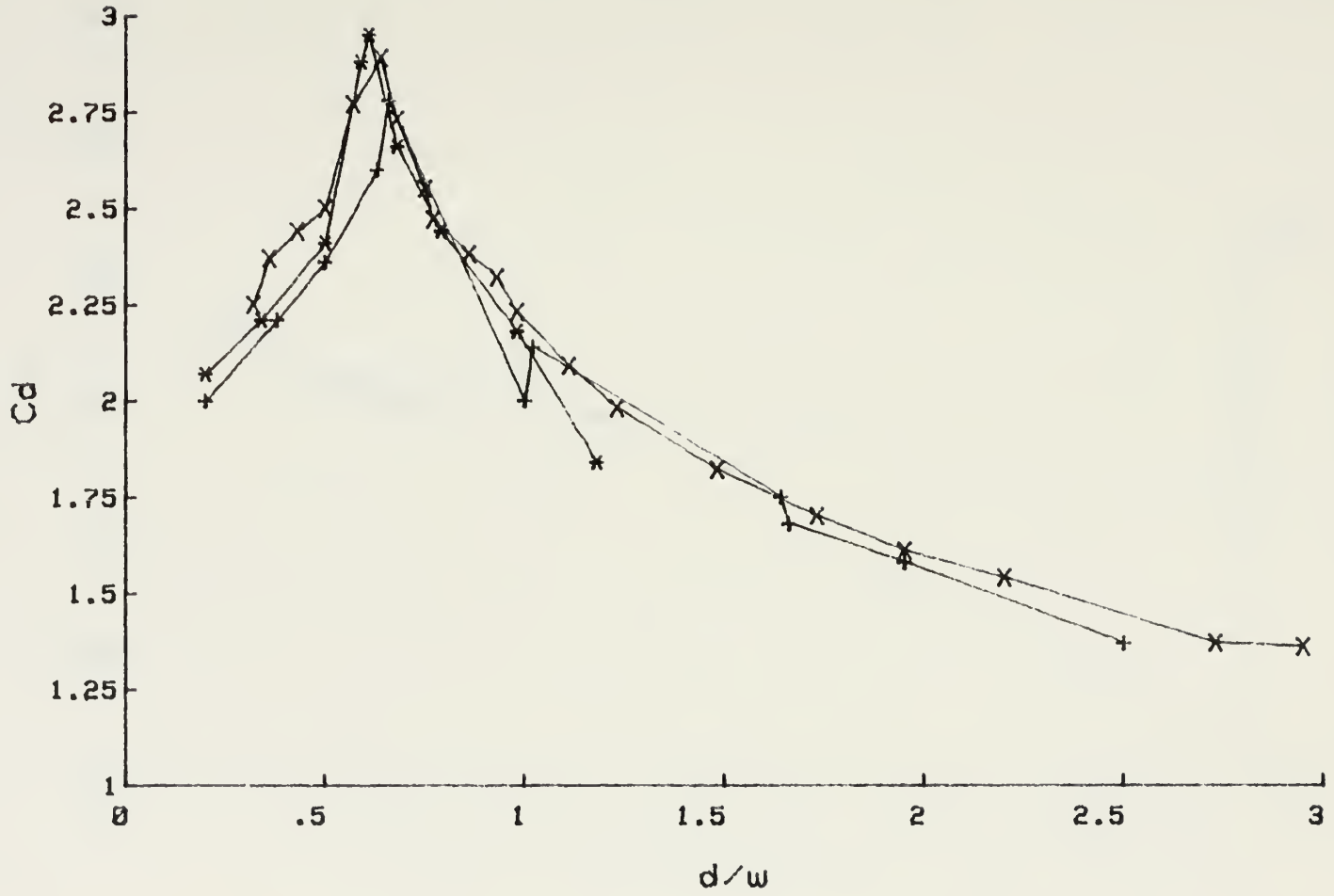

Figure 2. Cd vs. d/w on Rectangular Sections.

* Bearman and Tureman [3], Re = 2~7 x 10^4,
\+ Nakaguchi et al. [2], Re = 2~6 x 10^4,
X Courchesne and Laneville [6], Re = 4 x 10^4.

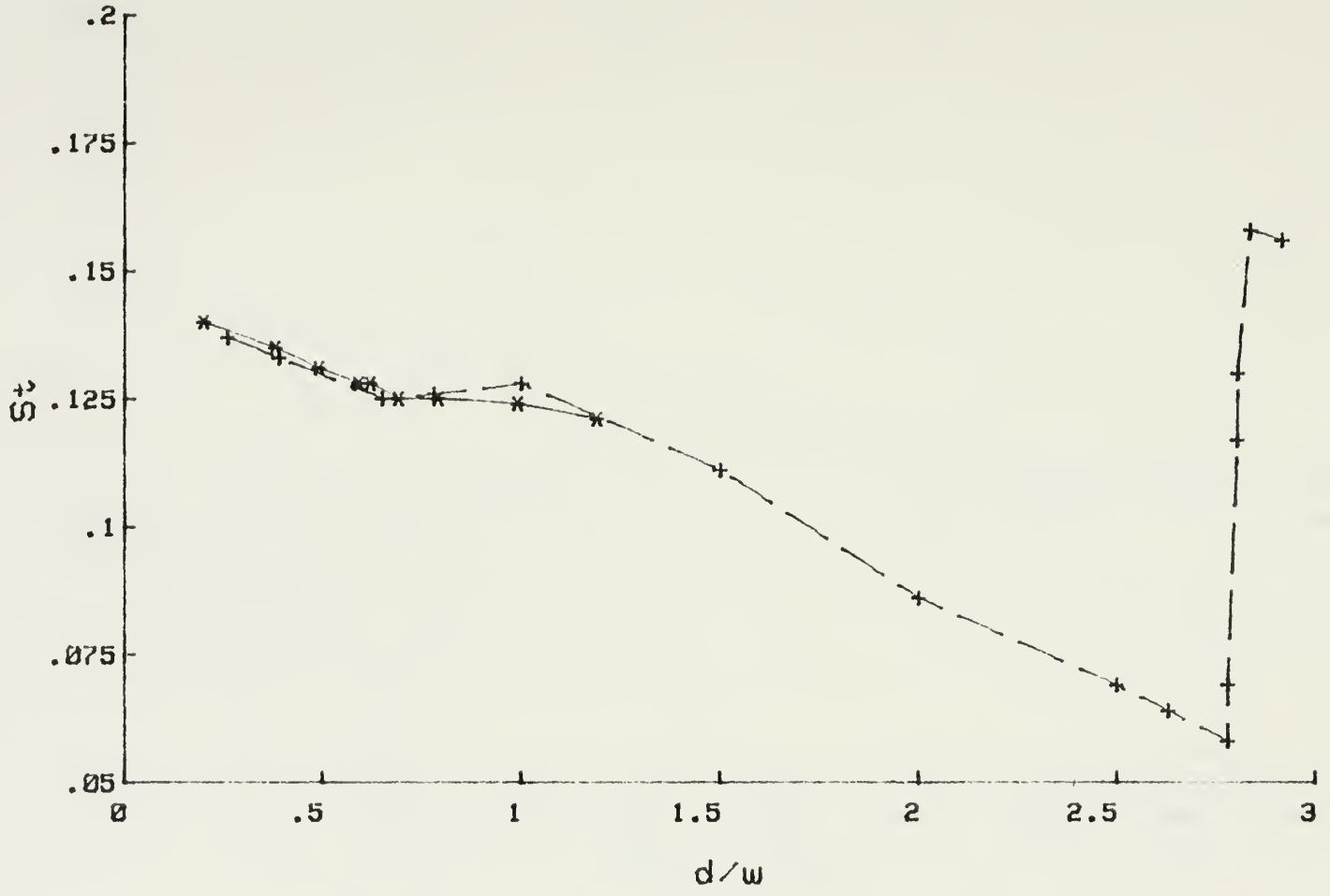

Figure 3. St vs. d/w on Rectangular Sections.

* Bearman and Trueman [3], Re = 2~7 x 10^4,

\+ Nakaguchi et al. [2], Re = 2~6 x 10^4.

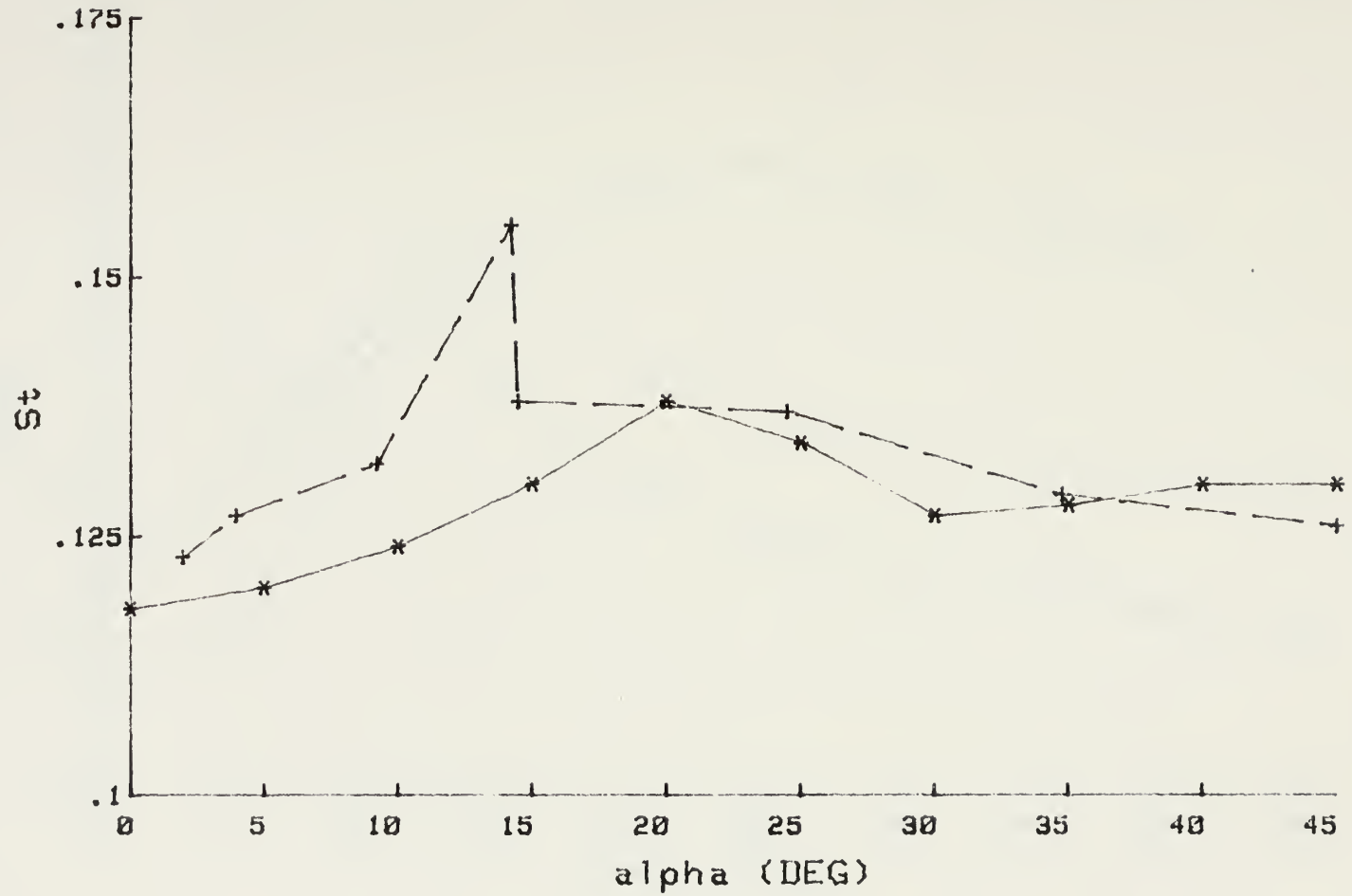

Figure 4. St vs. α on Square Prisms.

* Vickery [9], + Knauss [5].

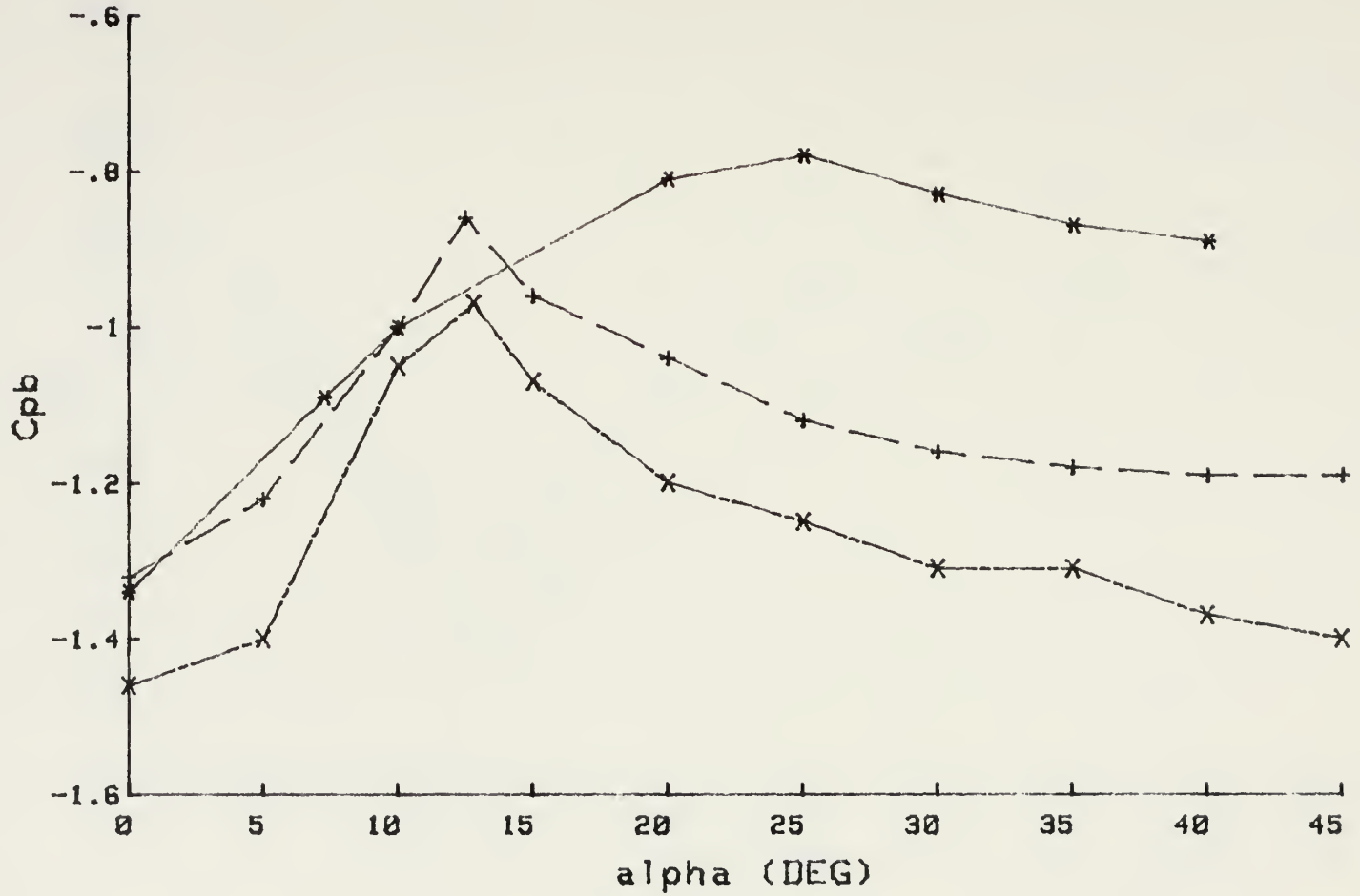

Figure 5. Cpb vs. α on Square Prisms.
* Vickery [9], + Lee [1], X Obasaju [7].

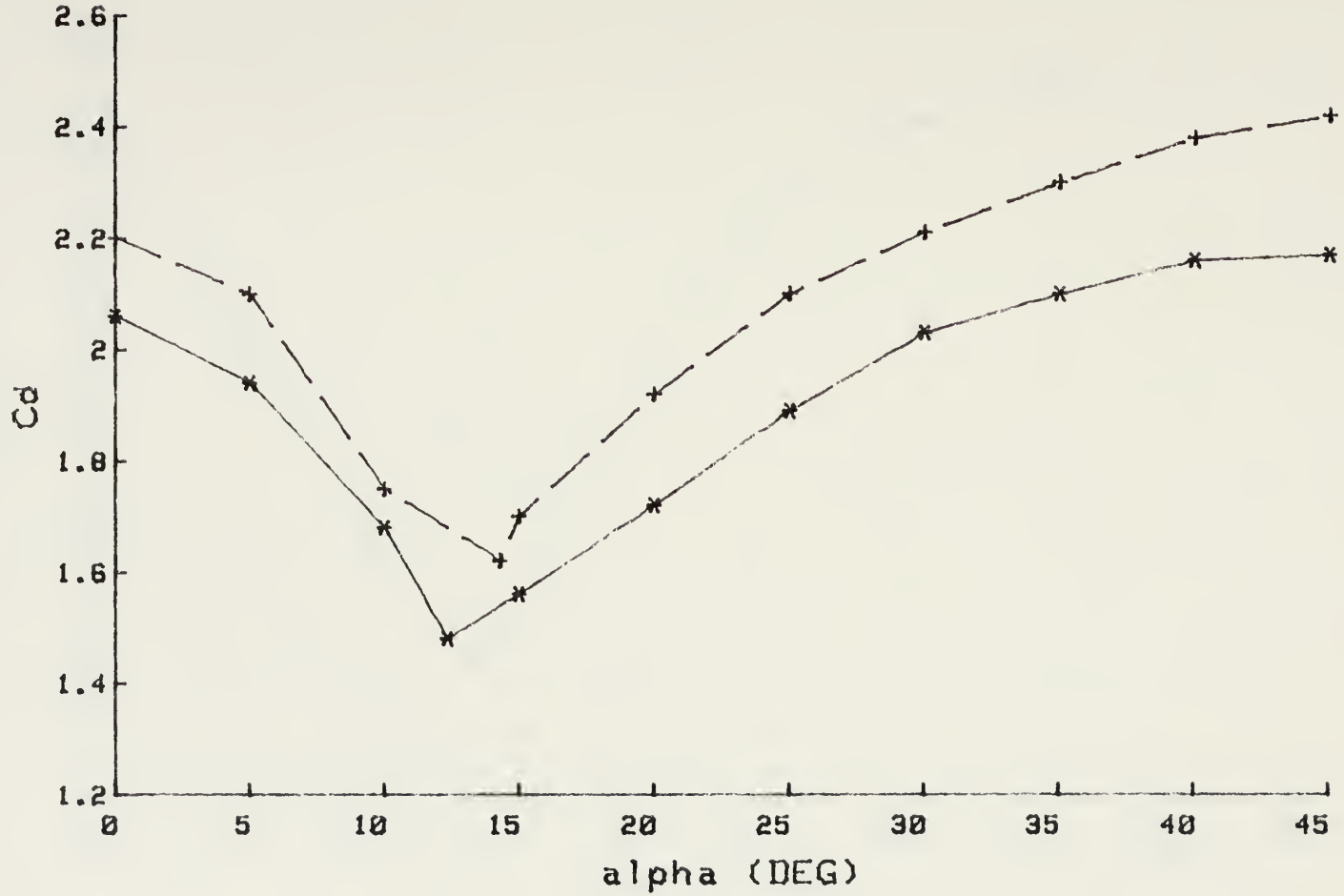

Figure 6. Cd vs. α on Square Prisms.
* Lee [1], Re = 1 x 10^5, + Obasaju [7], Re = 5 x 10^4.

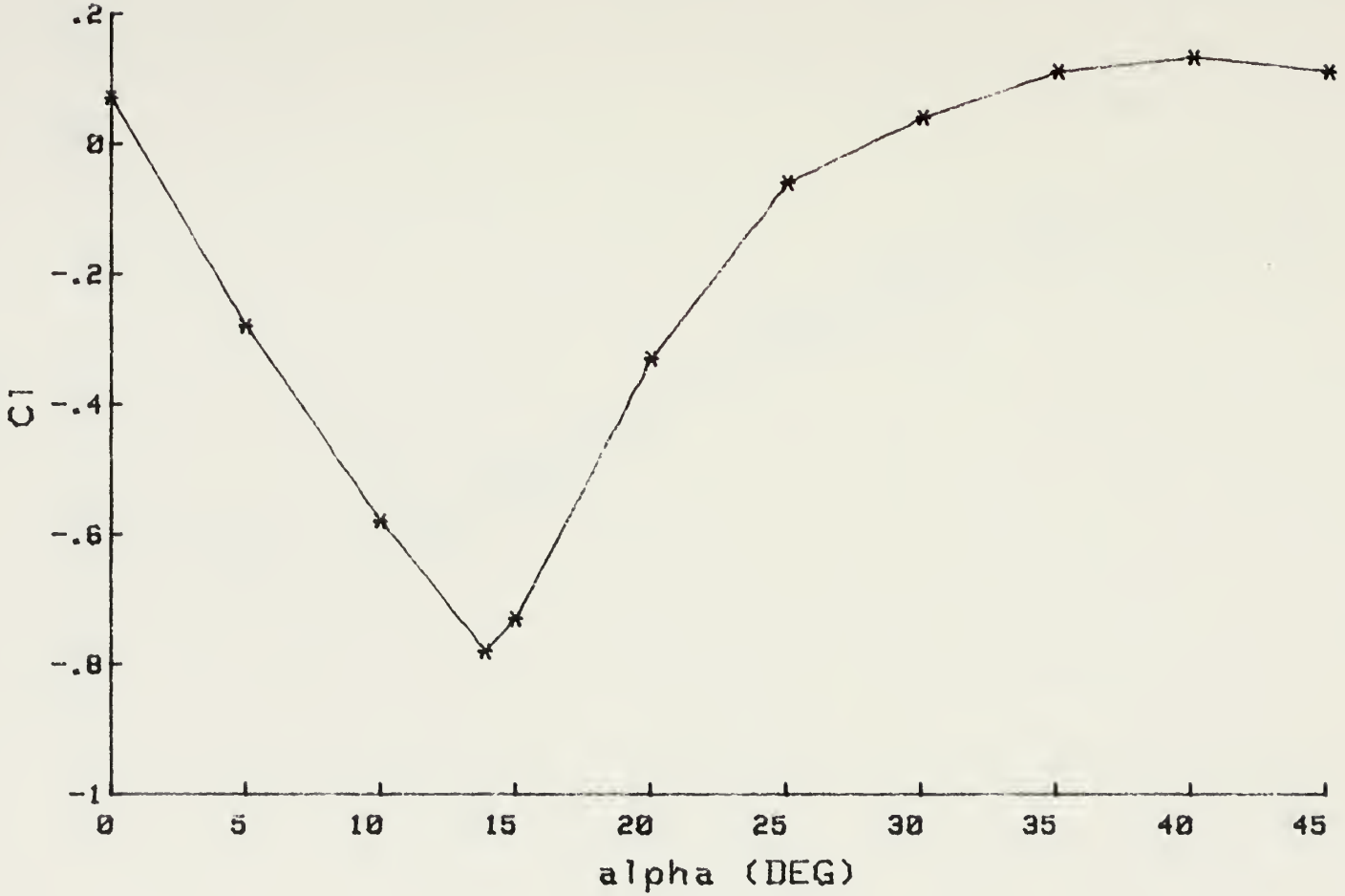

Figure 7. Cl vs. α on Square Prisms.

* Lee [1], Re = 1 x 10^5.

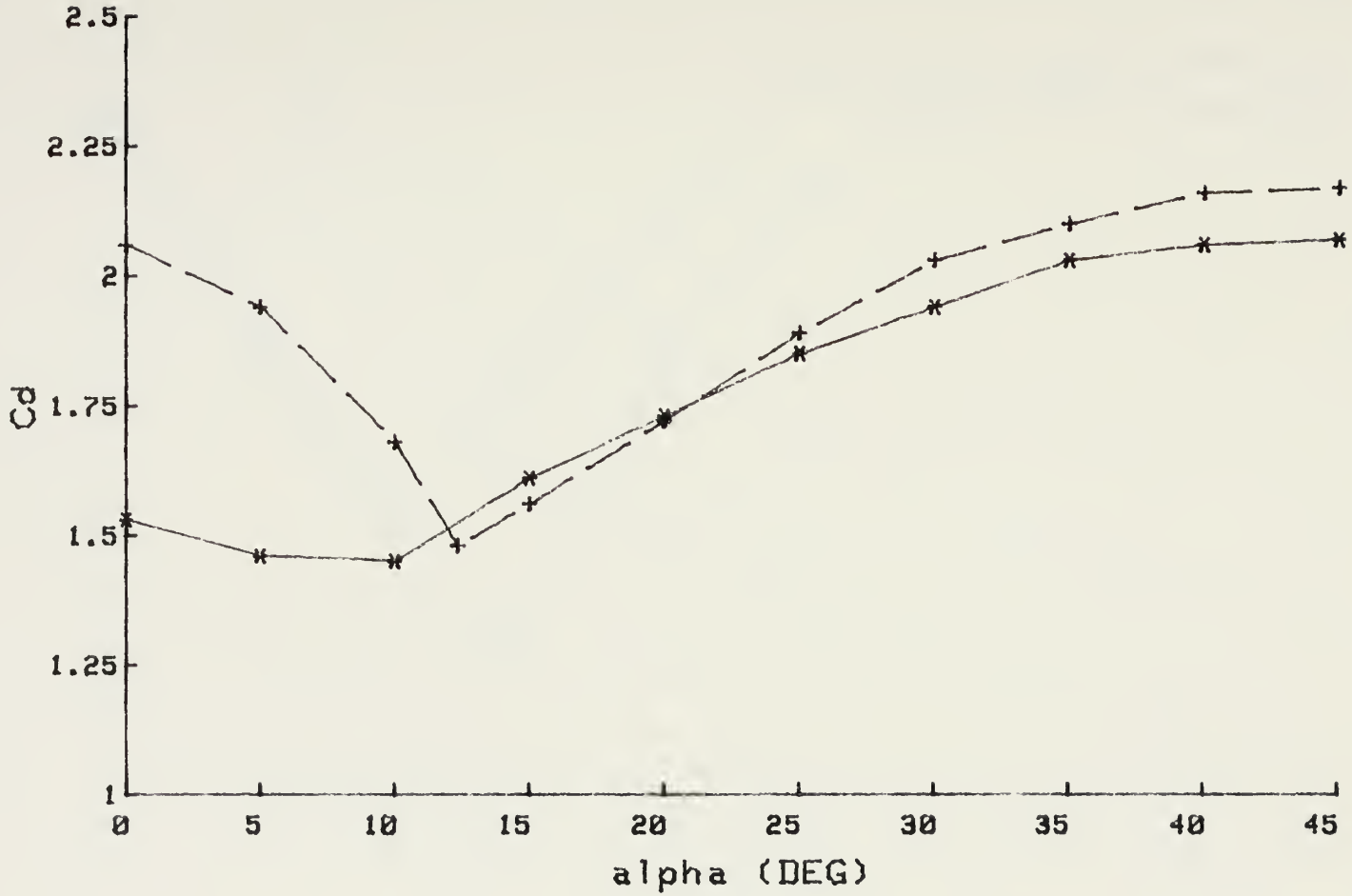

Figure 8. Cd vs. α with Varying Turbulence Intensity.
+ ε = .5%, * ε = 12.5% Lee [1].

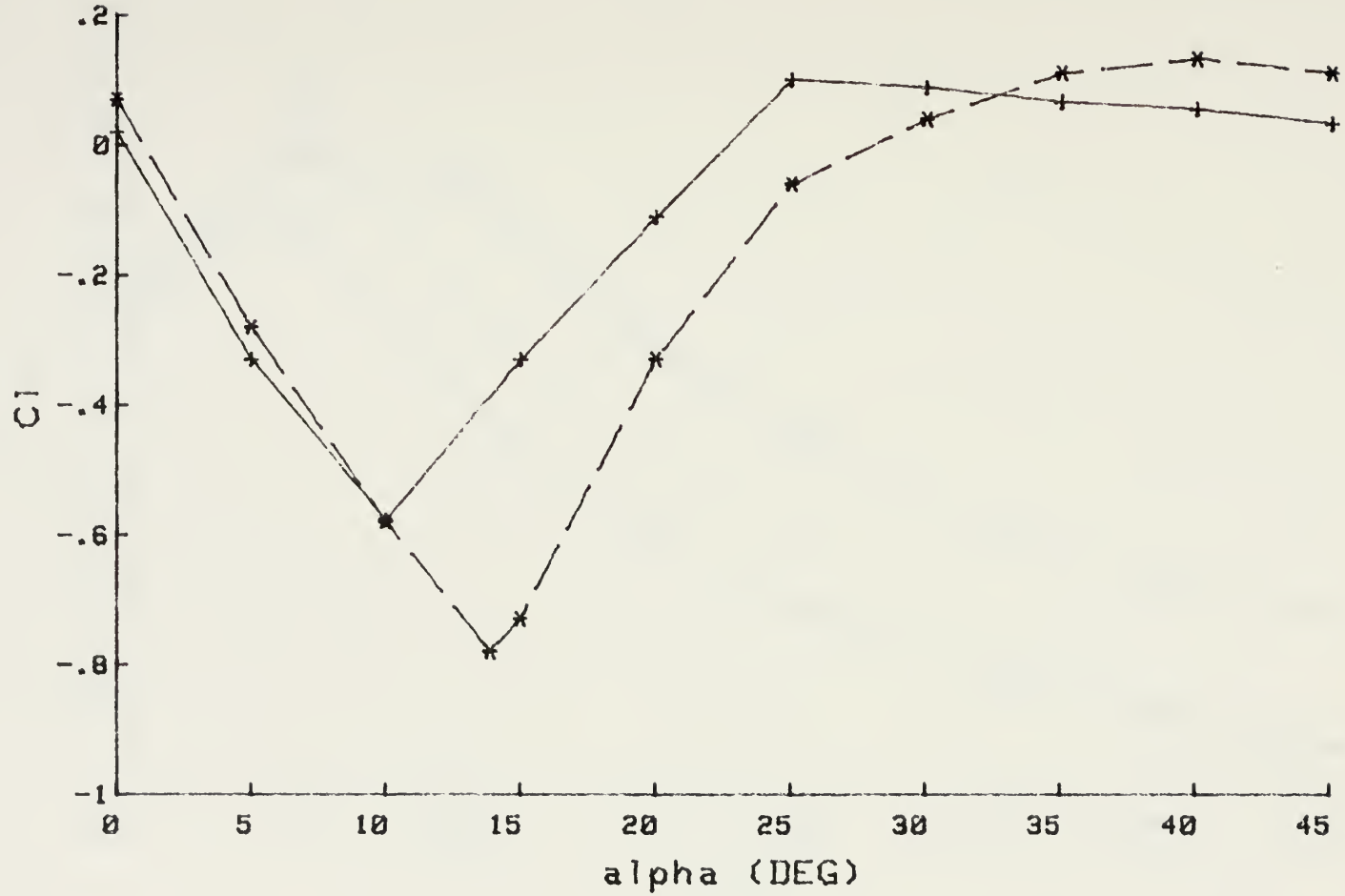

Figure 9. Cl vs. α with Varying Turbulence Intensity.
* ε = .5%, + ε = 12.5% Lee [1]

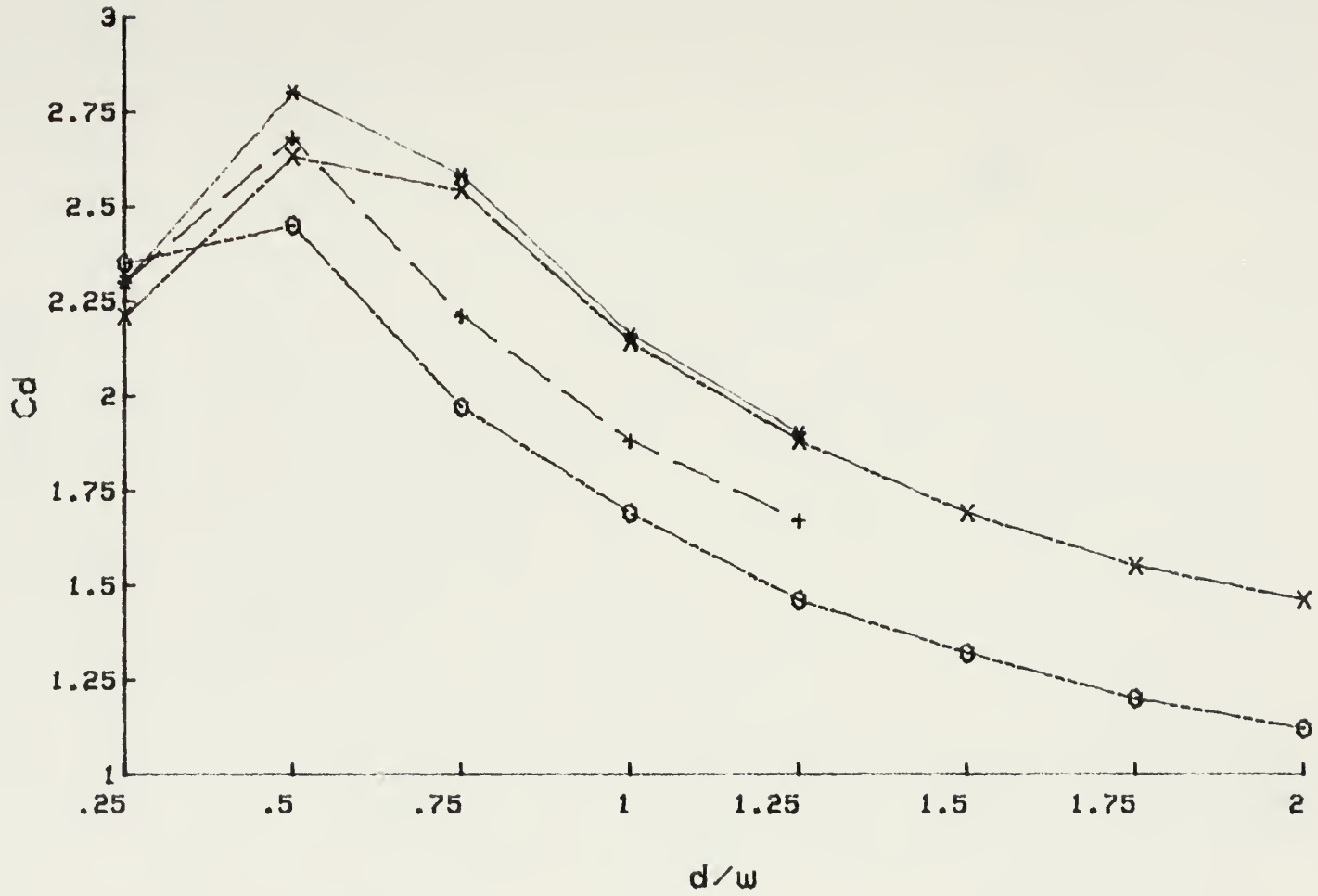

Figure 10. Cd vs. d/w with Varying Turbulence Intensity.

* ε = 4.9% Nakamura and Tomonari [12], + ε = 11.1% Nakamura and Tomonari [12], X ε = 2.6% Courchesne and Laneville [13], 0 ε = 13.5% Courchesne and Laneville [13].

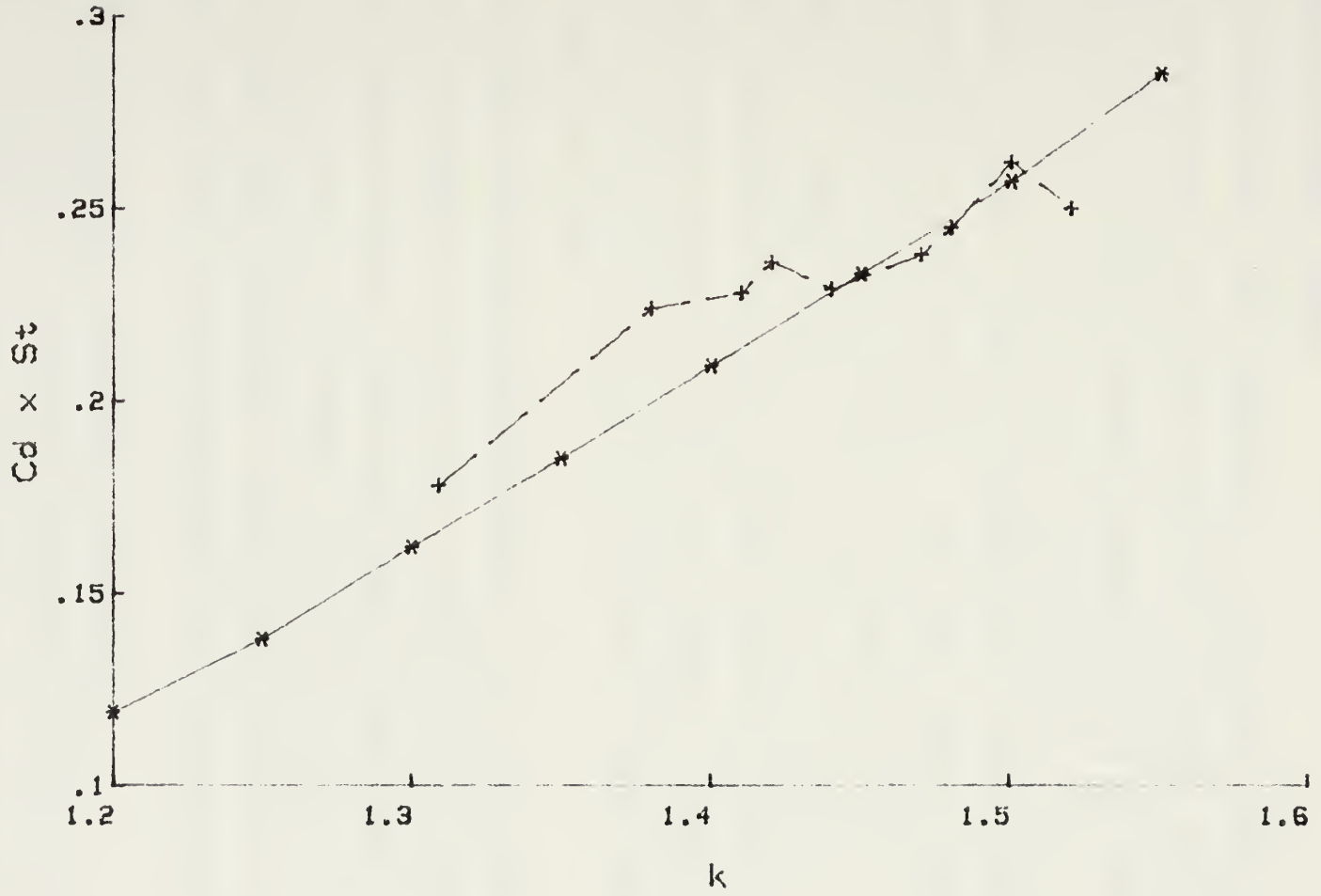

Figure 11. Cd x St vs. k.

* Bearman and Trueman [3], + Lee [1].

III. EXPERIMENTAL EQUIPMENT AND PROCEDURES

A. VERTICAL WATER TUNNEL

The experiments were conducted in a vertical water tunnel which was previously used and described in detail in the study of impulsive flow about submarine-shaped bodies performed in 1981 [Ref. 17]. A quick-release valve located at the base of the tunnel is used to create an impulsively-started flow of nearly constant linear velocity. The valve seats against an 'O' ring inserted on the bottom of the seating surface so that no leakage is present prior to initiating fluid motion.

The operation of the quick-release valve is controlled by a three-way valve mounted beneath the tunnel. A solenoid valve provides on-off control of the quick-release valve and, therefore, the flow itself.

Following the rapid initial opening, which accelerates the flow in 0.1 seconds or less, slower further opening of the quick-release valve sustains a controlled drop of the tunnel water level. This controlled slowdown of the rate at which the quick-release valve opens, provided steady flow velocities of about 0.9 feet per second for the experiments described herein.

B. FLUID DISPLACEMENT AND FORCE MEASUREMENTS

The displacement of fluid was measured through the use of a variable resistance probe. An eight foot long platinum wire,

placed vertically in the tunnel and mounted away from the walls, provided tunnel water level indication to an amplifier-recorder assembly. Prior to taking data, trial impulsive flow was initiated several times. Adjustments to the quick-release valve control system were made, as necessary, to ensure a linear slope on the elevation versus time plot on the recorder. As the slope was not exactly linear a third order polynomial was fitted to the elevation versus time plot in order to have an accurate means of calculating the displacement of the fluid, S, as a function of time and its derivative, velocity U(t).

10kg-capacity load transducers were used to measure the instantaneous drag and lift forces on the test bodies. Special housings were built for each gage so that they could be mounted on the tunnel at each end of the test body. A complete description of the force measurement assemblies and calibration procedures may be found in [Ref. 17].

C. TEST BODIES AND TESTING PROCEDURES

Five rectangular cylinders were tested during this investigation. The geometrical characteristics of the test bodies are shown in Table I. The test Bodies A, C, D and E were constructed from solid plexiglas, turned on a milling machine and then polished for a smooth finish. The Body B was constructed from a square aluminum tube. The length of each cylinder was cut so that a gap of approximately 0.06 in. was present between the tunnel wall and each end. A complete description of the mounting arrangements and procedures can be found in [Ref. 17].

Each body was tested at various angles of attack for drag and lift measurement. At least two runs were conducted for drag and lift, respectively, at each reference angle. Velocity was indicated by an elevation versus time plot which was generated for every run.

Raw analog data was produced from the force transducers and the variable resistance probe by connecting their outputs to individual electronic amplifiers and then to a strip-chart recorder which was operated at a speed of 50 mm per second for each run. This analog data was processed in accordance with the governing equations described in Chapter II.

TABLE I

Geometrical Characteristics of the Test Bodies.

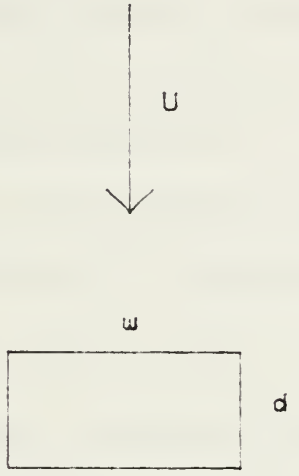

(Repeated from Figure 1.)

Dimensions (d X w X L)	Configuration (d/w)	Designation
3.00 X 3.00 X 23.78 in	1	Body A
1.98 X 1.98 X 23.75 in	1	Body B
1.75 X 2.75 X 23.78 in	.64	Body C
2.75 X 1.75 X 23.78 in	1.57	Body D
.875 X 1.375 X 23.78 in	.64	Body E

IV. EXPERIMENTAL RESULTS

A. PRESENTATION

The drag and lift coefficients, Cd and Cl, for each test body are presented primarily in graphical form as a function of the relative fluid displacement S/w. Since not all of the large volume of data are discussed herein, representative data have been assembled in the appendices by test body designation and reference angle (angle of attack).

B. DEFINITION OF THE FORCE-TRANSFER COEFFICIENTS

The drag and lift coefficients for the test bodies were computed using Equations (2) and (3). The positive directions of drag and lift along with the angle of attack with respect to the direction of impulsive flow are shown in Figure 1. The normalized displacement used for the test bodies is S/w where

$$S = \int_{o}^{T} U(t)\, dt$$

C. EFFECTS OF THE FORCE TRANSFER PARAMETERS

At zero-degrees angle of attack, all of the test bodies exhibit large overshoots in Cd between 1.8 to 2.4 near S/w = 5 and secondary peaks near S/w = 7.5. The relative magnitude of the drag peaks decreases for bodies with larger d/w. Following the secondary peaks in drag, Cd drops rapidly and

approaches asymptotically mean values ranging from Cd = 1.5 to 2.8, depending on the shape and the angle of attack of the body. These values are consistent with those obtained in steady flow. The asymptotic values of Cd (within the range of larger S/w values attained) decrease with test bodies of larger d/w as shown in Figures 12 through 16.

The phenomenon of vortex shedding is non-stationary in the early stages of impulsive motion and consequently a single vortex shedding frequency does not exist. However, an estimate of the vortex shedding frequency, f_v, was made from Figures 17 through 19. Time intervals between consecutive peaks of the lift-coefficient curves were used to derive a Strouhal number, St, in terms of the period defined by those time intervals. Analysis shows that for an angle of attack of 10 degrees, the approximate Strouhal numbers, St f_v w/U, were: St = 0.143 for Body C, St = 0.132 for Body A and St =0.125 for Body D. As found in earlier steady flow experiments, St decreased with test bodies of larger d/w (see Figure 3).

By carefully controlling the flow mechanism in the vertical water tunnel, repeatable velocities were maintained. The Reynolds number, Re = Uw/ν, range was 10,000 to 20,000. Thus, it was not possible to examine the variation of Cd or St with the Reynolds number.

Strong variations in the force-transfer coefficients are observed as the angle of attack is increased. Extremely

large drag overshoots were present with Cd reaching values of 2.3 to 4.4. Dramatic effects are associated with the growth of the first three or four vortices shed from the body following the initiation of impulsive flow. At the start of motion, the vortices grow rapidly and at a rate of growth such that the vorticity accumulates to an amount far in excess of that found in the later stages of the motion. This excess vorticity reduces the base pressure and causes a large drag overshoot. Cd is seen to rise to about 2.1 (at S/w = 4) to 2.7 (at about S/w = 6.5) in Figures 20 and 21. The first and second vortices appear to be shed at S/w = 4 and S/w = 6.5 in Figures 22 and 23. The relative magnitude of the drag overshoots in the early stages of the flow increased with the angle of attack for all test bodies. The asymptotic mean values of Cd in the final stages of the flow increased for angles of attack greater than 20 degrees. In contrast, mean Cd values approached minimum values of 1.3 to 2.3 for angles of attack between 10 and 20 degrees.

Figures 24 through 28 reveal net lift coefficients approaching minimum values of Cl = -0.2 to -1.4 at angles of attack between 10 and 20 degrees. Figures 29 through 34 exhibit positive net lift coefficients for square prisms with angles of attack 30 degrees and higher. These observations with respect to the final stages of impulsive flow are in accord with results of previous experimental results in steady flows, (see Figures 6 and 7). As evidenced from

Figures 35 and 36, Bodies C and D, unlike the square prisms, display a net negative lift coefficient for angles of attack 30 degrees and higher.

Evaluation of approximate Strouhal numbers for Bodies A and B yielded values which reached a maximum of St = 0.150 to 0.154, at an angle of attack of 20 degrees. These results are in consonance with earlier investigations, Figure 4. No such correlation was evident for Bodies C and D.

The effects of turbulence were not evaluated in this study as the impulsive flow developed in the vertical water tunnel was smooth, $\varepsilon = 0$.

The aspect ratios of the test bodies in this work varied from L/w = 7.9 to 17.3. The models were sharp-edged, resulting in fixed separation points and in excellent spanwise coherence of the vorticies. End plates were not used and the experimental results do not indicate the presence of appreciable end effects or a loss of two-dimensionality.

Wall blockage effects were evaluated by comparing Figures 37 through 41 and Figures 42 through 46 for Bodies A and B. Blockage correction formulae for the early stages of impulsive flow do not exist and their development is beyond the scope of this work. Equations (7) and (8) were used to make blockage corrections for the drag coefficients of Bodies A and B for the late stages of low, i.e., for S/w = 16 to 18. The corrected Cd values varied between 1.98 and 2.18 for an angle of attack of 20 degrees. Body A and B corrected Cd

values varied by no more than 6 percent between the two bodies. The magnitude of the individual corrections for Body A were about 15 to 16 percent of the uncorrected Cd values. For Body B, however, the magnitude of the corrections were within the limits of experimental error. Hence, Body A results do reflect some blockage effect. Blockage corrections were not applied to the results contained herein for reasons of uniformity and comparison.

Calculations were performed to determine the magnitude of the effect of the acceleration parameter on the drag coefficient. The acceleration was determined from the polynomial for displacement, S, and the force contribution due to added mass was computed. The net effect was no more than a 3 percent variation in Cd, within the limits of experimental error and was considered negligible.

Extensive study of the plots of the lift coefficients as compared to the drag coefficients indicates that the onset of vortex shedding was the predominant factor in determining the behavior of the force transfer coefficients. In all cases investigated, the drag coefficients oscillated at twice the vortex shedding frequency. As the angle of attack was increased, vortex strength increased as inferred directly from the larger amplitude oscillations in Cd and Cl, (see Figures 47 through 52). Also noted at higher angles of attack are secondary and tertiary peaks in Cd associated with the shedding of the third and fourth vortices which

are of significant magnitude and even larger than the initial drag overshoots in some cases, (see Figures 39, 45 and 49 through 52).

Of special interest is the behavior of the transverse force. The initial lift force on Bodies A and B was positive for all angles of attack and for Body C through an angle of attack of 20 degrees. In contrast, the initial lift force for Body C at an angle of attack of 40 degrees and for Body D at all angles was negative. It should be noted that the profile presented to the flow by Body C and D at 40 degrees angle of attack was nearly identical. The growth and motion of the first vortex sets up a circulation about the body which is equal in magnitude and opposite in direction to that of the first shed vortex. As a result, the velocity increases and the pressure decreases on the opposite side of the body relative to the first vortex. The differential pressure creates a transverse force. The direction of the initial lift force is fixed by the asymmetry of the body in that the force is away from the shed vortex and normal to the direction of ambient flow. The subsequent shedding of vortices from opposite sides of the body results in an alternating lift force as shown in Figures 17 and 18 and Figures 22 through 36.

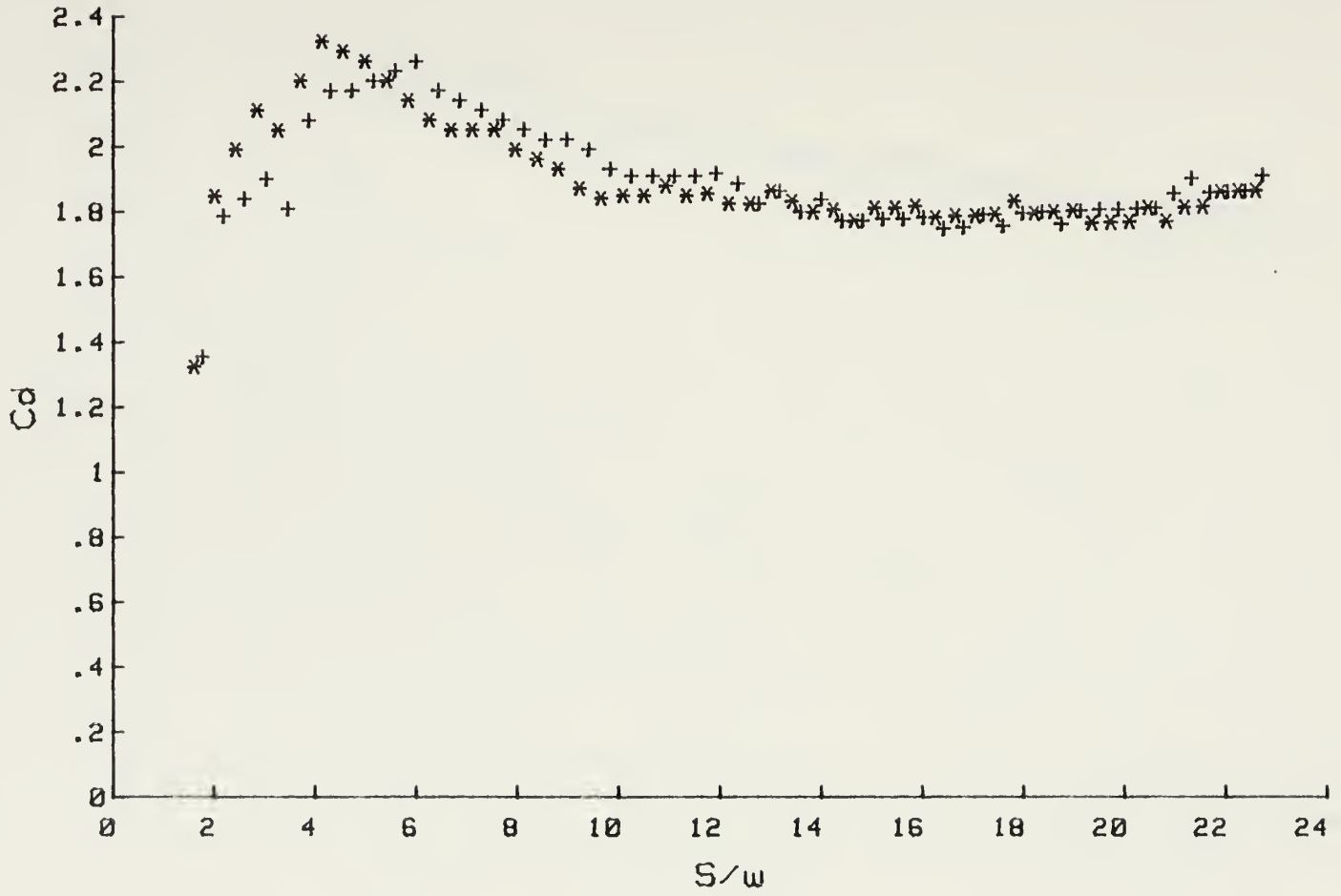

Figure 12. Cd vs. S/w for Body C at 0deg.

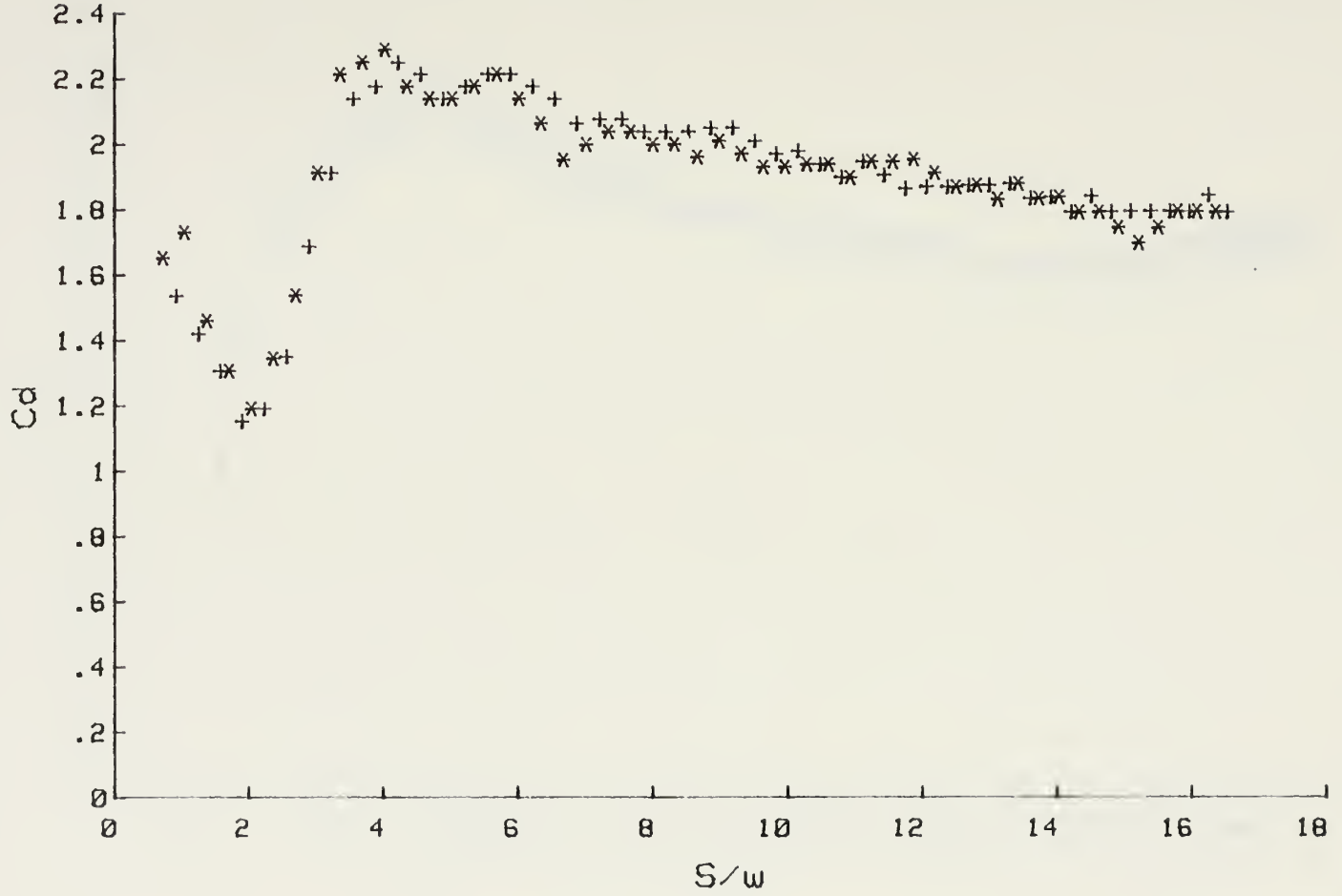

Figure 13. Cd vs. S/w for Body A at 0deg.

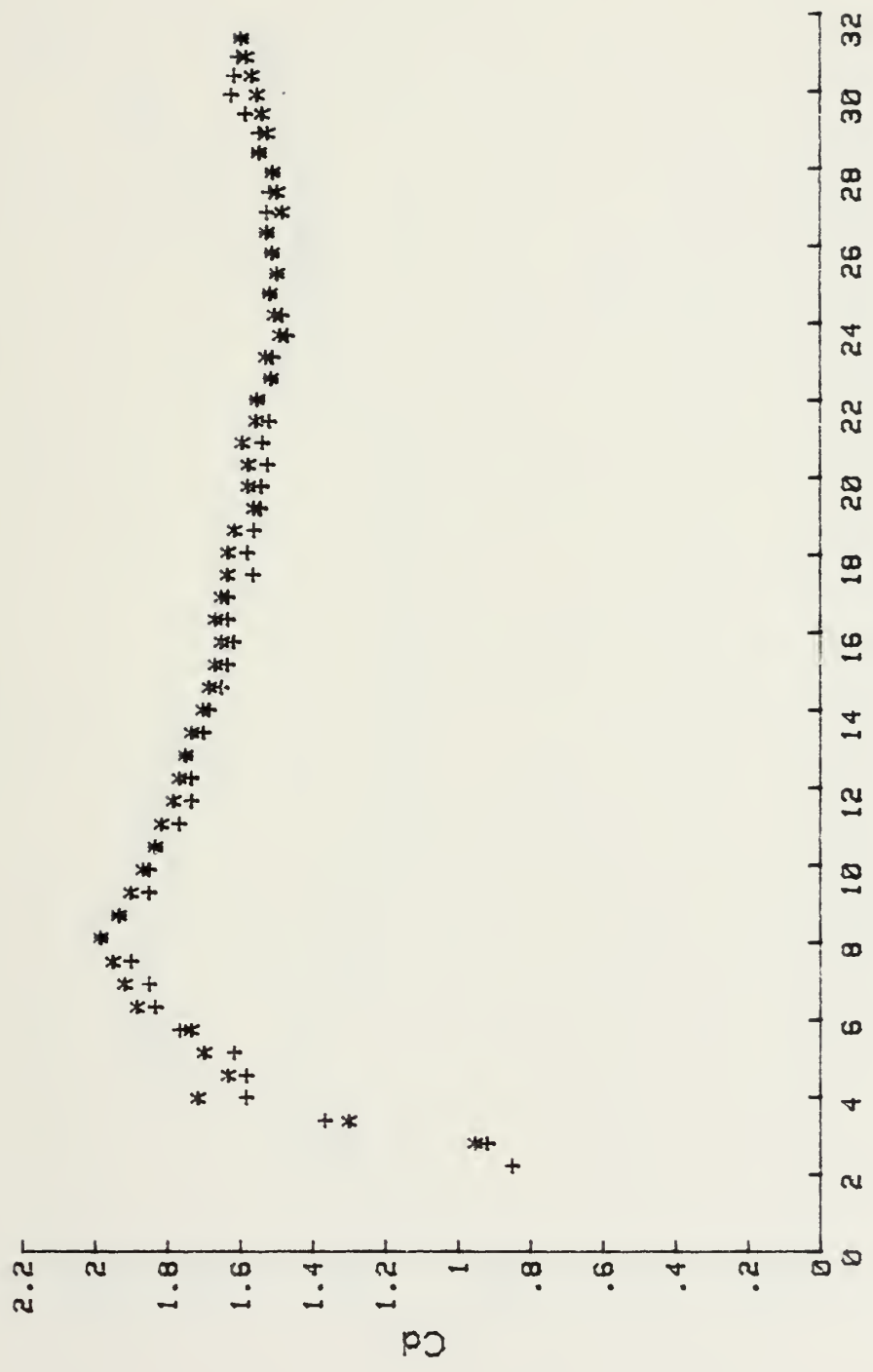

Figure 14. Cd vs. S/w for Body B at 0deg.

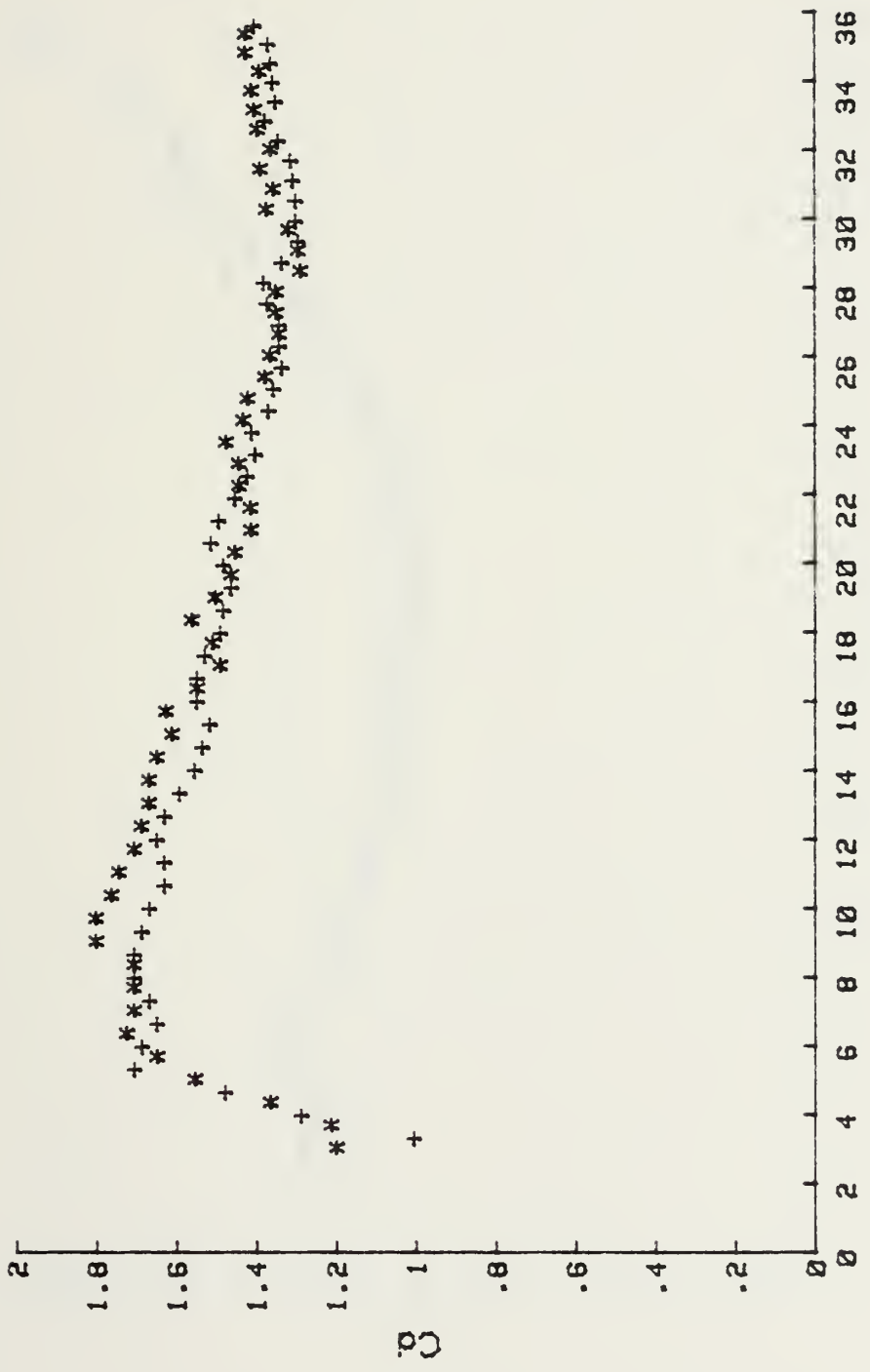

Figure 15. Cd vs. S/ω for Body D at 0 deg.

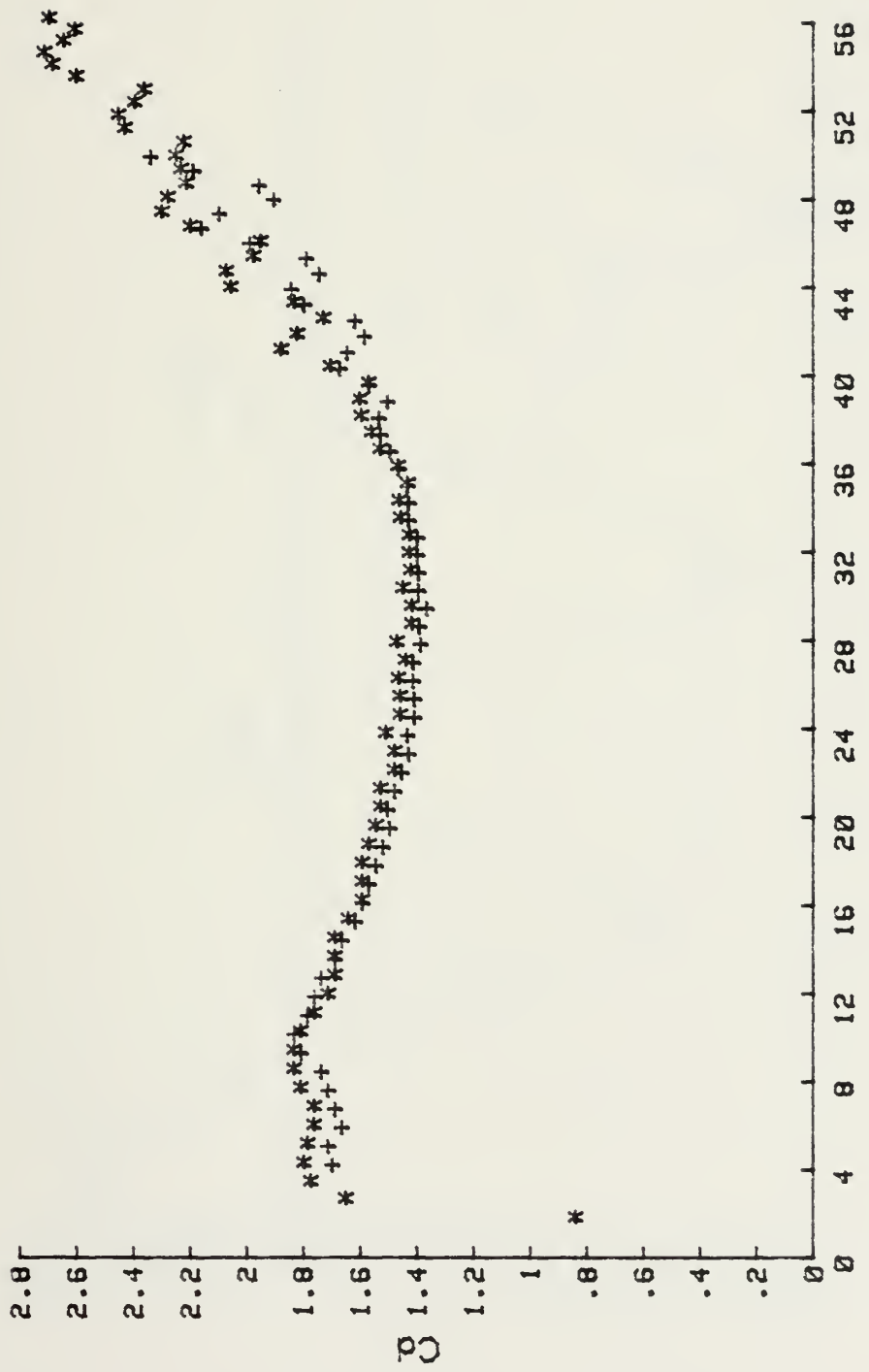

Figure 16. Cd vs. S/w for Body E at 0 deg.

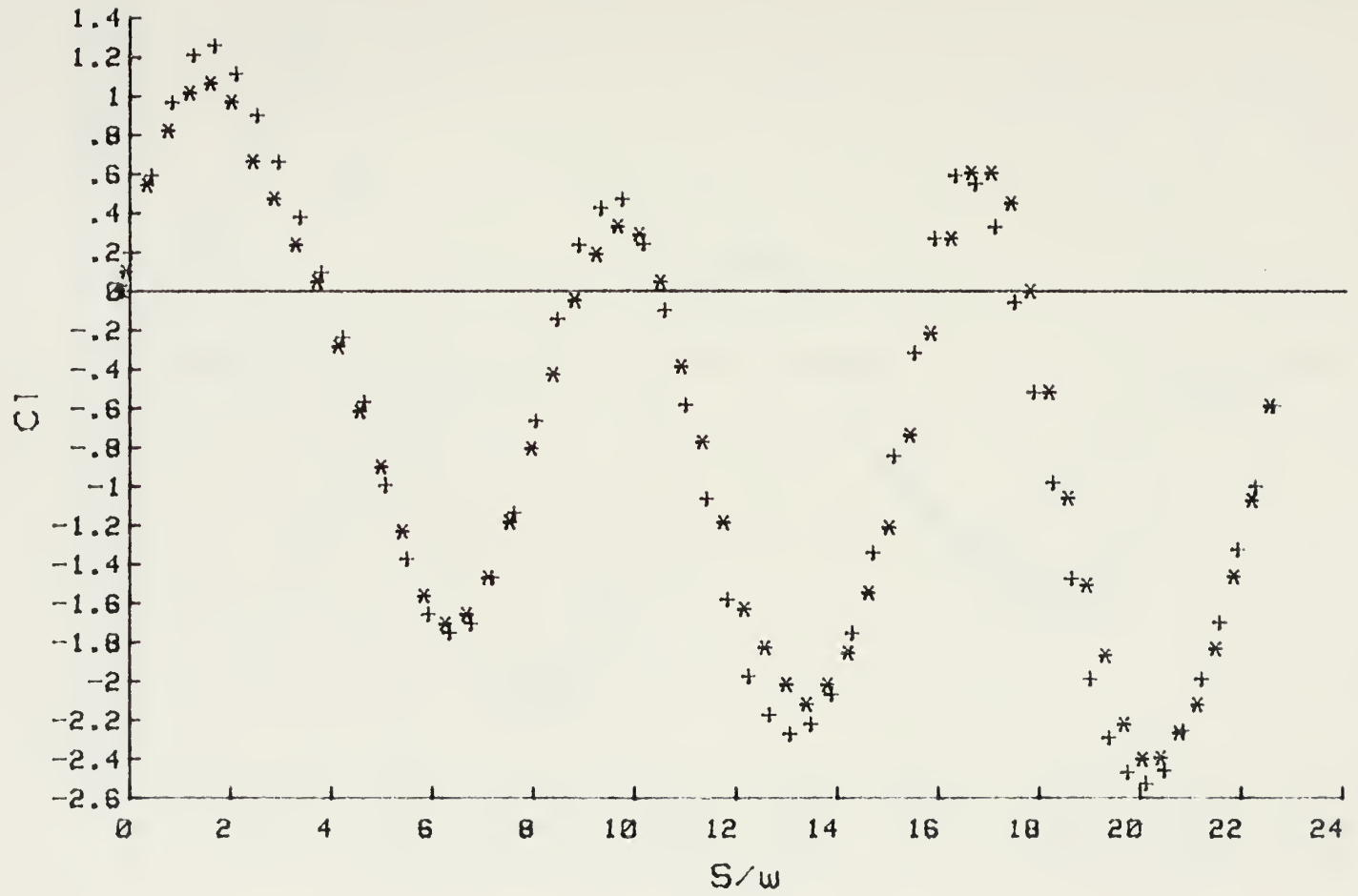

Figure 17. Cl vs. S/w for Body C at 10deg.

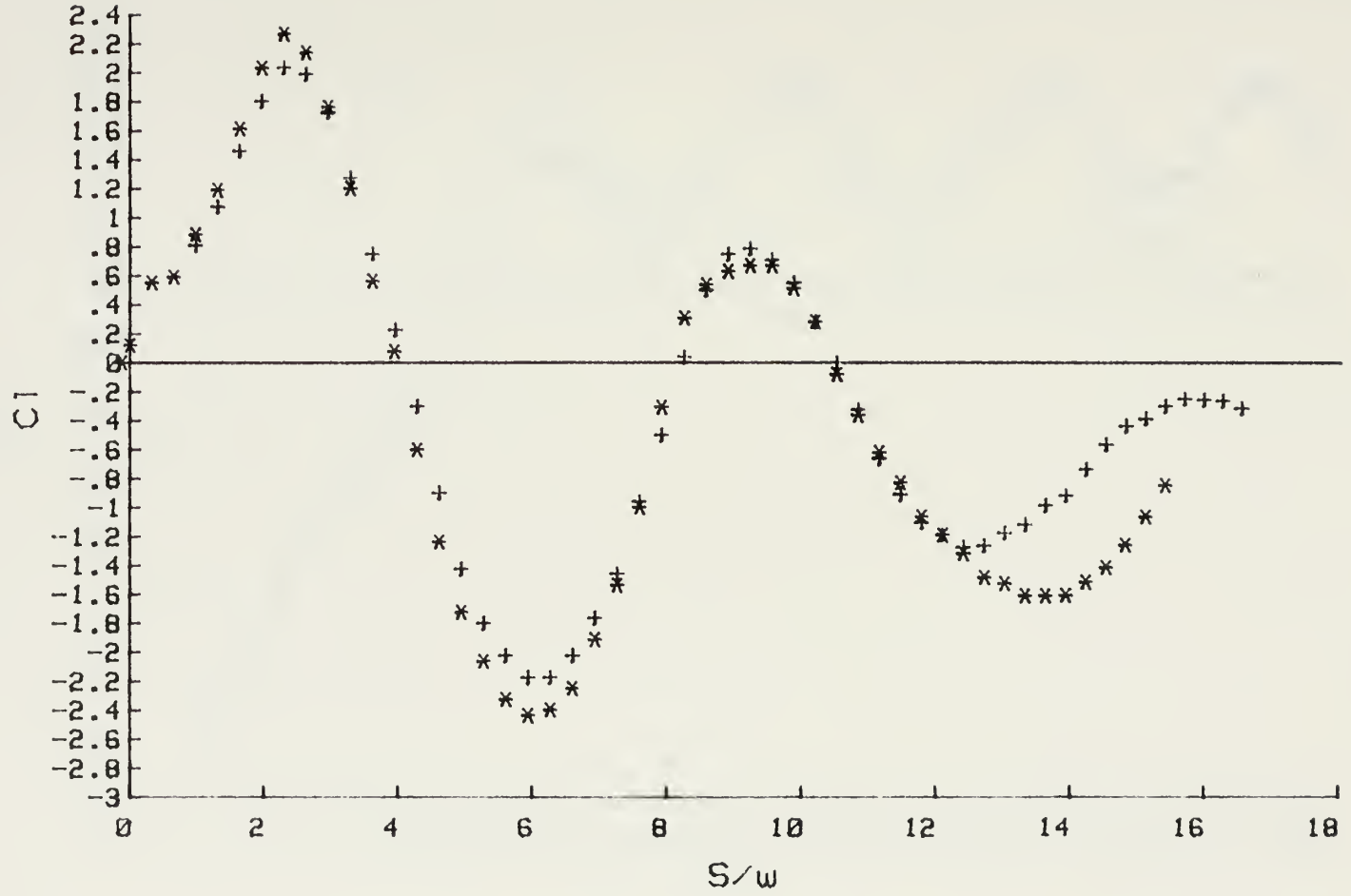

Figure 18. Cl vs. S/w for Body A at 10deg.

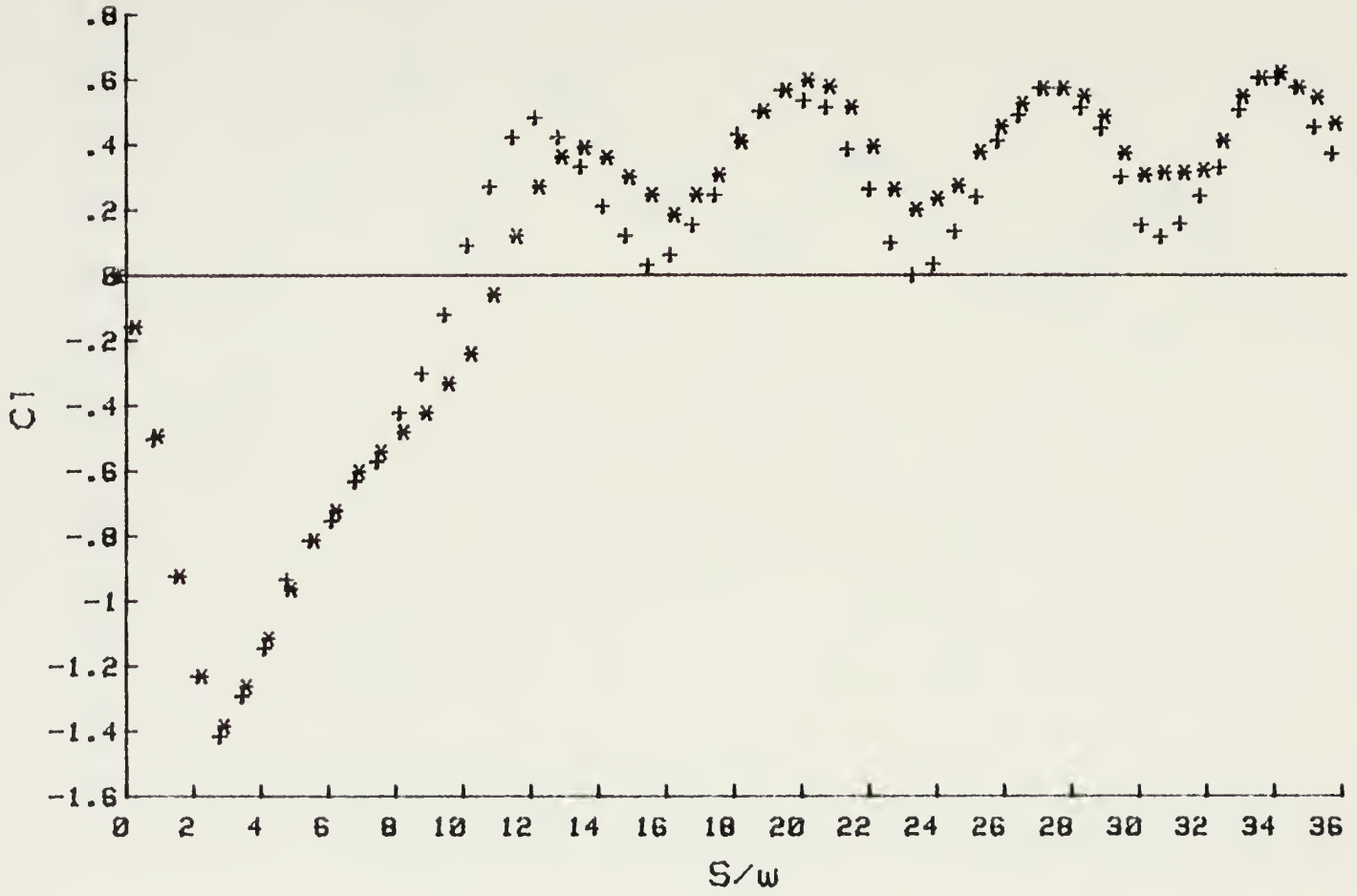

Figure 19. Cl vs. S/w for Body D at 10deg.

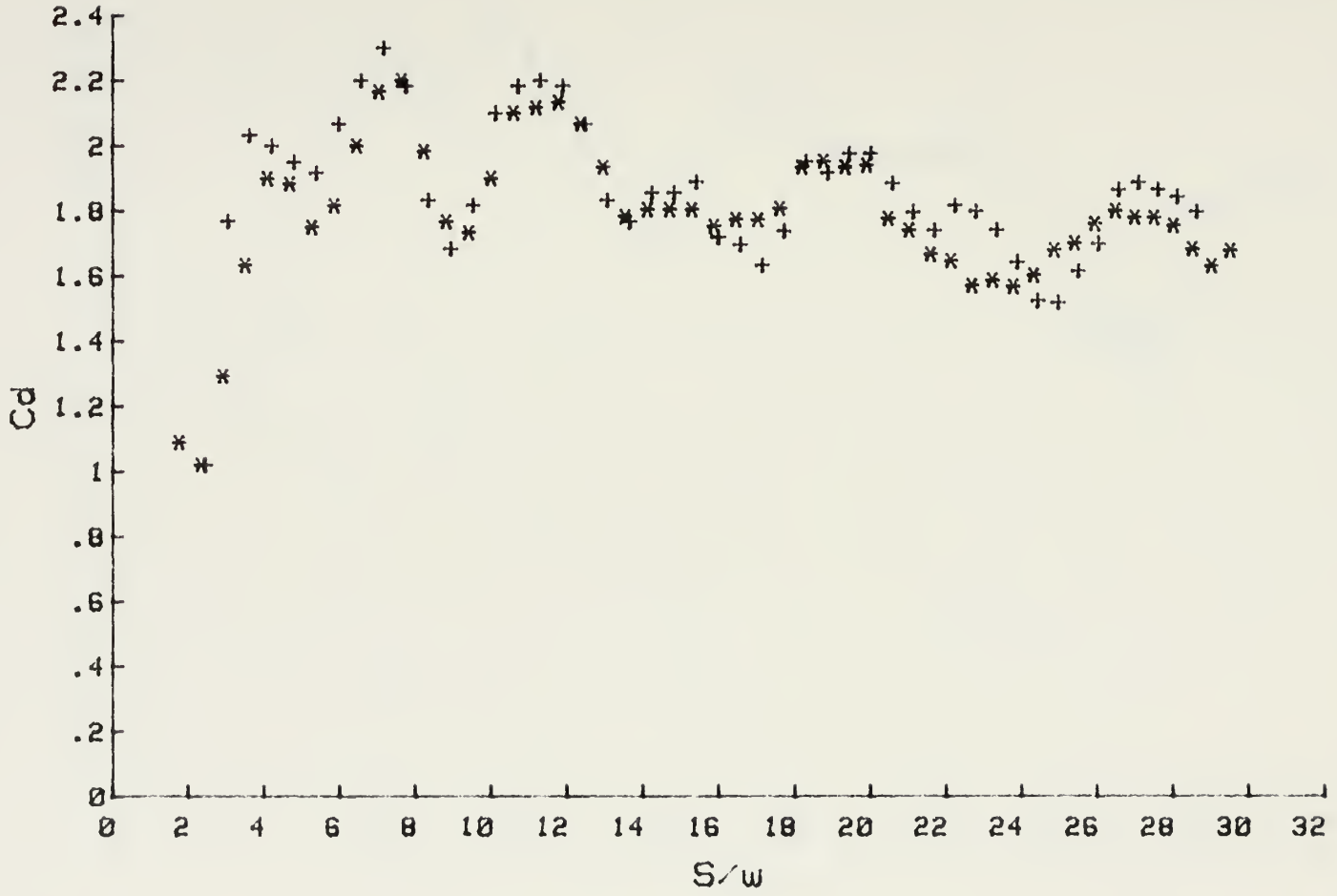

Figure 20. Cd vs. S/w for Body B at 5 deg.

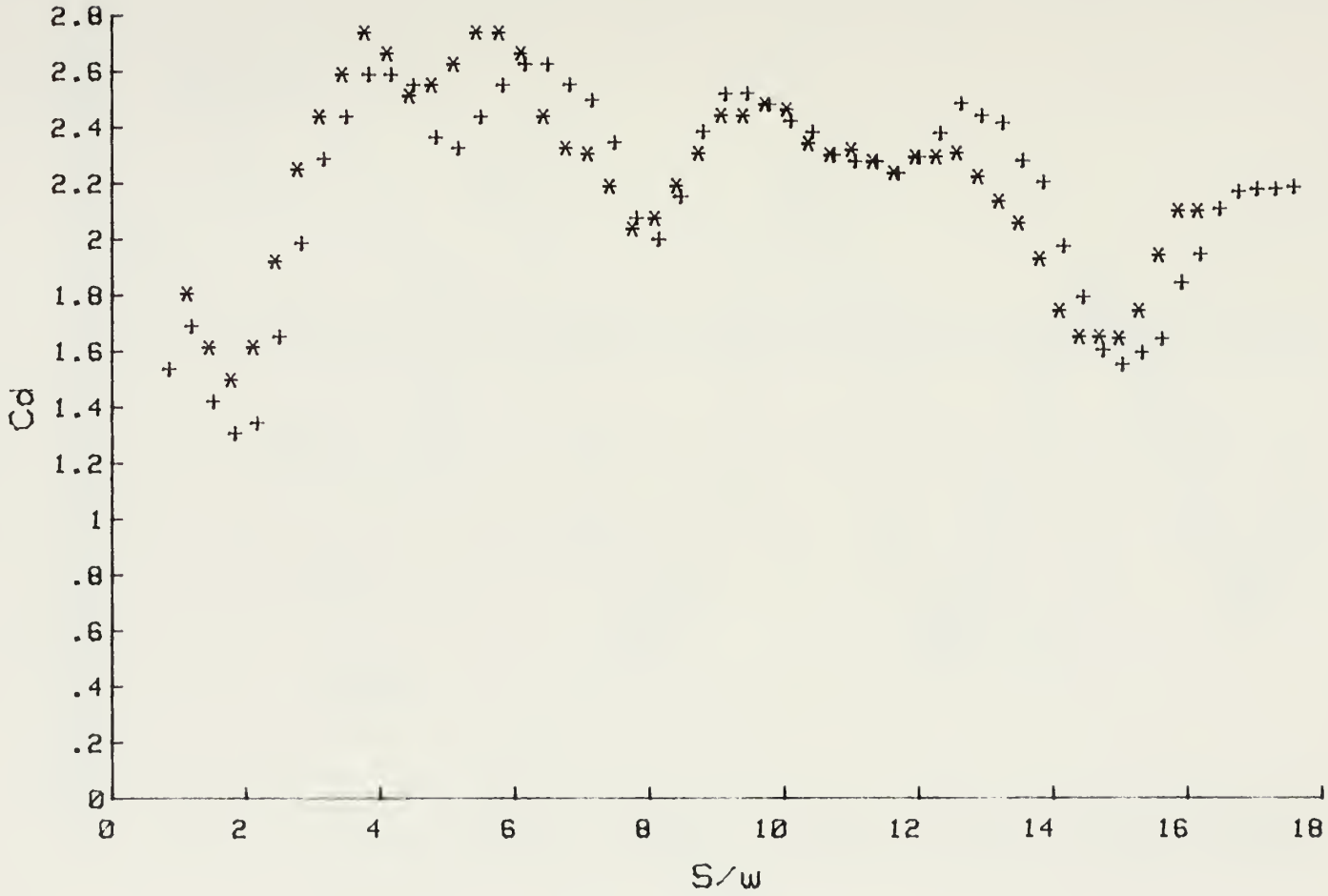

Figure 21. Cd vs. S/w for Body A at 5 deg.

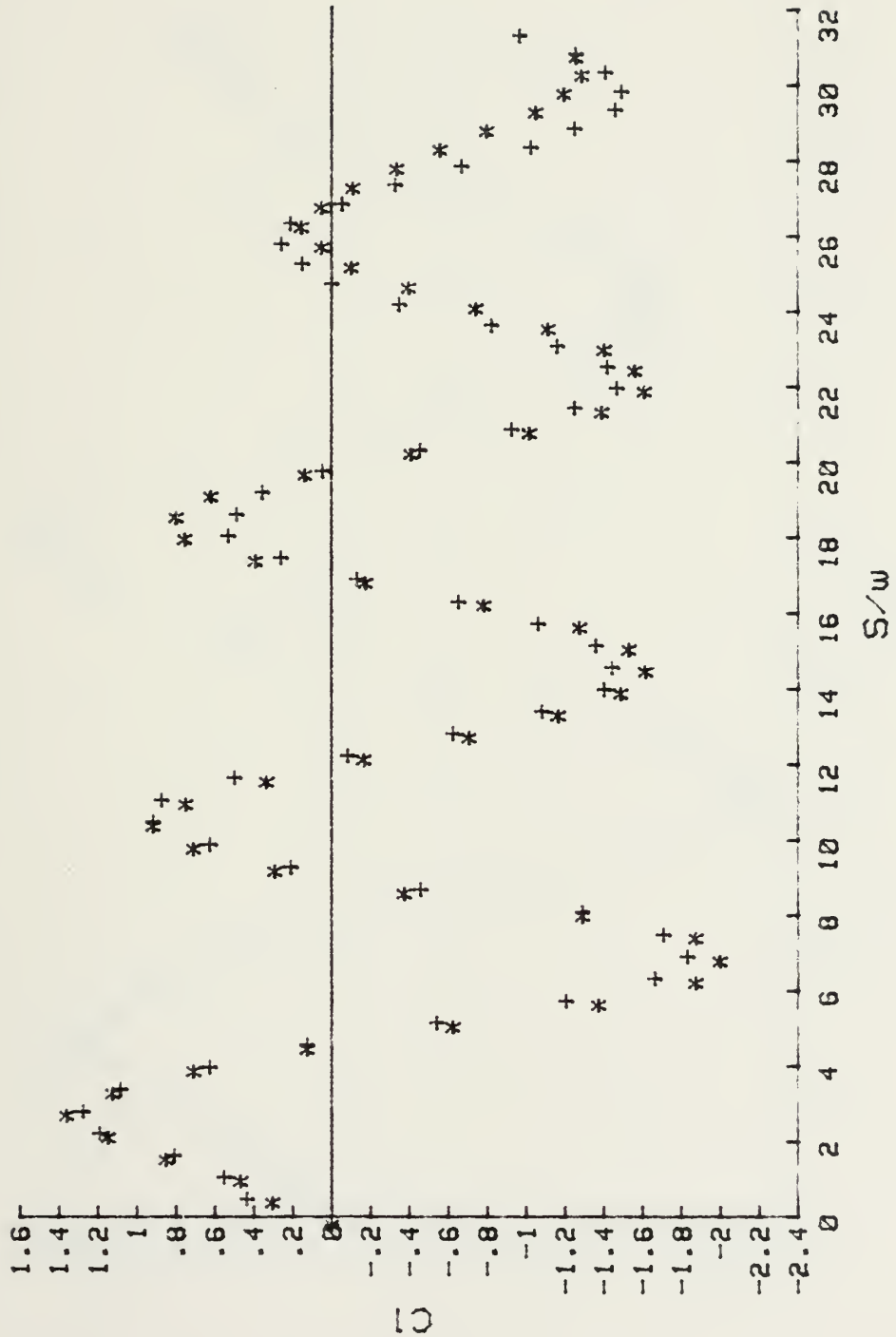

Figure 22. Cl vs. S/w for Body B at 5 deg.

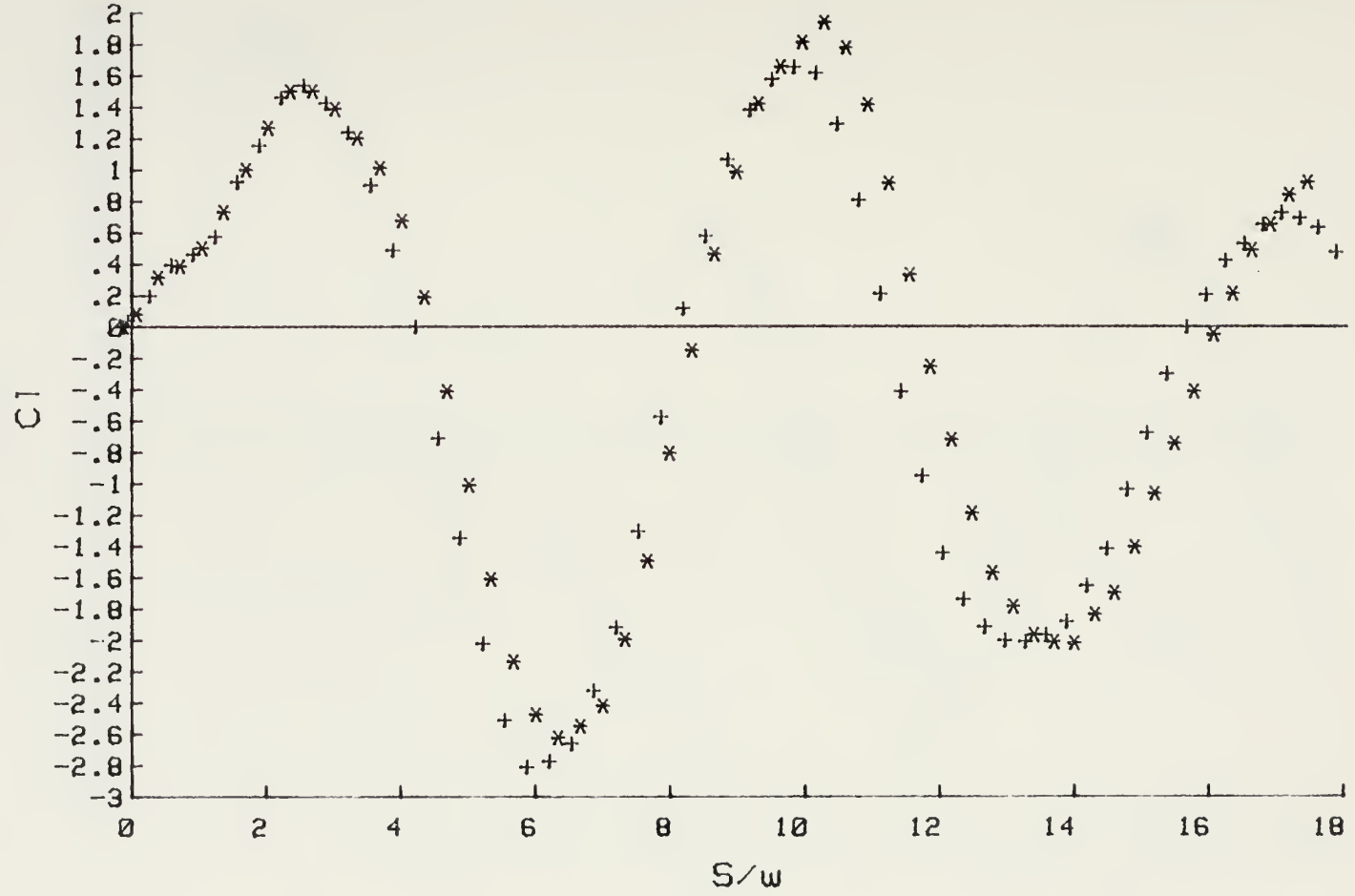

Figure 23. Cl vs. S/w for Body A at 5 deg.

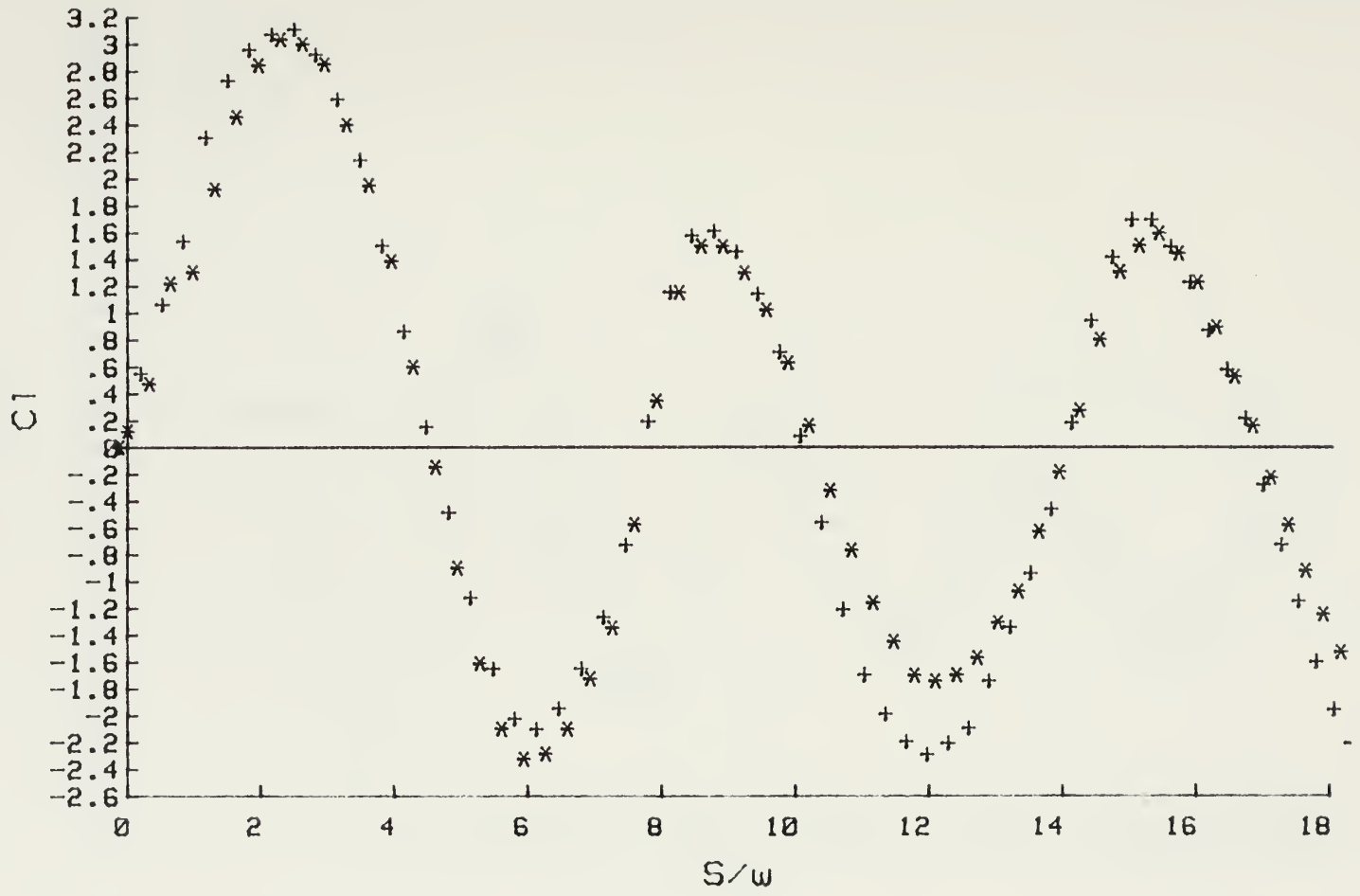

Figure 24. Cl vs. S/w for Body A at 20deg.

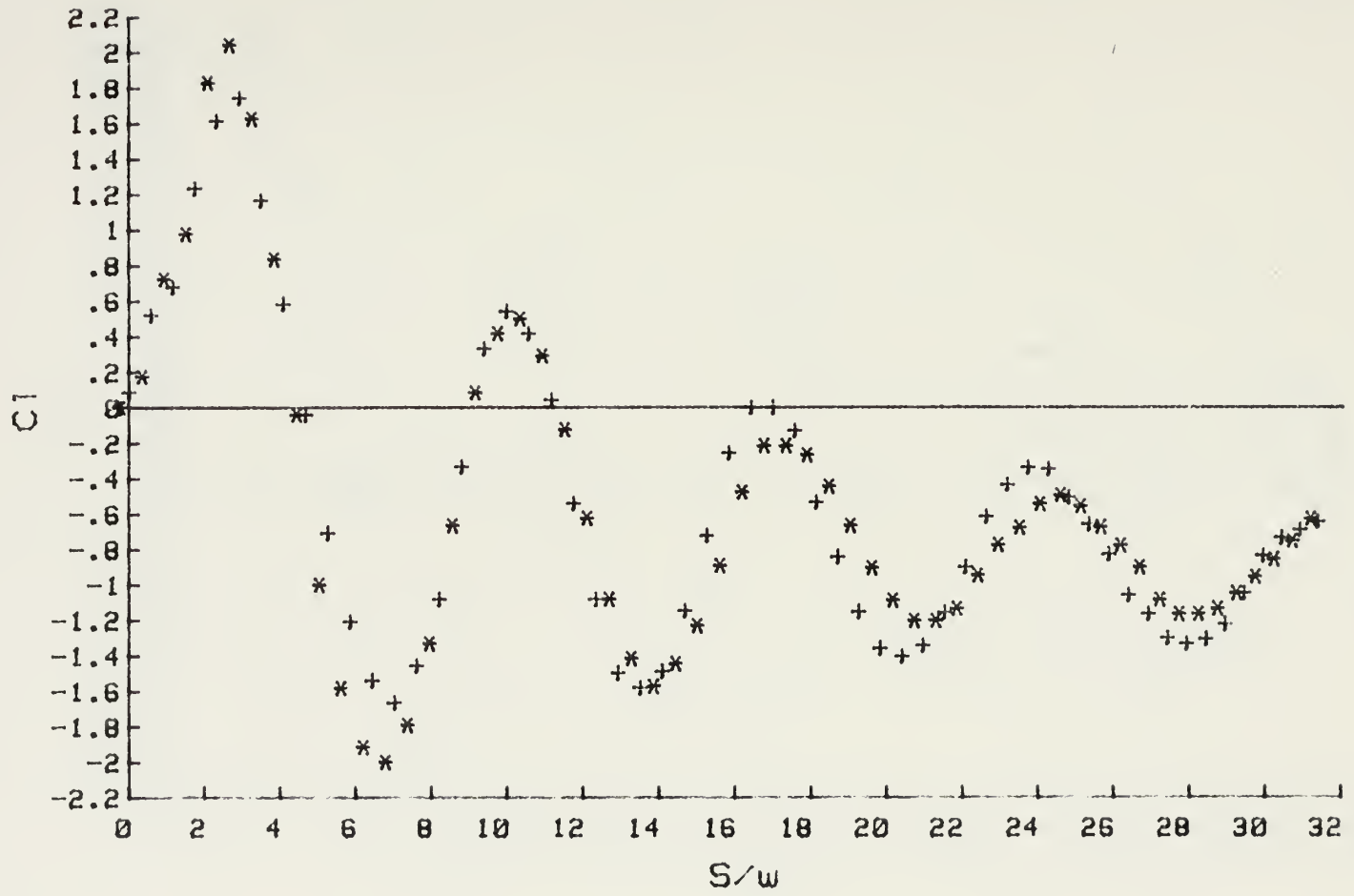

Figure 25. Cl vs. S/w for Body B at 10deg.

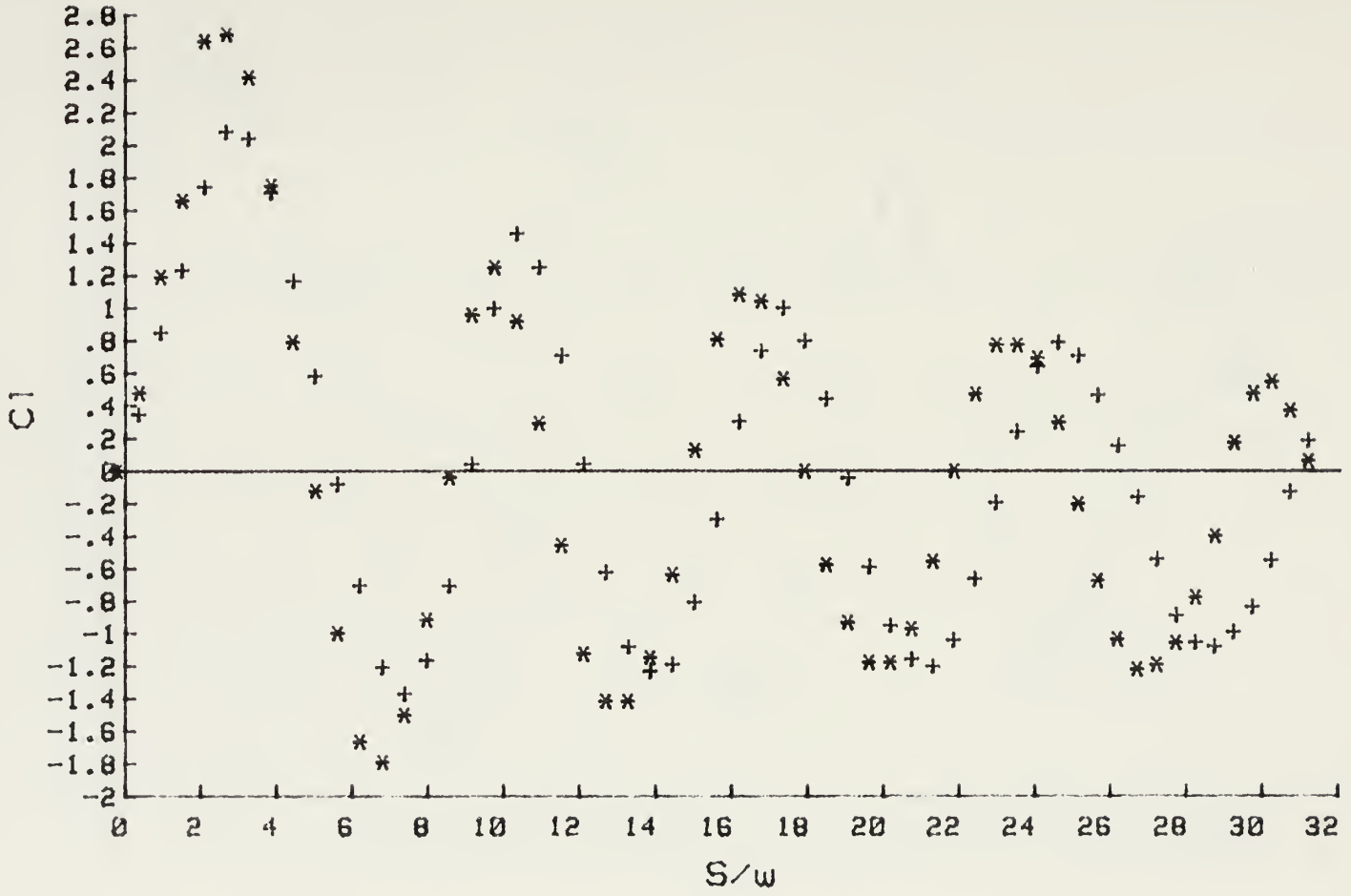

Figure 26. Cl vs. S/w for Body B at 20deg.

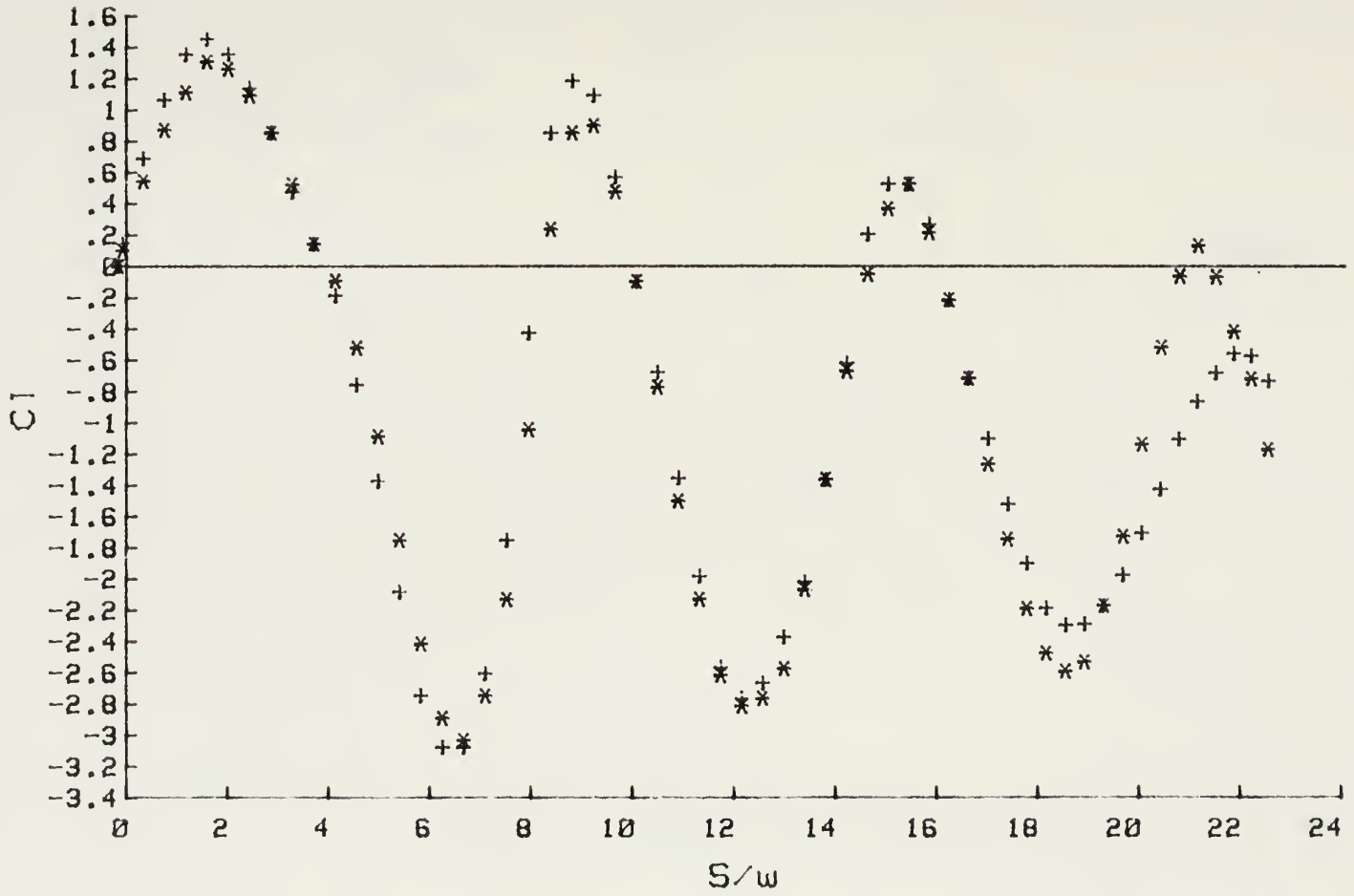

Figure 27. Cl vs. S/w for Body C at 20deg.

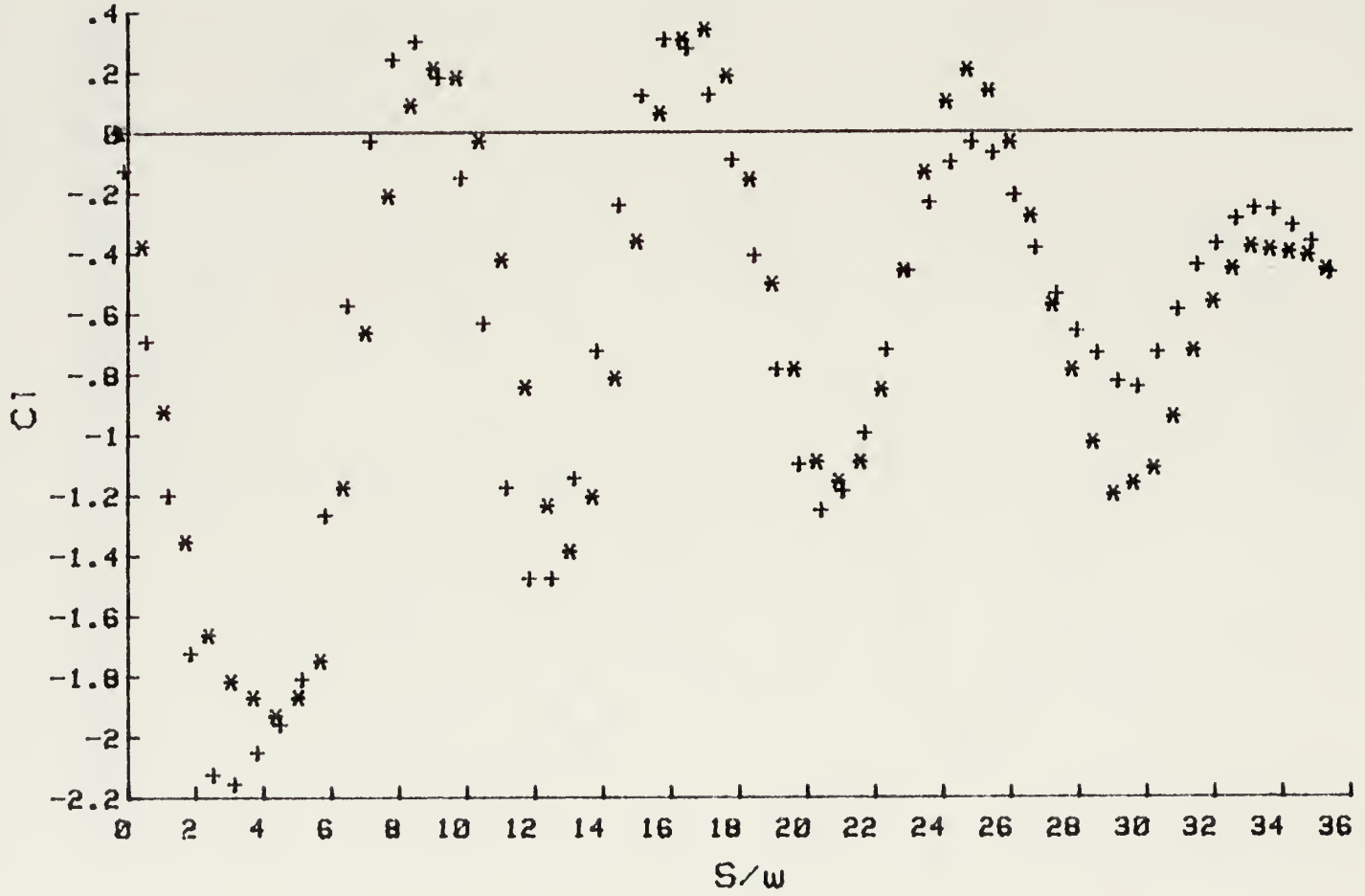

Figure 28. Cl vs. S/w for Body D at 20deg.

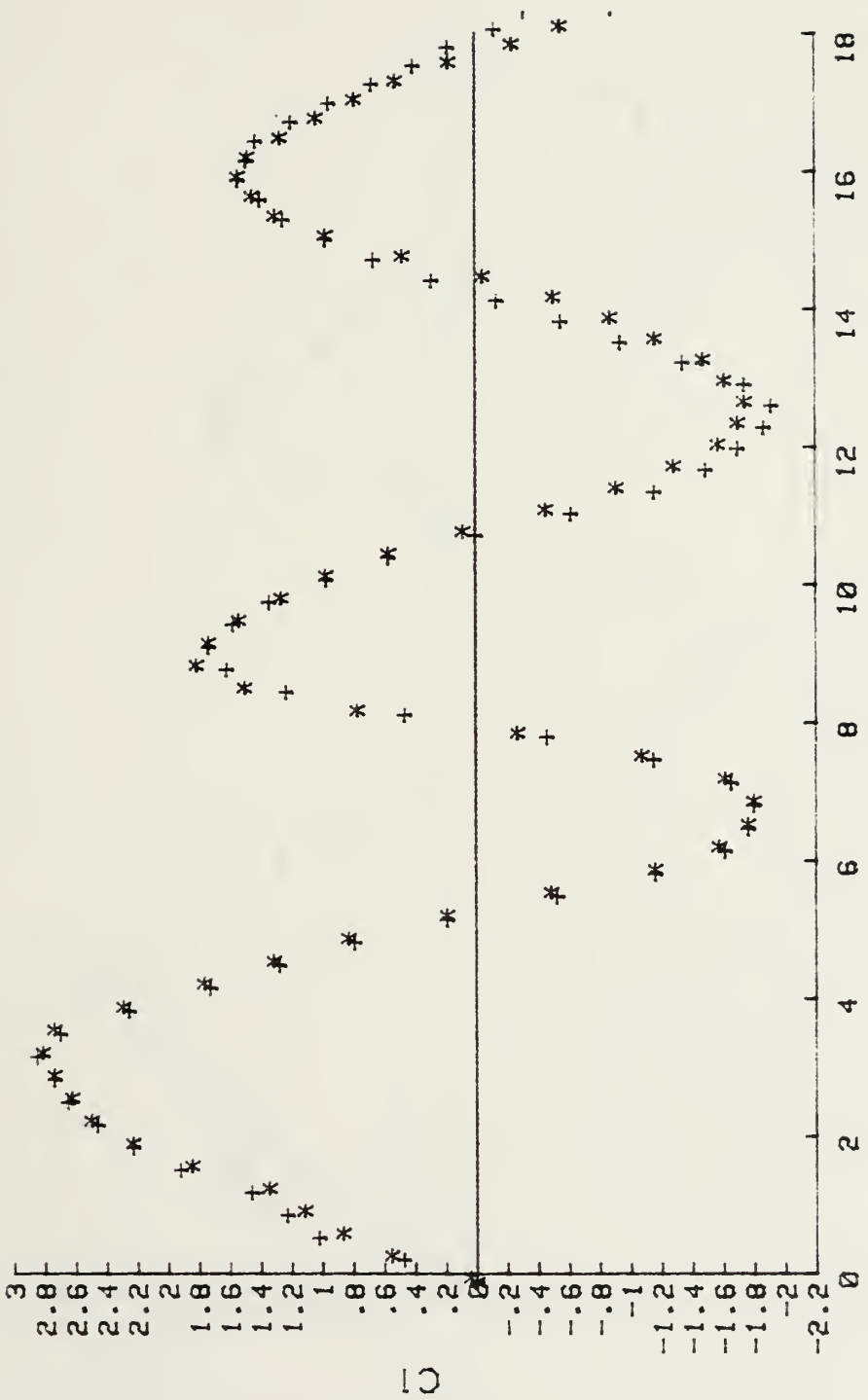

Figure 29. Cl vs. S/w for Body A at 30deg.

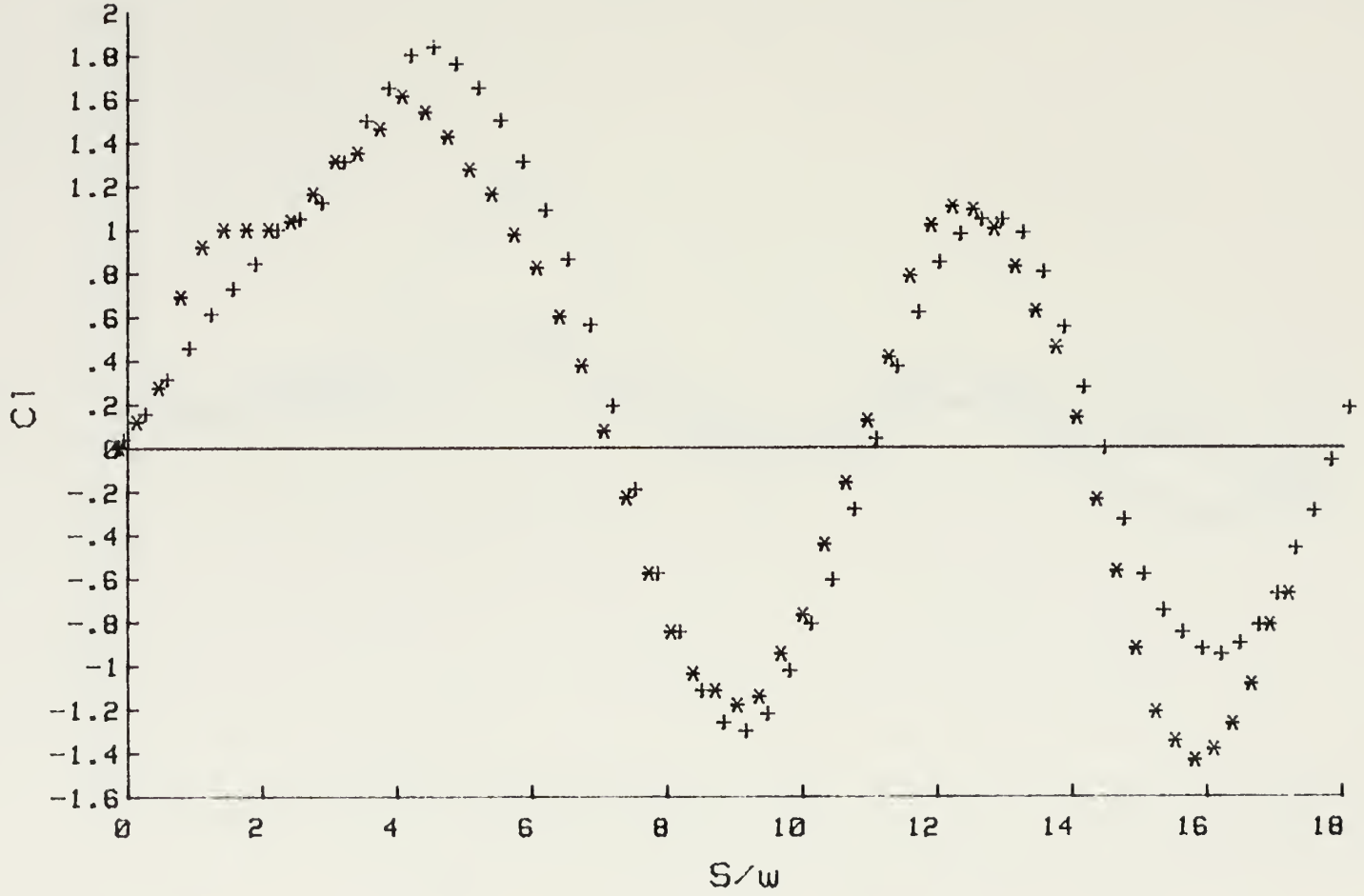

Figure 30. Cl vs. S/w for Body A at 40deg.

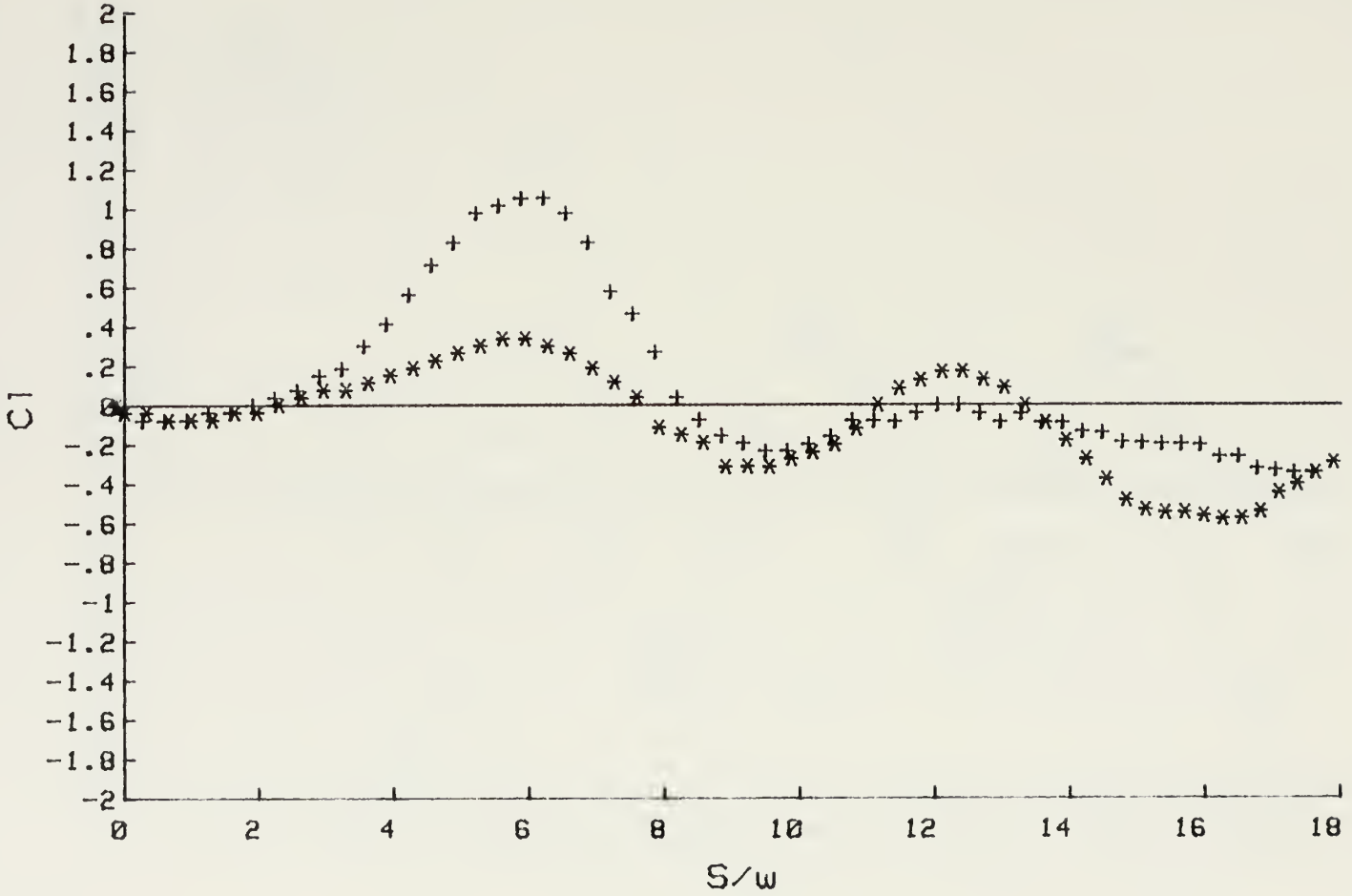

Figure 31. Cl vs. S/w for Body A at 45 deg.

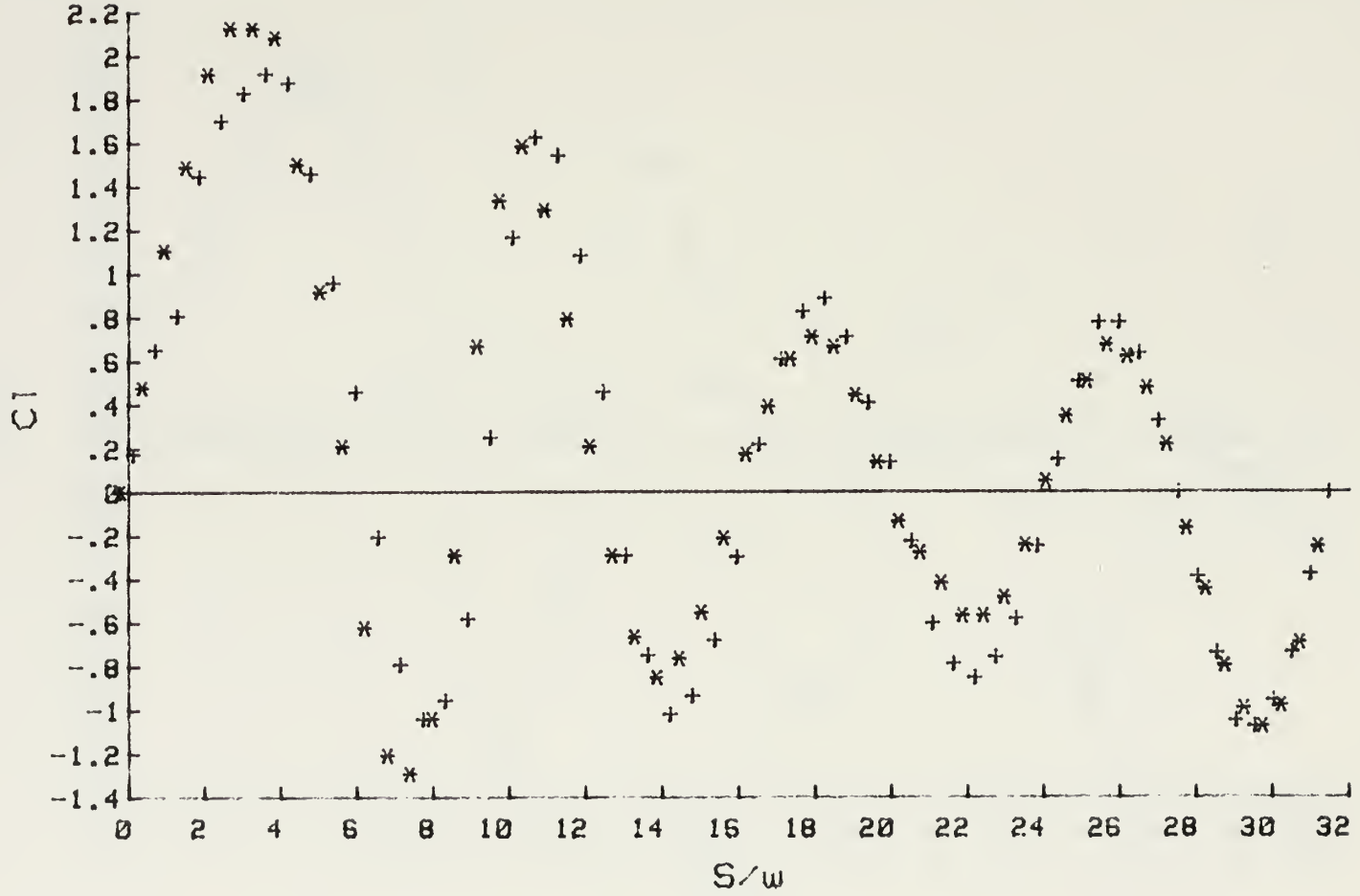

Figure 32. Cl vs. S/w for Body B at 30 deg.

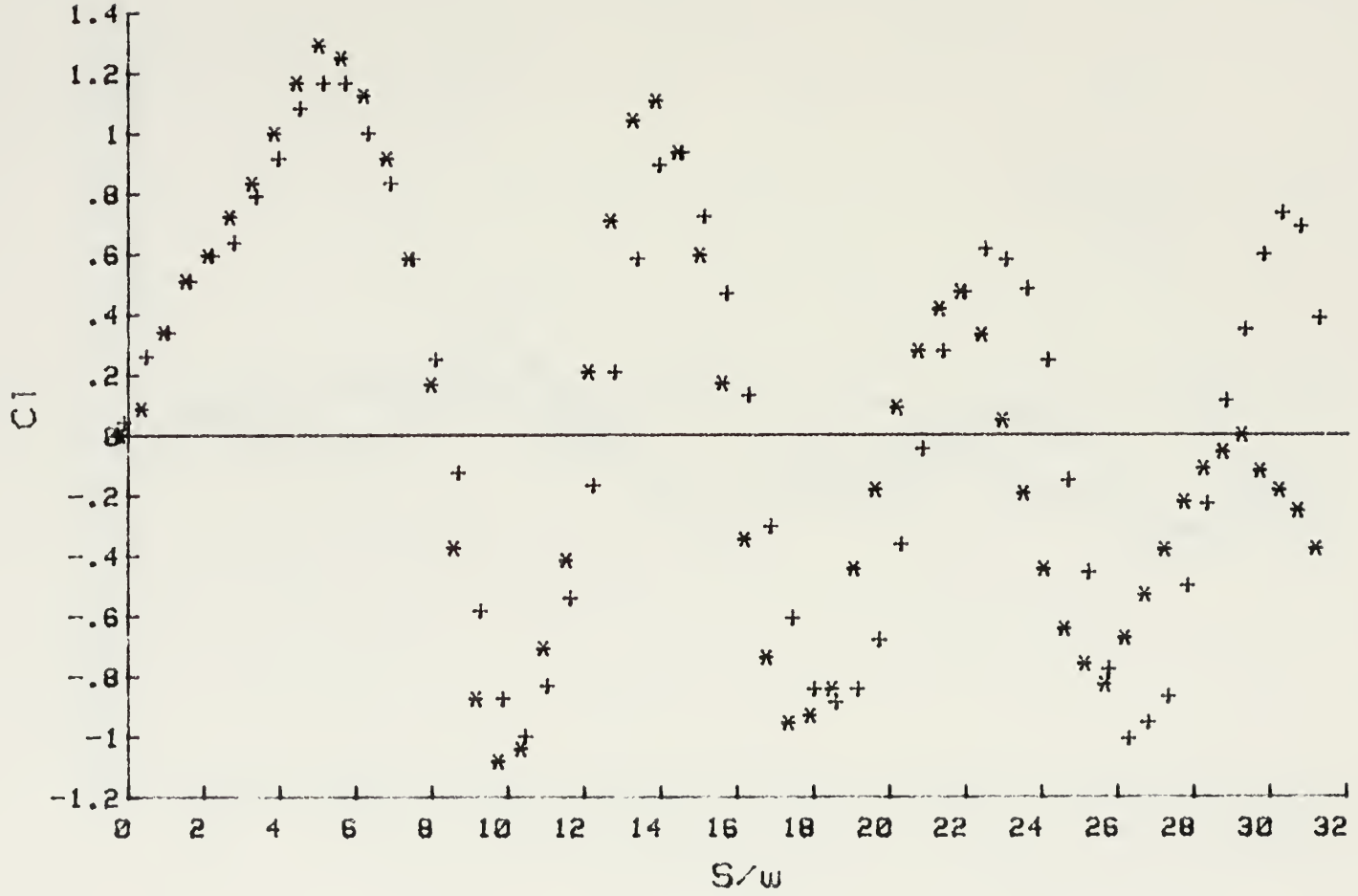

Figure 33. Cl vs. S/w for Body B at 40deg.

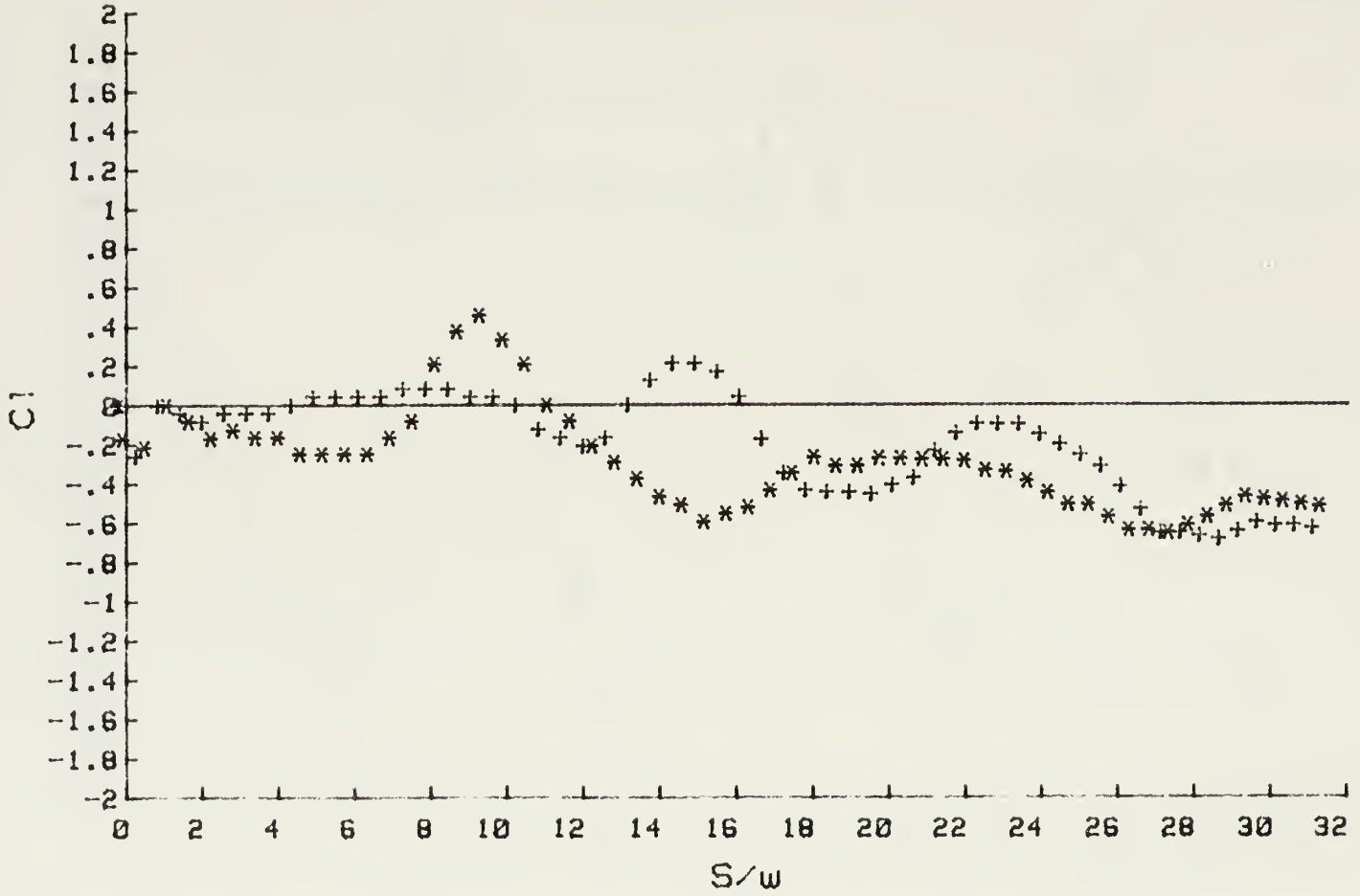

Figure 34. Cl vs. S/w for Body B at 45 deg.

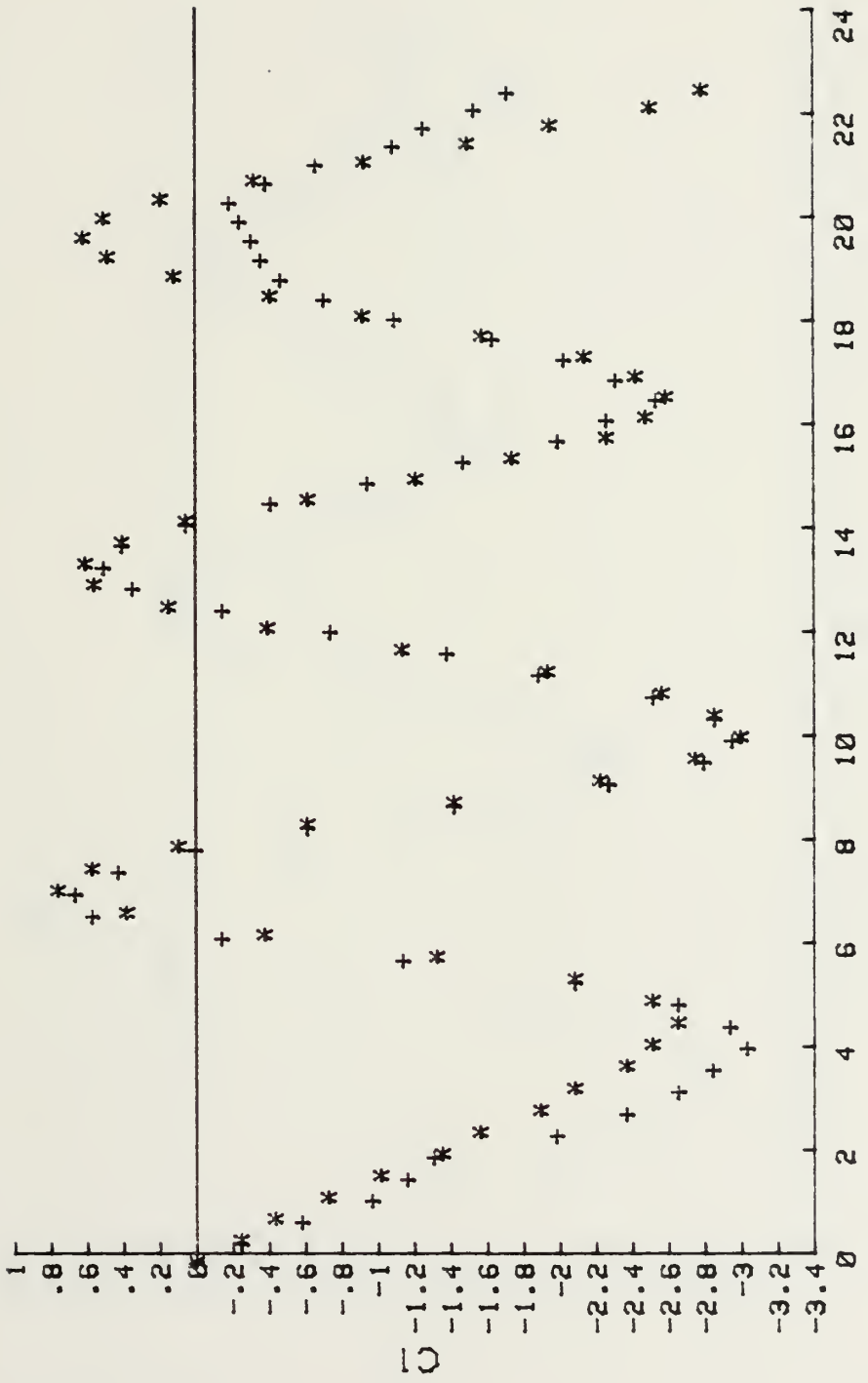

Figure 35. Cl vs. S/w for Body C at 40 deg.

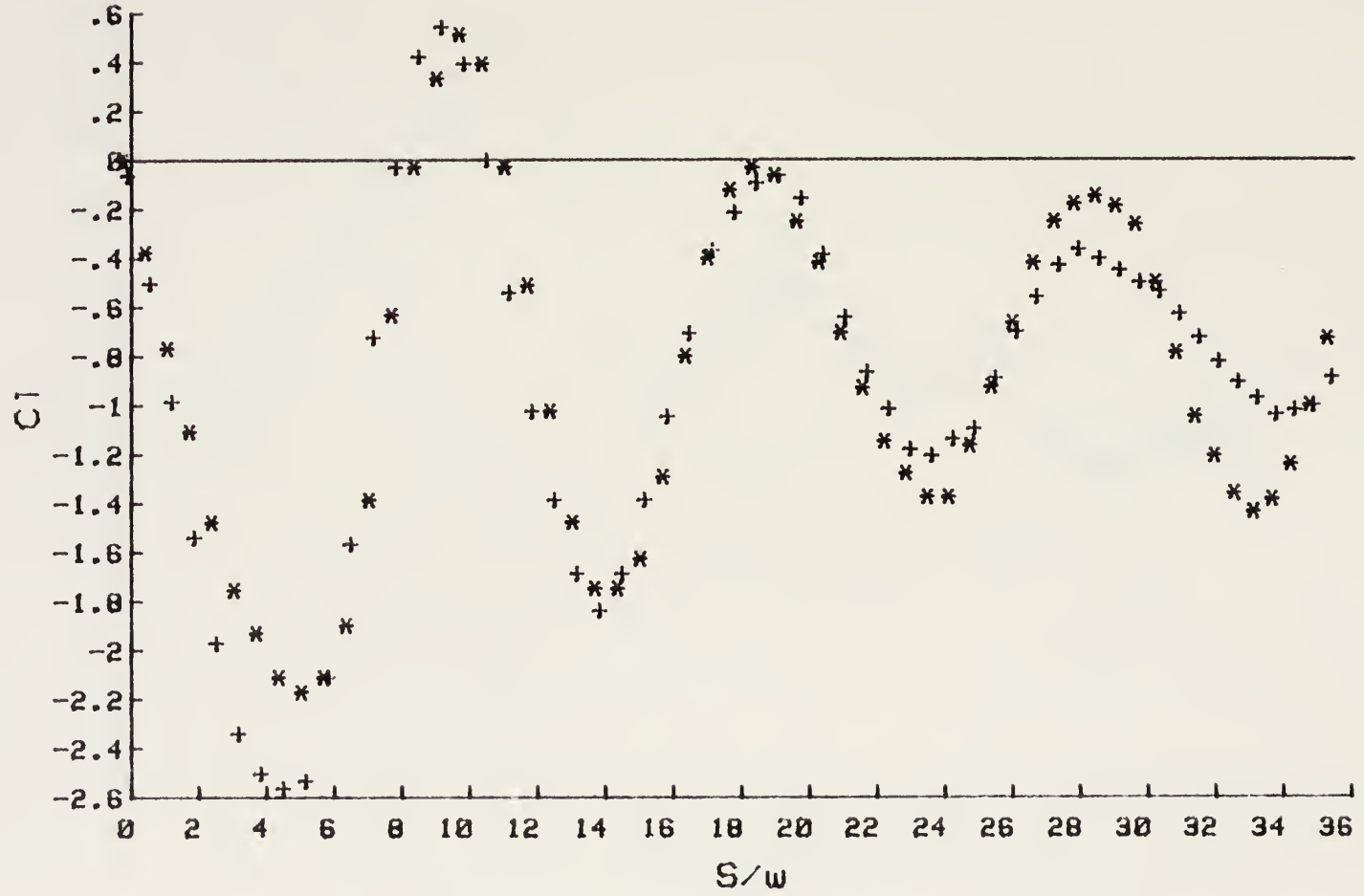

Figure 36. Cl vs. S/w for Body D at 40deg.

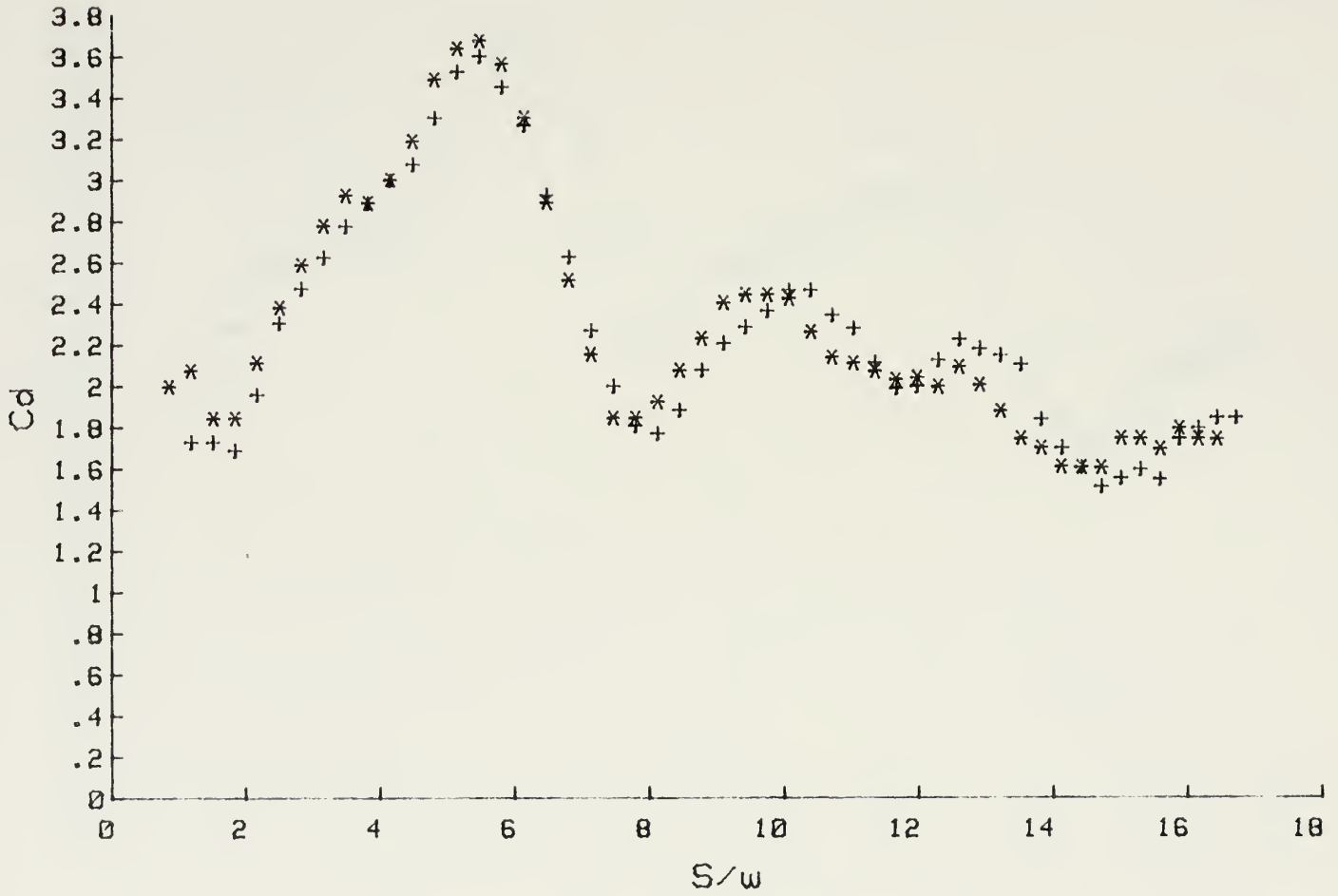

Figure 37. Cd vs. S/w for Body A at 10deg.

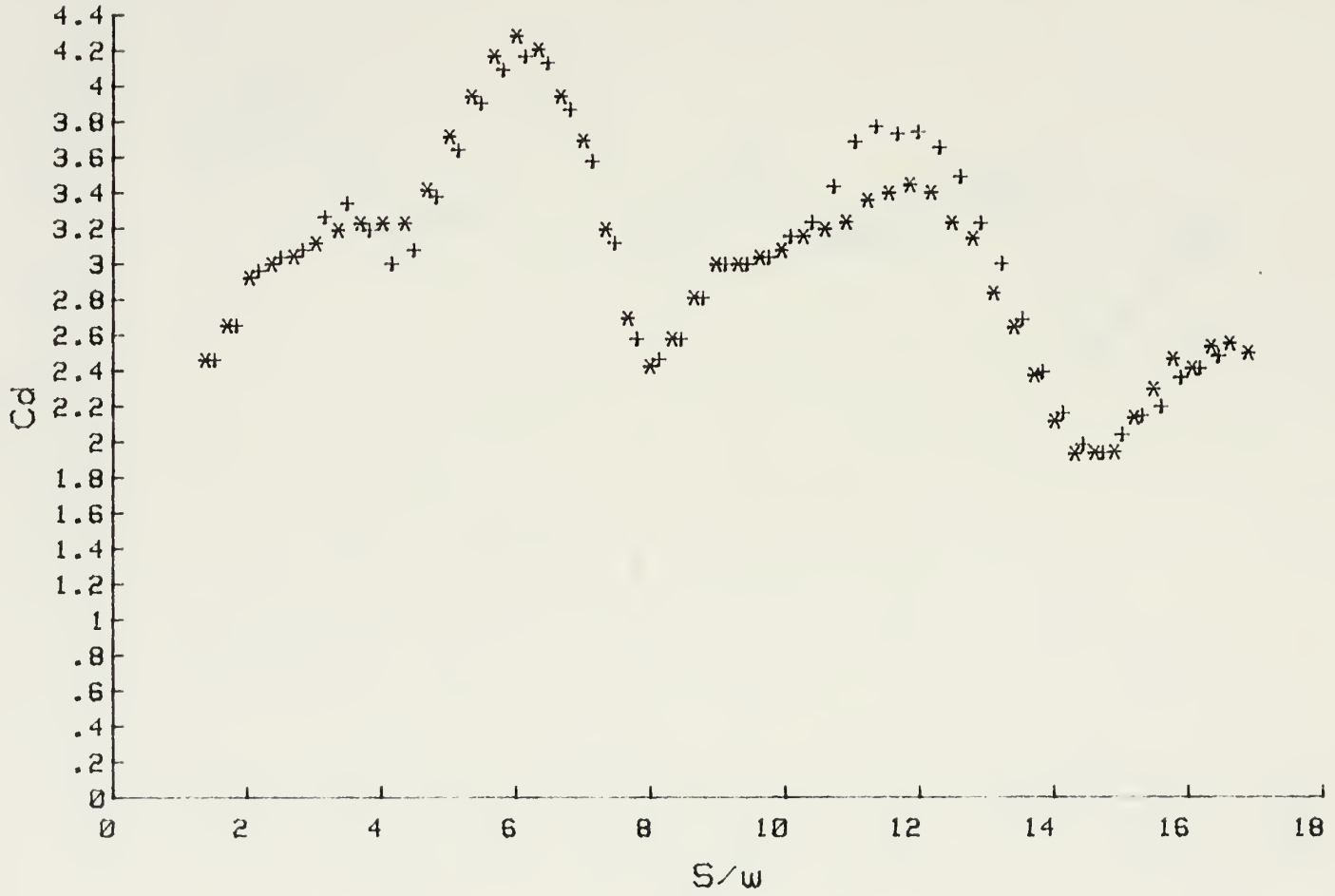

Figure 38. Cd vs. S/w for Body A at 20deg.

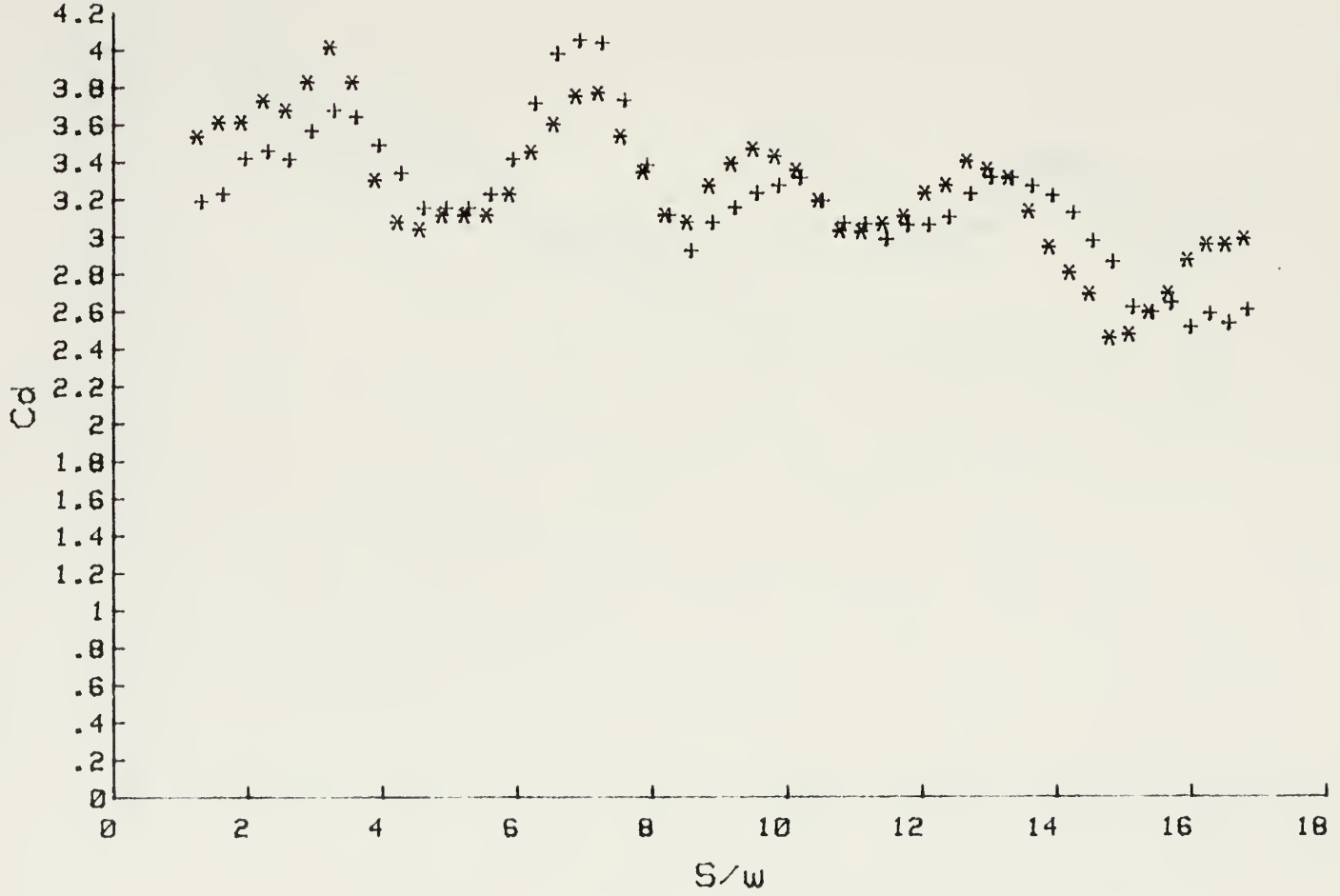

Figure 39. Cd vs. S/w for Body A at 30deg.

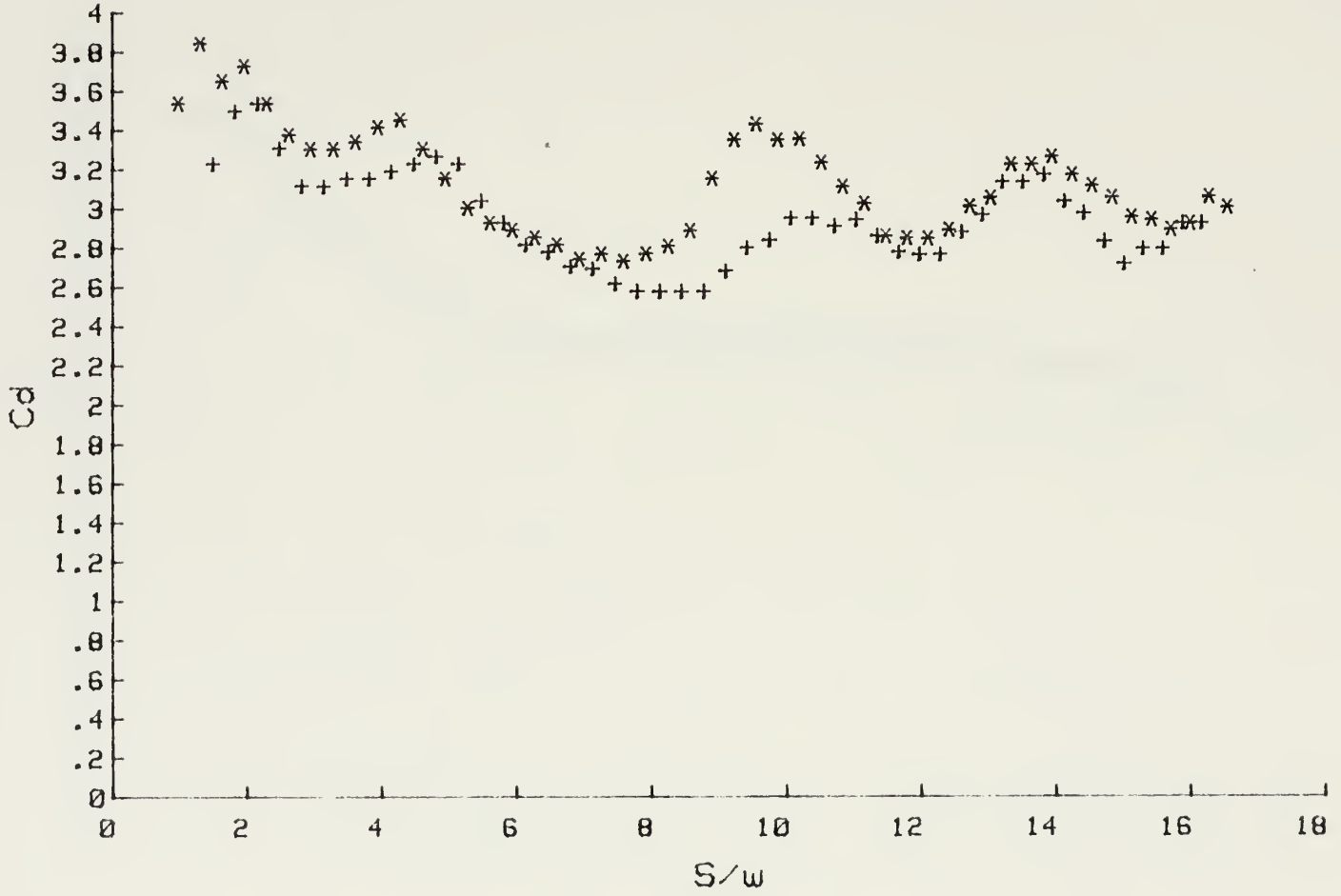

Figure 40. Cd vs. S/w for Body A at 40deg.

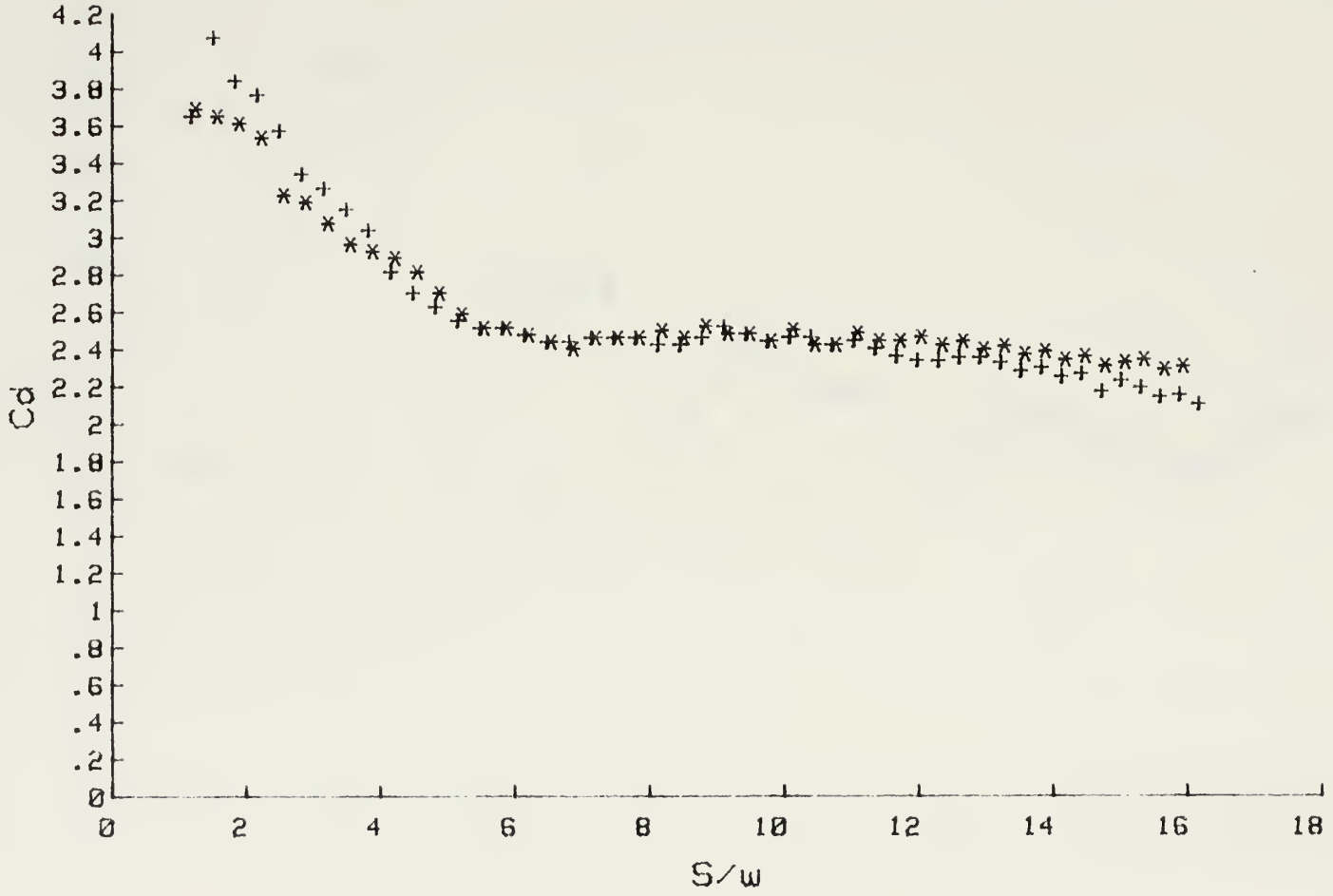

Figure 41. Cd vs. S/w for Body A at 45 deg.

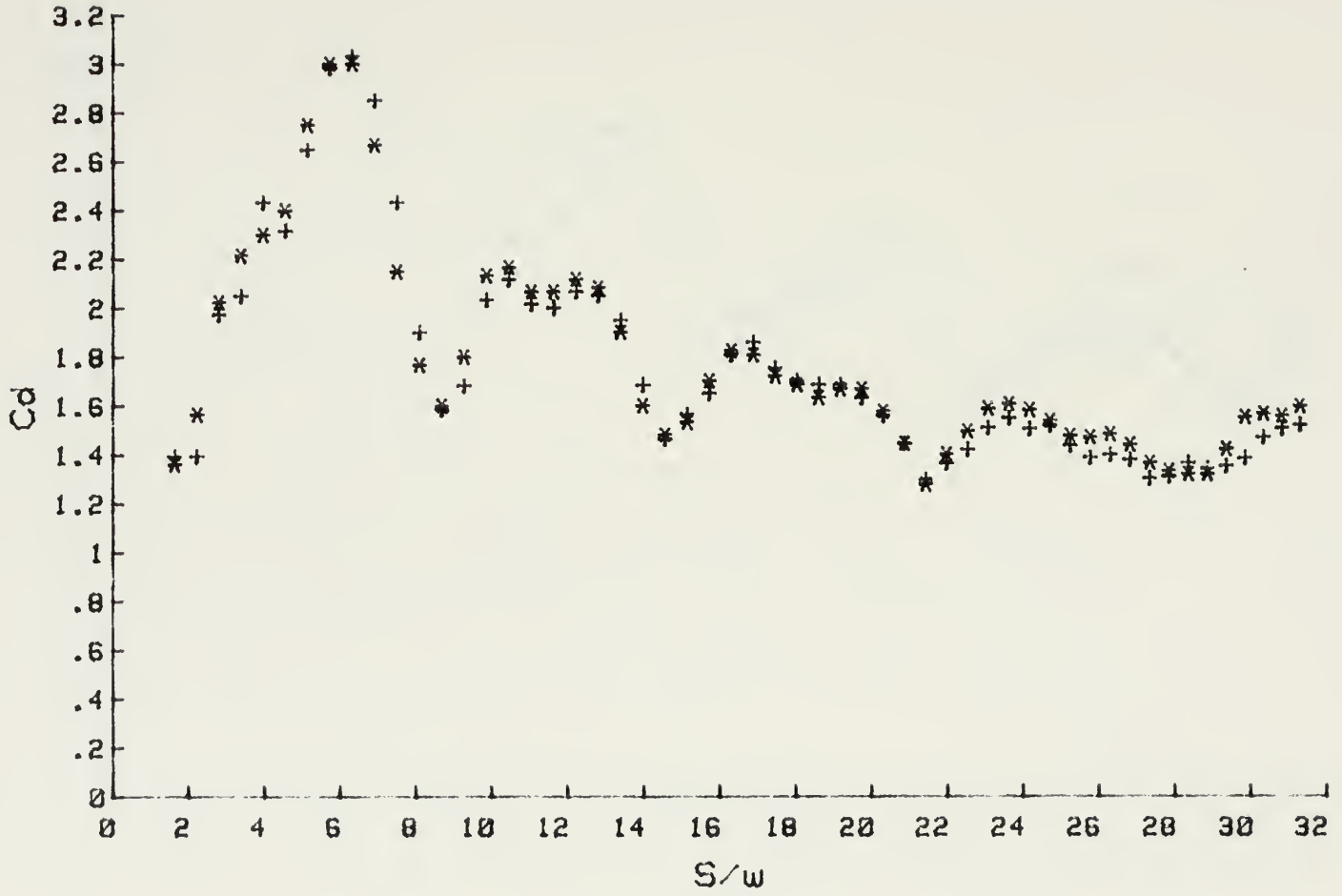

Figure 42. Cd vs. S/w for Body B at 10deg.

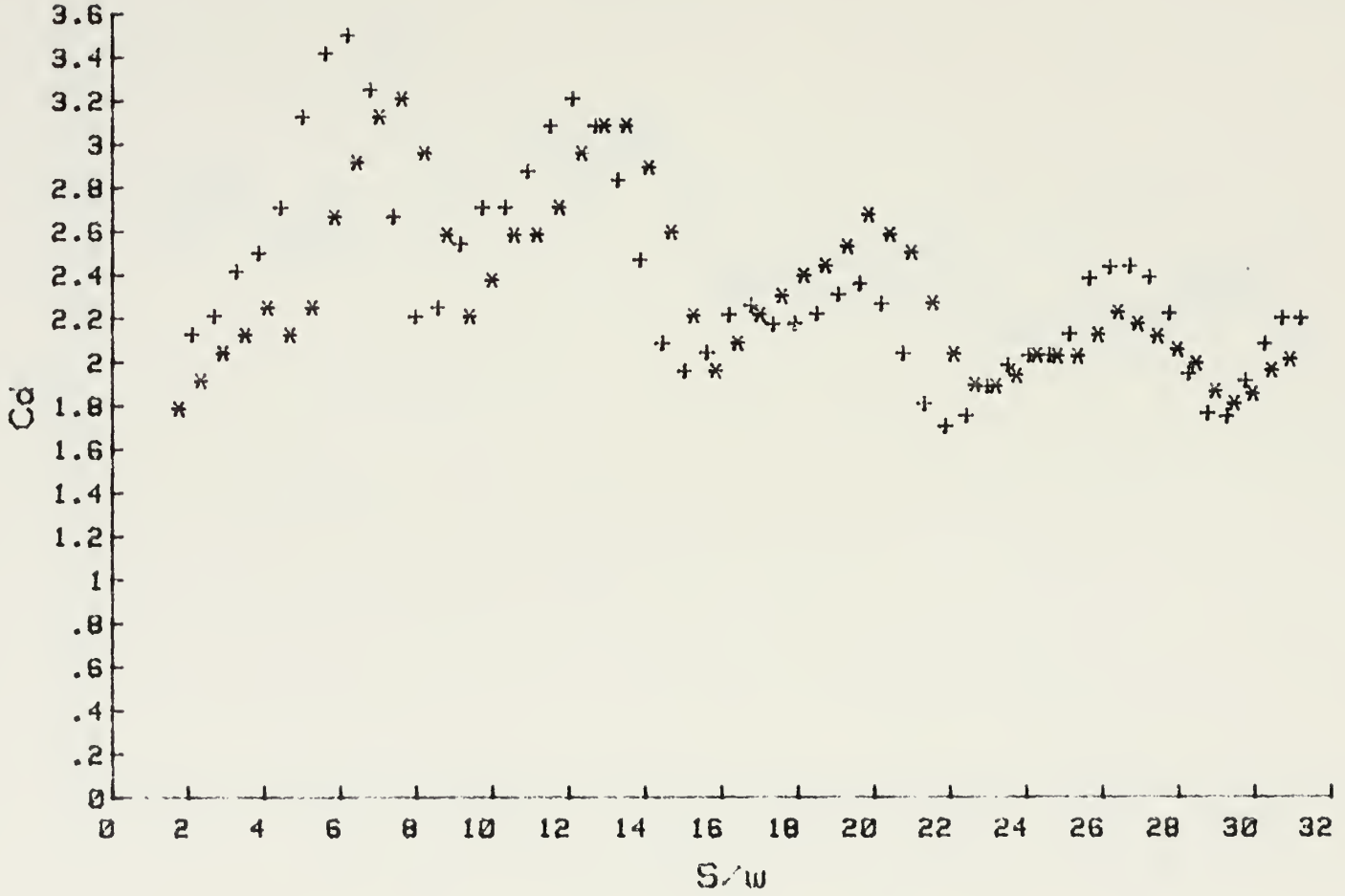

Figure 43. Cd vs. S/w for Body B at 20 deg.

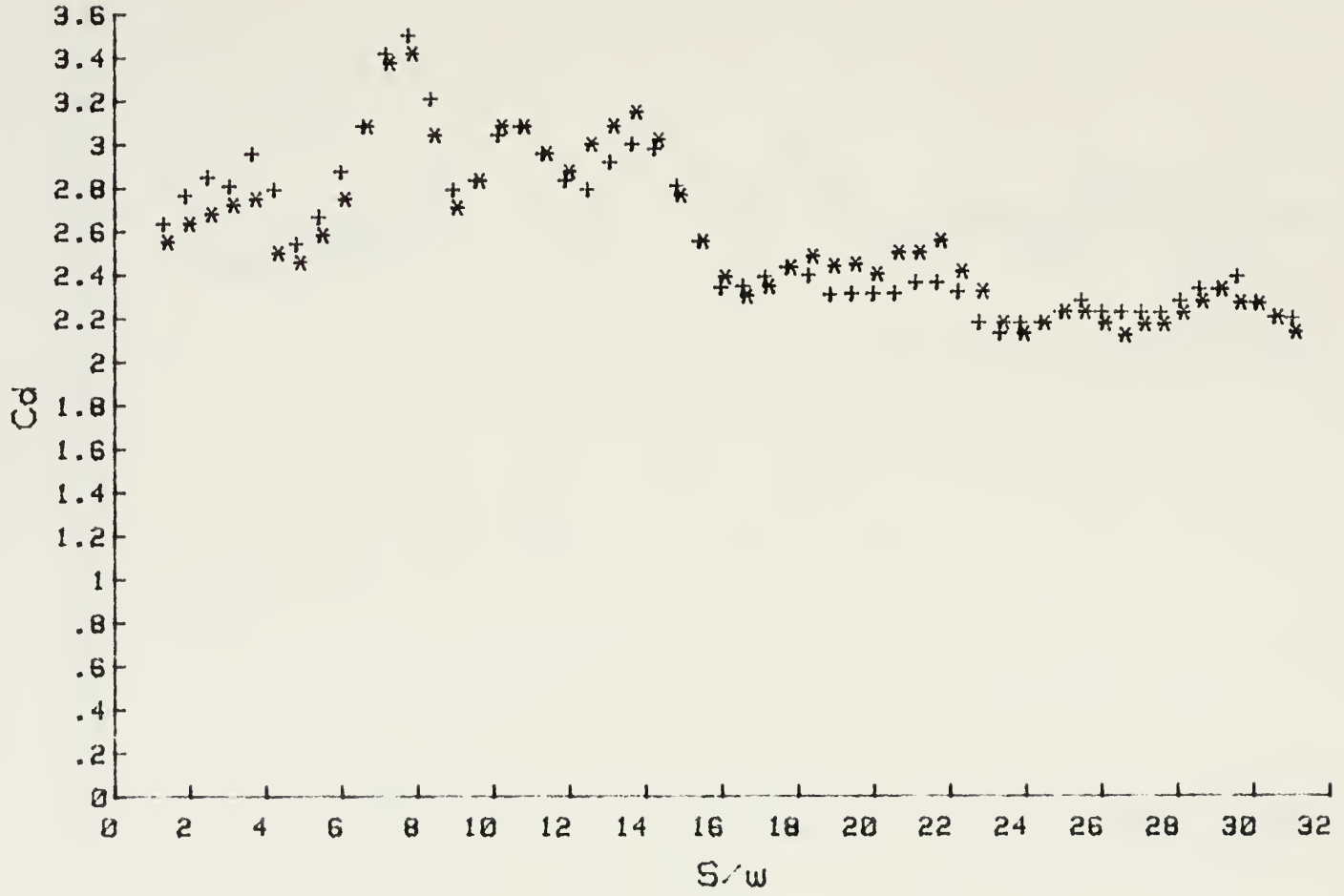

Figure 44. Cd vs. S/w for Body B at 30deg.

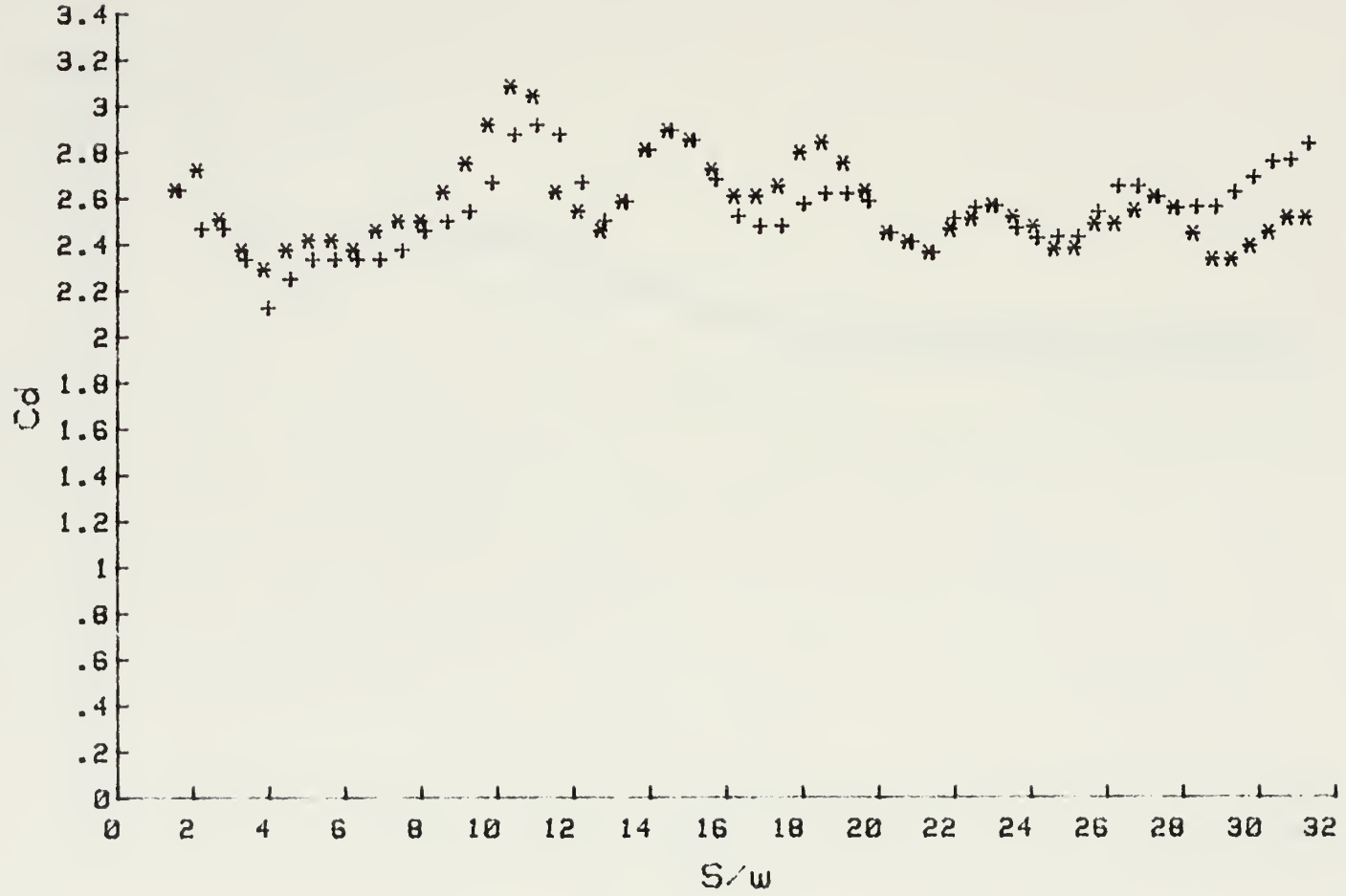

Figure 45. Cd vs. S/w for Body B at 40deg.

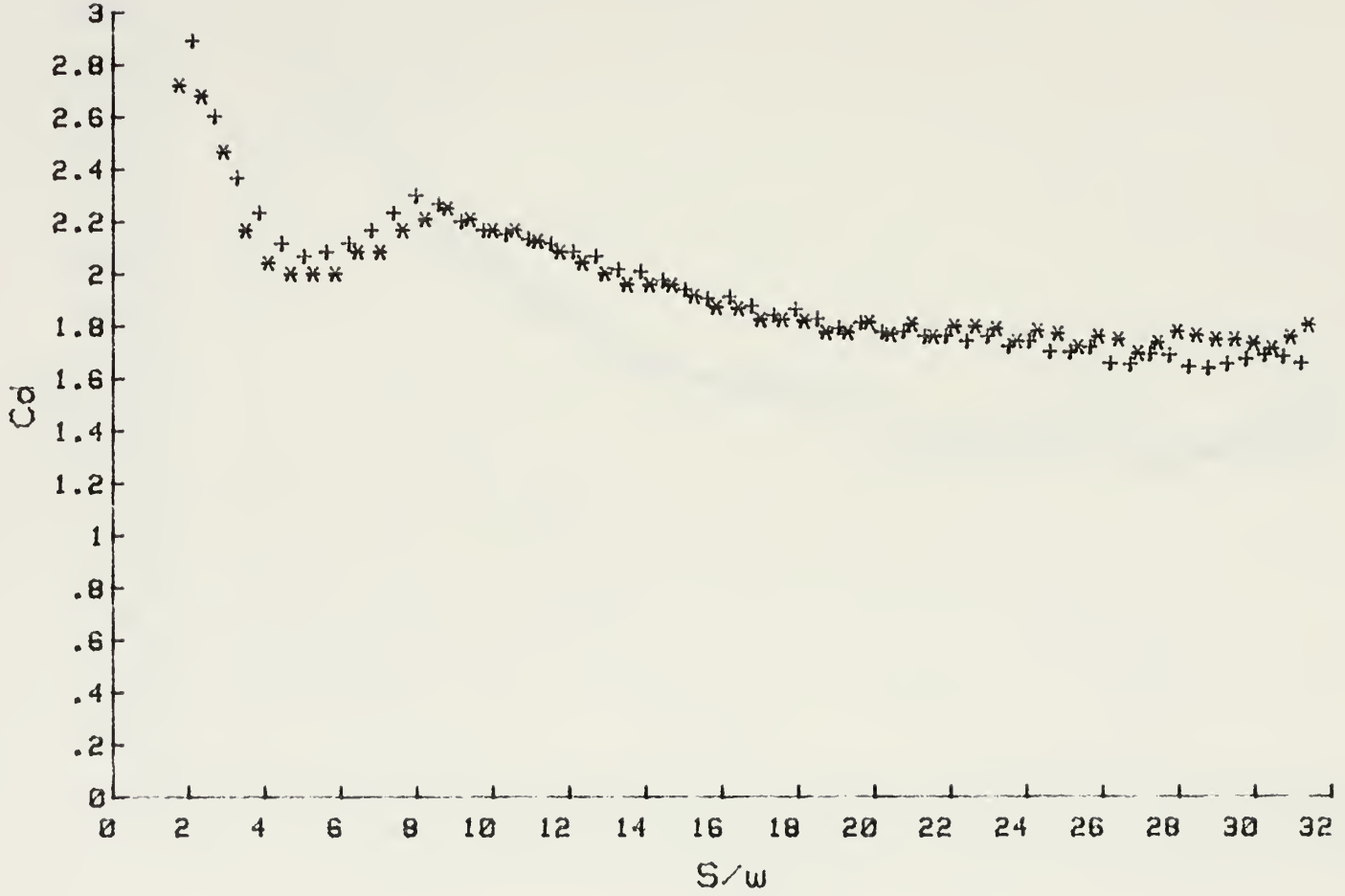

Figure 46. Cd vs. S/w for Body B at 45 deg.

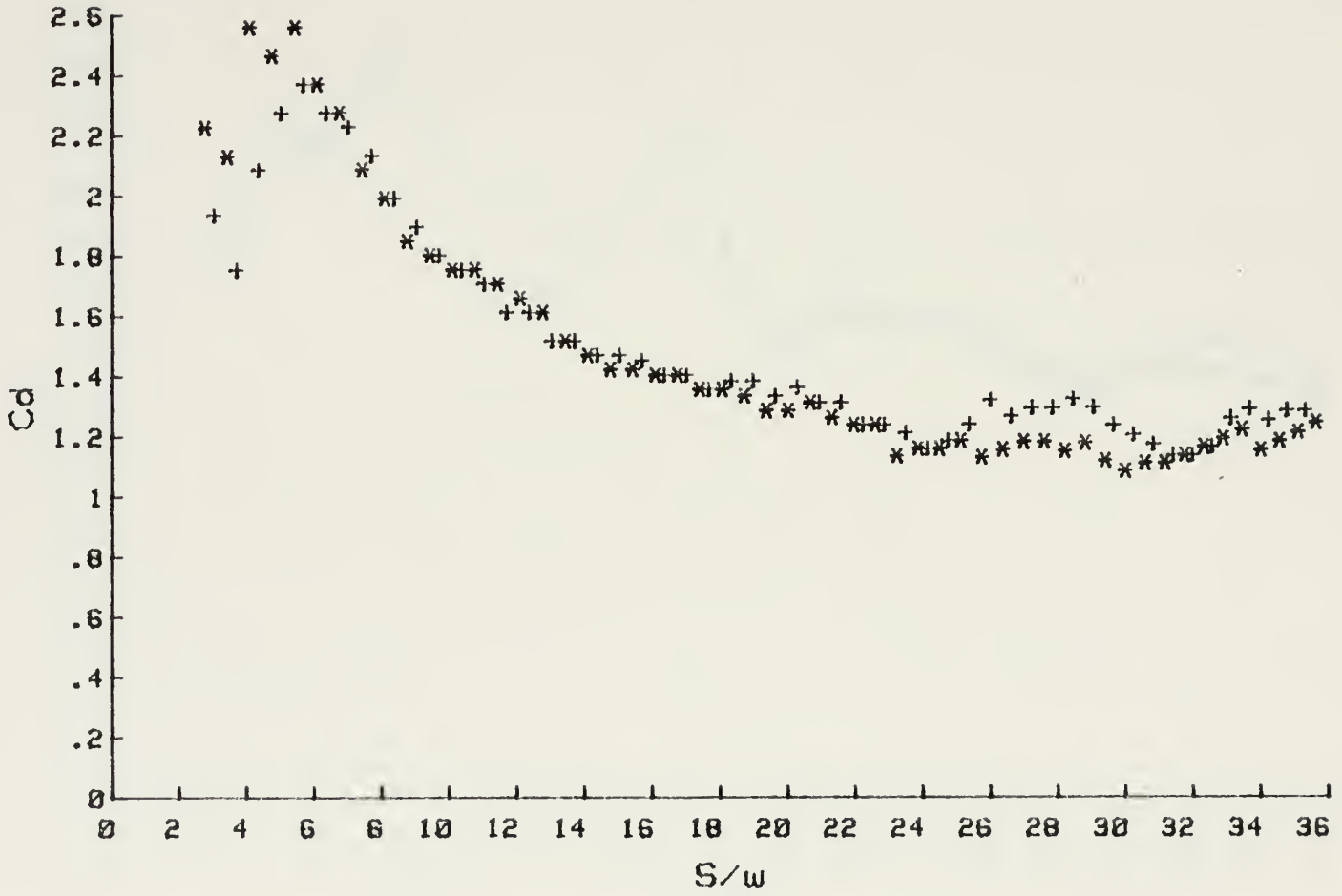

Figure 47. Cd vs. S/w for Body D at 10deg.

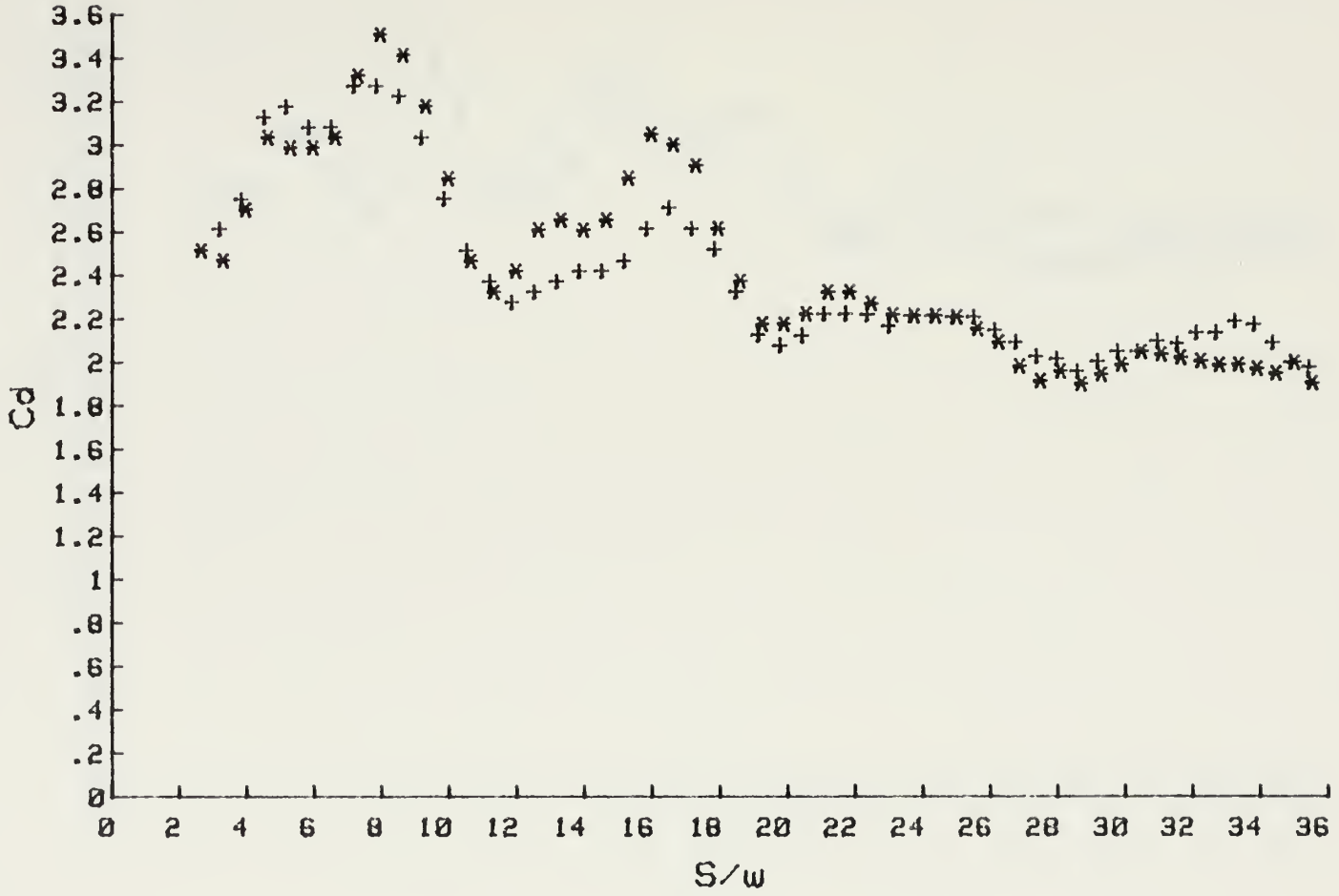

Figure 48. Cd vs. S/w for Body D at 20deg.

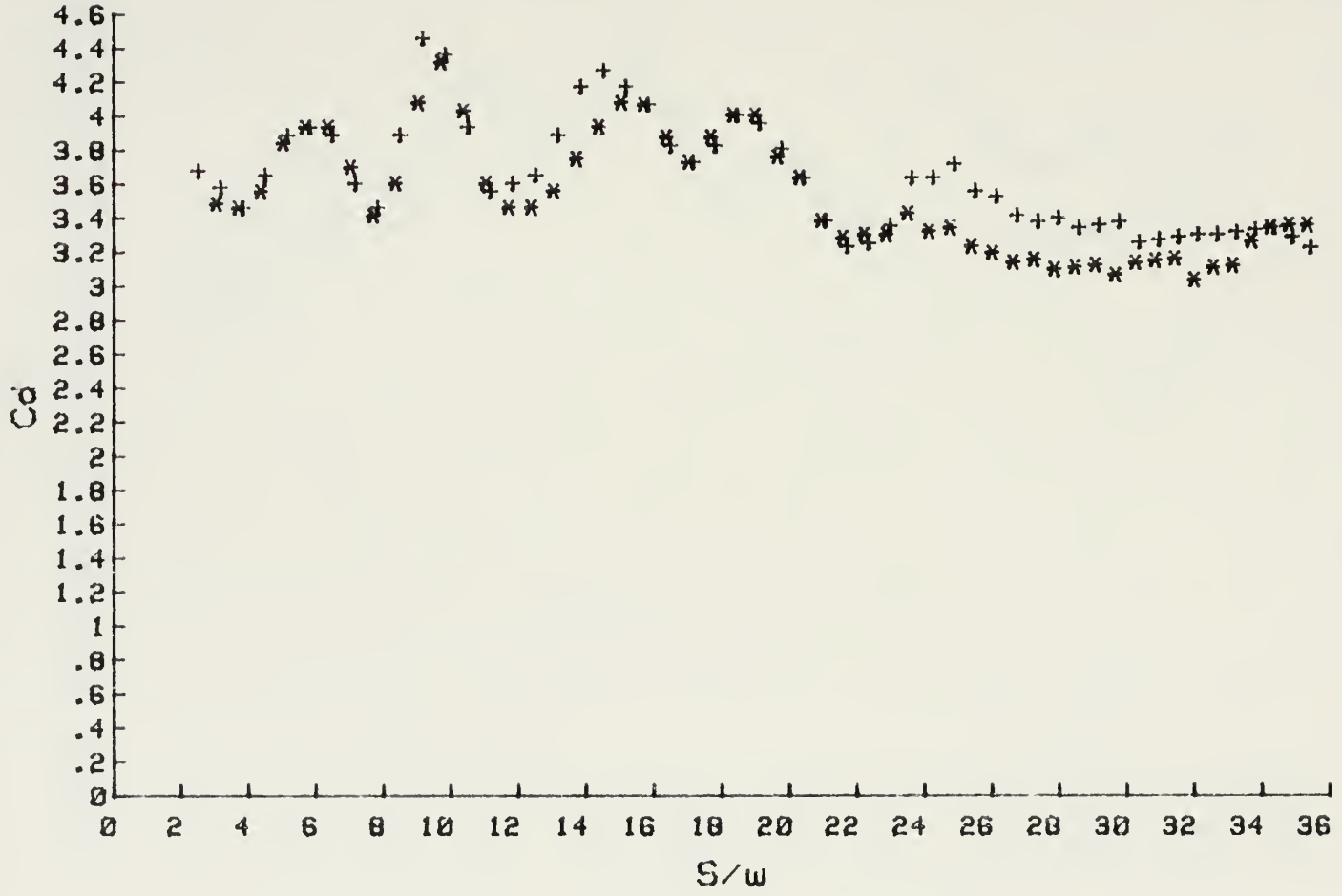

Figure 49. Cd vs. S/w for Body D at 40deg.

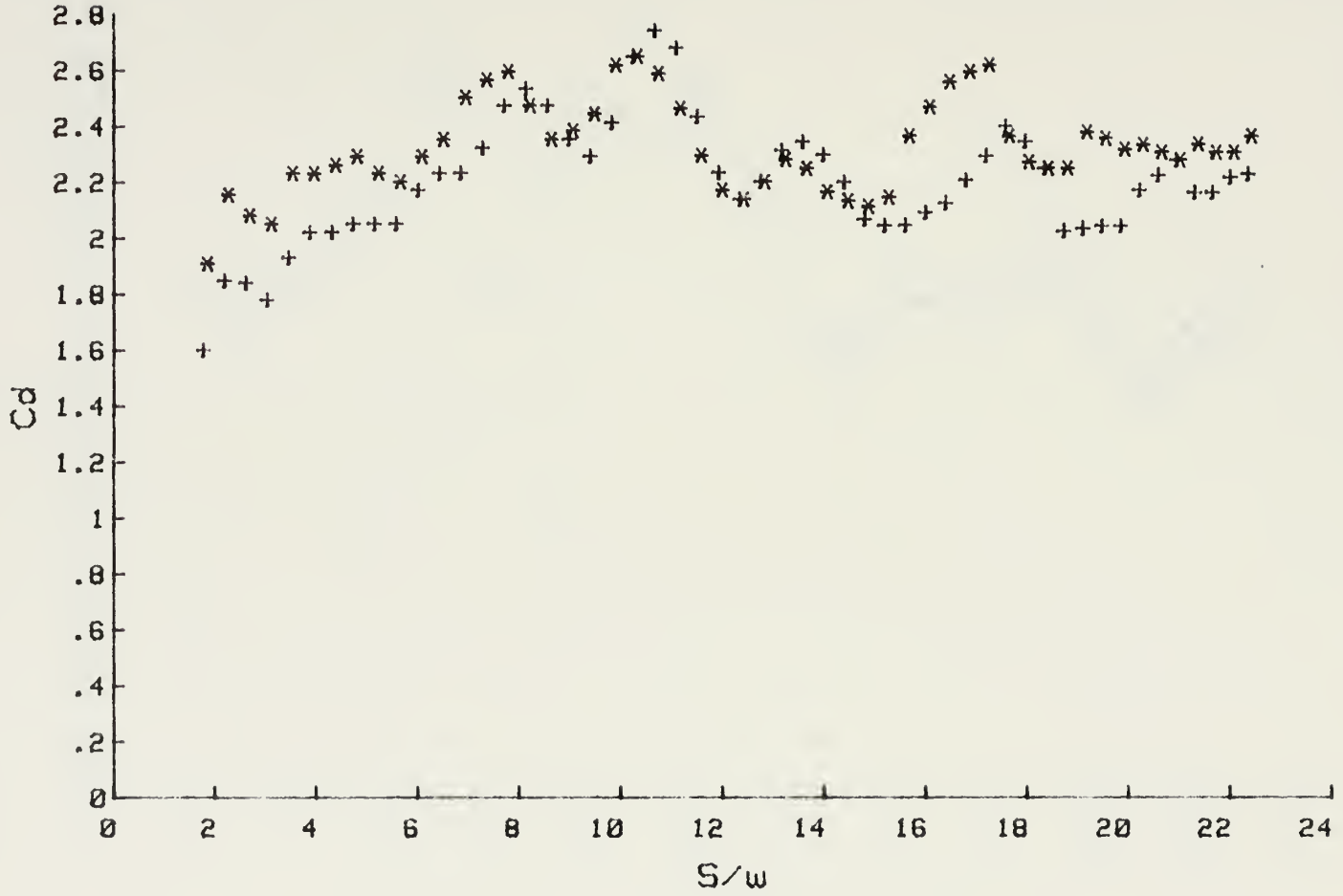

Figure 50. Cd vs. S/w for Body C at 10deg.

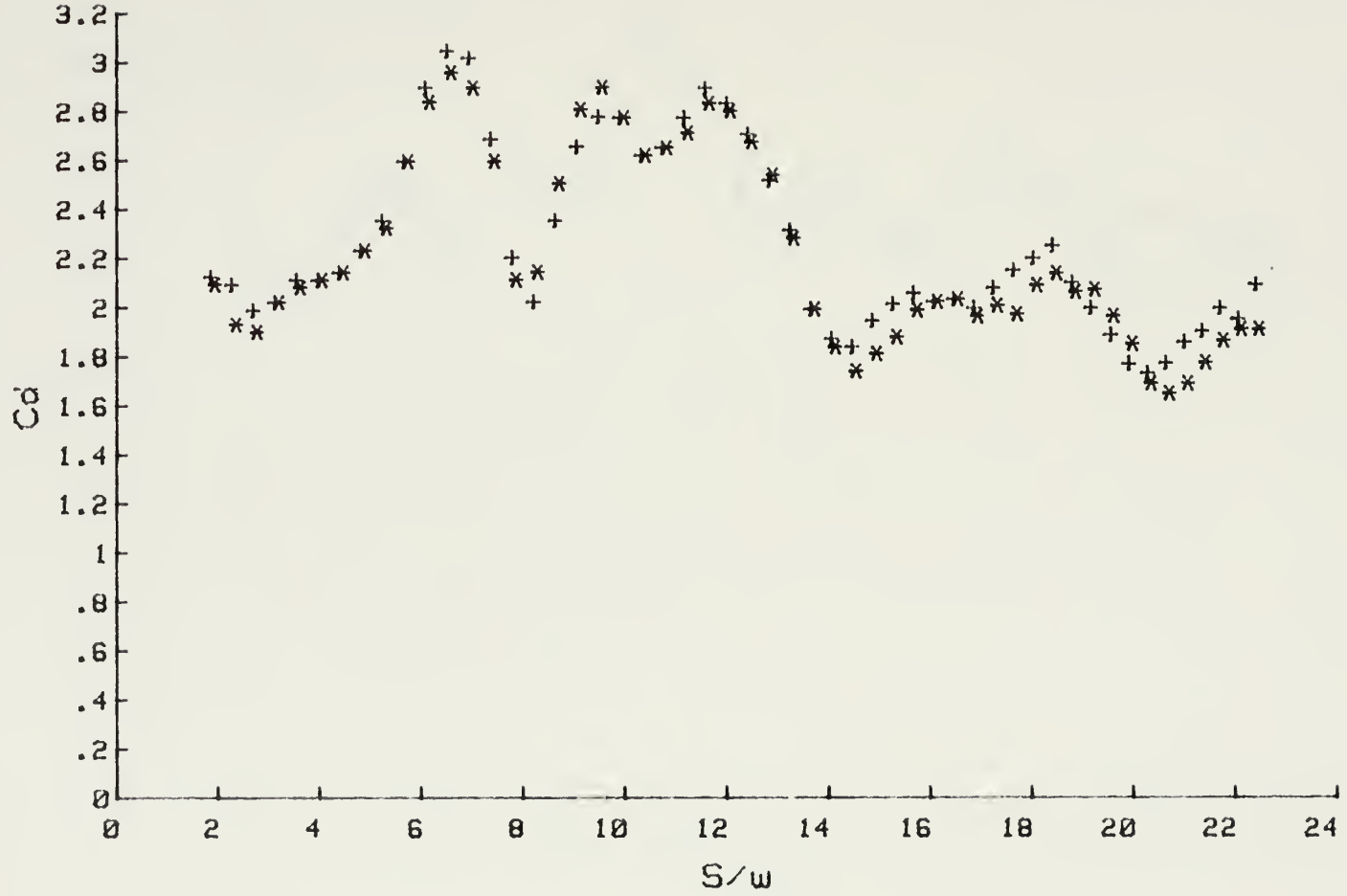

Figure 51. Cd vs. S/w for Body C at 20deg.

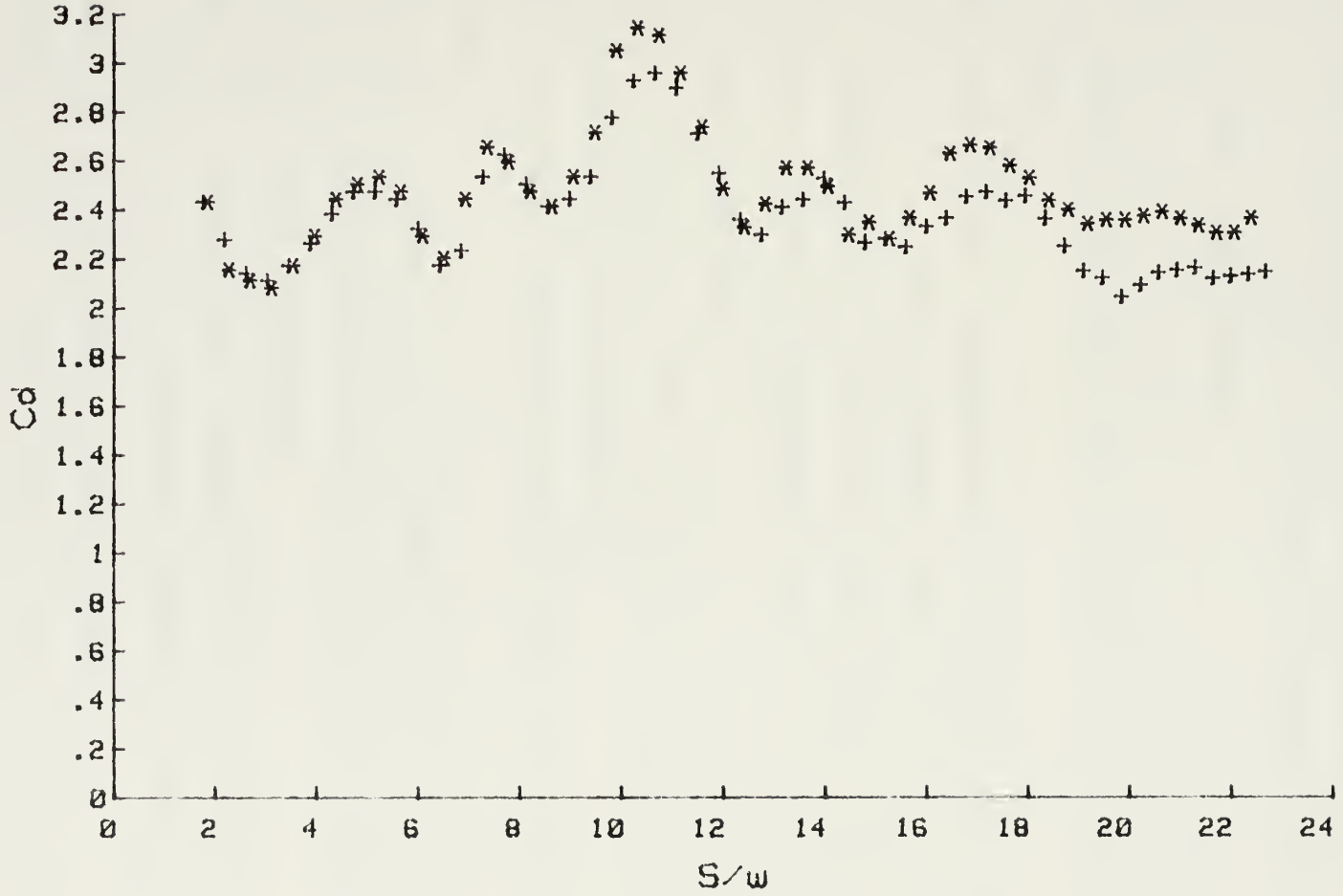

Figure 52. Cd vs. S/w for Body C at 40deg.

V. CONCLUSIONS

The experimental investigation of the impulsively-started flow about several rectangular cylinders resulted in the following conclusions:

1. Shedding of the first two or three vortices from the test bodies produced significant drag overshoot of as much as fifty percent.
2. Drag coefficients asymptotically approached values in the range of 2.4 to 2.8 for S/w greater than 30 to 50 for Bodies C and E, respectively; 1.8 to 2 for S/w greater than 16 and 22 for Bodies A and B, respectively; and 1.5 to 1.6 for S/w greater than 30 for Body D.
3. For the rectangular bodies studied, the asymptotic values of Cd decreased with increasing d/w.
4. Peak Cd values increased with the angle of attack for all test bodies.
5. Mean Cd values approached a minimum between angles of attack of 10 and 20 degrees, then increased with angles of attack greater than 20 degrees.
6. Mean lift coefficients reached minimum values between 10 and 20 degrees angle of attack and approached positive values for angles of attack greater than 30 degrees.
7. Strouhal numbers ranged from 0.125 to 0.154 for Bodies A and B, from 0.143 to 0.166 for Body C and were nearly constant at about 0.125 for Body D.

8. For the rectangles studied, St decreased with increasing d/w.

9. For the square prism (Bodies A and B), St peaked to 0.151 to 0.154 for an angle of attack of 20 degrees and then decreased at angles of attack greater than 20 degrees.

10. Asymmetry of a body relative to the direction of the impulsive flow fixes the position of initiation of the first vortex and the initial direction of the lift force acting on the body.

VI. RECOMMENDATIONS FOR FURTHER RESEARCH

It is recommended that additional research on impulsively-started flow about bluff bodies be conducted in the following area:

1. Impulsive flow tests of the bodies presented herein should be conducted at significantly different, and preferably higher, Reynolds numbers.
2. Attempts should be made to determine the velocities and vortex strength either through flow visualization or through the use of a laser velocimeter.
3. The pressure distribution about the bodies should be measured and evaluated as a function of time from the start of fluid motion.
4. Extensive flow visualization photographs of the tests on these bodies should be conducted with attempts to monitor the flow for S/w values of 100 or more. Accurate correlation of the time sequence of the photographs with the analog traces of the forces should be an important part of this effort.
5. The present results should be extended to larger S/w values (in connection with the recommendation above) in order to verify the asymptotic behavior of the drag coefficients and to calculate Strouhal numbers for larger times.
6. Impulsive flow tests of the bodies presented herein should be conducted at other angles of attack, specifically near 15 degrees to monitor the apparent minima in Cd and Cl near this angle.

7. These investigations should be expanded to cover general three-dimensional bluff bodies, on which there is very little or no research, save for the sphere.

8. The effect of ambient flow turbulence on the impulsively-started flow should be investigated in order to understand the initiation of the vortex asymmetry on axisymmetric bodies.

9. Numerical models based on solutions to the Navier-Stokes equations or discrete vortex methods should be developed and or refined so as to be compared to experimental results such as contained in this study.

LIST OF REFERENCES

1. Lee, B. E., "The Effect of Turbulence on the Surface Pressure Field of a Square Prism," Journal of Fluid Mechanics, Vol. 69, pp. 263-282, 1975.

2. Nakaguchi, H., Hashimoto, K. and Muto, S., "An Experimental Study of Aerodynamic Drag of Rectangular Cylinders," Journal of the Japan Society of Aeronautical and Space Sciences, Vol. 16, pp. 1-5, 1968.

3. Bearman, P. W. and Trueman, D. M., "An Investigation of the Flow Around Rectangular Cylinders," Aeronautical Quarterly, Vol. XXIII, Part 3, pp. 229-237, 1972.

4. Bostock, B. R. and Mair, W. A., "Pressure Distributions and Forces on Rectangular and D-Shaped Cylinders," Aeronautical Quarterly, Vol. XXIII, Part 1, pp. 1-6, 1972.

5. Knauss, D. T., The Influence of Flow Orientation on the Vortex Frequencies of Bluff Cylinders at Low Reynolds Numbers, Ph.D. Thesis, University of Maryland, 1974.

6. Courchesne, J. and Laneville, A., "A Comparison of Correction Methods Used in the Evaluation of Drag Coefficient Measurements for Two-Dimensional Rectangular Cylinders," Journal of Fluids Engineering, Vol. 101, pp. 506-510, December 1974.

7. Obasaju, E. D., "On the Effect of End Plates on the Mean Forces on Square Sectioned Cylinders," Journal of Industrial Aerodynamics, Vol. 5, pp. 179-188, 1979.

8. Davis, R. W. and Moore, E. F., "A Numerical Study of Vortex Shedding from Rectangles," Journal of Fluid Mechanics, Vol. 116, pp. 475-506, 1982.

9. Vickery, B. J., "Fluctuating Lift and Drag on a Long Cylinder of Square Cross-Section in a Smooth and in a Turbulent Stream," Journal of Fluid Mechanics, Vol. 25, pp. 481-494, 1966.

10. Rockwell, D. O. "Organized Fluctuations due to Flow Past a Square Cross Section Cylinder," Journal of Fluids Engineering, Vol. 99, pp. 511-516, 1977.

11. Lee, B. E., "Some Effects of Turbulence Scale on the Mean Forces on Bluff Bodies," Journal of Industrial Aerodynamics, Vol. 1, pp. 361-370, 1975/1976.

12. Nakamura, Y. and Tomonari, Y., "The Effect of Turbulence on the Drag of Rectangular Prisms," Journal of the Japan Society of Aeronautical and Space Sciences, Vol. 19, No. 44, pp. 81-86, June 1976.

13. Courchesne, J. and Laneville, A., "An Experimental Evaluation of Drag Coefficient for Rectangular Cylinders Exposed to Grid Turbulence," Journal of Fluids Engineering, Vol. 104, pp. 523-528, December 1982.

14. Graham, J.M.R., "The Effect of End-Plates on the Two-Dimensionality of a Vortex Wake," Aeronautical Quarterly, Vol. 20, Part 3, pp. 237-247, August 1969.

15. Lee, B. E., "The Susceptibility of Tests on Two-Dimensional Bluff Bodies to Incident Flow Variations," Journal of Industrial Aerodynamics, Vol. 2, pp. 133-148, 1977.

16. Awbi, H.B., "An Assessment of the Universal Strouhal Number Concept for Two-Dimensional Bluff Bodies," Aeronautical Journal, Vol. 85, No. 850, pp. 467-469, December 1981.

17. Kline, H. K., Impulsively-Started Flow About Submarine-Shaped Bodies, M.S.M.E. Thesis, Naval Postgraduate School, Monterey, CA, 1981.

APPENDIX A: REPRESENTATIVE DATA FOR BODY A AT 0 DEGREES

S/w	Cd	S/w	Cl
1.05	1.73		
1.71	1.31		
2.36	1.34		
3.03	1.91		
3.69	2.25		
4.35	2.17		
5.01	2.14		
5.68	2.21		
6.34	2.06		
7.00	2.00		
7.66	2.04		
8.31	2.00		
8.97	2.01		
9.62	1.93		
10.26	1.94		
10.90	1.90	NEGLIGIBLE	
11.53	1.95		
12.16	1.91		
12.78	1.87		
13.39	1.88		
14.00	1.84		
14.59	1.79		
15.18	1.70		
15.76	1.79		
16.32	1.79		

APPENDIX B: REPRESENTATIVE DATA FOR BODY A AT 5 DEGREES

S/w	Cd	S/w	Cl
1.18	1.69	.07	.08
1.84	1.31	.72	.38
2.50	1.65	1.38	.73
3.16	2.29	2.04	1.27
3.82	2.59	2.68	1.50
4.48	2.55	3.36	1.20
5.15	2.32	4.02	.67
5.81	2.55	4.68	-.41
6.47	2.62	5.35	-1.61
7.13	2.50	6.01	-2.47
7.79	2.07	6.67	-2.55
8.44	2.15	7.33	-2.00
9.10	2.52	7.98	-.81
9.74	2.48	8.64	.46
10.39	2.38	9.29	1.42
11.03	2.28	9.94	1.81
11.66	2.23	10.58	1.78
12.28	2.38	11.22	.91
12.90	2.44	11.85	-.25
13.52	2.28	12.47	-1.19
14.12	1.97	13.09	-1.79
14.71	1.60	13.70	-2.01
15.30	1.59	14.30	-1.84
15.87	1.84	14.89	-1.41
16.44	2.11	15.47	-.75
17.26	2.18	16.04	-.05
16.71	2.17	16.60	.49
		17.15	.84

APPENDIX C: REPRESENTATIVE DATA FOR BODY A AT 10 DEGREES

S/w	Cd	S/w	Cl
1.18	2.07	.99	.92
1.84	1.84	1.64	1.69
2.50	2.38	2.30	2.38
3.16	2.77	2.96	1.69
3.82	2.89	3.62	.49
4.48	3.19	4.28	-.86
5.15	3.64	4.95	-1.99
5.81	3.56	5.61	-2.55
6.47	2.89	6.27	-2.51
7.13	2.15	6.93	-1.87
7.79	1.84	7.59	-.65
8.44	2.07	8.25	.65
9.10	2.40	8.90	.87
9.74	2.44	9.55	.87
10.39	2.26	10.20	.12
11.03	2.11	10.84	-.69
11.66	2.03	11.47	-1.24
12.28	2.00	12.10	-1.53
12.90	2.00	12.72	-1.52
13.52	1.74	13.33	-1.30
14.12	1.61	13.94	-.96
14.71	1.60	14.53	-.66
15.30	1.74	15.12	-.24
15.87	1.79	15.70	0.00
16.44	1.74	16.27	-.05
		16.82	-.22

APPENDIX D: REPRESENTATIVE DATA FOR BODY A AT 20 DEGREES

S/w	Cd	S/w	Cl
1.71	2.65	.01	.12
2.36	3.00	.66	1.22
3.03	3.11	1.31	1.92
3.69	3.22	1.97	2.84
4.35	3.22	2.63	3.00
5.01	3.71	3.29	2.40
5.68	4.15	3.95	1.39
6.34	4.20	4.62	-.15
7.00	3.69	5.28	-1.61
7.66	2.69	5.94	-2.32
8.31	2.57	6.60	-2.10
8.97	2.99	7.26	-1.34
9.62	3.03	7.92	.35
10.26	3.15	8.58	1.50
10.90	3.23	9.23	1.30
11.53	3.39	9.87	.63
12.16	3.40	10.52	-.32
12.78	3.14	11.15	-1.16
13.39	2.64	11.78	-1.70
14.00	2.11	12.41	-1.70
14.59	1.93	13.03	-1.31
15.18	2.13	13.64	-.63
15.76	2.46	14.24	.28
16.32	2.53	14.83	1.31
16.88	2.50	15.41	1.59
		15.99	1.23
		16.55	.53
		17.10	-.22
		17.64	-.92
		18.16	-1.53
		18.67	-1.82

APPENDIX E: REPRESENTATIVE DATA FOR BODY A AT 30 DEGREES

S/w	Cd	S/w	Cl
1.58	3.61	.20	.47
2.23	3.73	.85	1.23
2.89	3.82	1.51	1.92
3.55	3.82	2.17	2.46
4.22	3.07	2.83	2.74
4.88	3.11	3.49	2.70
5.54	3.11	4.15	1.72
6.21	3.45	4.81	.79
6.87	3.75	5.48	-.52
7.53	3.53	6.14	-1.61
8.18	3.11	6.80	-1.80
8.84	3.27	7.46	-1.15
9.49	3.46	8.12	.46
10.13	3.35	8.77	1.61
10.77	3.03	9.42	1.57
11.41	3.06	10.07	.97
12.04	3.23	10.71	0.00
12.66	3.40	11.34	-1.16
13.27	3.31	11.97	-1.70
13.88	2.94	12.60	-1.92
14.48	2.69	13.21	-1.34
15.06	2.47	13.82	-.55
15.64	2.69	14.42	.28
16.21	2.95	15.01	.97
16.77	2.98	15.59	1.40
		16.16	1.49
		16.71	1.19
		17.26	.67
		17.80	.18
		18.32	-.32
		18.83	-.65
		19.32	-.83

APPENDIX F: REPRESENTATIVE DATA FOR BODY A AT 40 DEGREES

S/w	Cd	S/w	Cl
1.31	3.84	.14	.20
1.97	3.73	.79	.38
2.63	3.37	1.44	.69
3.29	3.30	2.10	.88
3.95	3.41	2.76	1.05
4.62	3.30	3.42	1.35
5.28	3.00	4.08	1.72
5.94	2.89	4.75	1.80
6.60	2.81	5.41	1.57
7.26	2.77	6.07	1.20
7.92	2.77	6.74	.67
8.58	2.88	7.39	-.12
9.23	3.35	8.05	-.85
9.87	3.35	8.71	-1.15
10.52	3.23	9.36	-1.14
11.15	3.02	10.00	-.81
11.78	2.84	10.64	-.08
12.41	2.89	11.28	.74
13.03	3.05	11.91	1.32
13.64	3.22	12.53	1.57
14.24	3.17	13.15	1.35
14.83	3.05	13.76	.83
15.41	2.94	14.36	.19
15.99	2.92	14.95	-.48
16.55	3.00	15.53	-1.00
		16.10	-1.28
		16.66	-1.36
		17.21	-1.01
		17.74	-.47

APPENDIX G: REPRESENTATIVE DATA FOR BODY A AT 45 DEGREES

S/w	Cd	S/w	Cl
1.51	4.07	.01	-.02
2.17	3.76	.66	-.04
2.83	3.34	1.31	-.04
3.49	3.15	1.97	-.08
4.15	2.81	2.63	-.24
4.81	2.62	3.29	0.00
5.48	2.51	3.95	0.00
6.14	2.47	4.62	.04
6.80	2.44	5.28	.07
7.45	2.46	5.94	.11
8.12	2.42	6.60	.07
8.77	2.46	7.26	.12
9.42	2.48	7.92	.04
10.07	2.46	8.58	0.00
10.71	2.42	9.23	-.08
11.34	2.40	9.87	-.12
11.97	2.34	10.52	-.04
12.60	2.35	11.15	0.00
13.21	2.33	11.78	-.04
13.82	2.30	12.41	-.13
14.42	2.26	13.03	-.22
15.01	2.23	13.64	-.27
15.59	2.14	14.24	-.23
16.16	2.10	14.83	-.19
		15.41	-.15
		15.99	-.10
		16.55	-.11
		17.10	-.11
		17.64	-.12
		18.16	-.12

APPENDIX H: REPRESENTATIVE DATA FOR BODY B AT 0 DEGREES

S/w	Cd	S/w	Cl
2.80	.92		
3.97	1.58		
5.15	1.62		
6.32	1.83		
7.50	1.90		
8.68	1.93		
9.86	1.85		
11.04	1.77		
12.22	1.73		
13.39	1.70		
14.56	1.65		
15.72	1.62		
16.88	1.63		
18.03	1.58	NEGLIGIBLE	
19.17	1.54		
20.30	1.52		
21.41	1.52		
22.52	1.51		
23.61	1.47		
24.69	1.52		
25.76	1.51		
26.80	1.53		
27.83	1.51		
28.85	1.55		
29.84	1.62		
30.81	1.61		

APPENDIX I: REPRESENTATIVE DATA FOR BODY B AT 5 DEGREES

S/w	Cd	S/w	Cl
2.34	1.02	.48	.43
3.50	1.63	1.64	.81
4.68	1.88	2.80	1.28
5.85	1.82	3.97	.62
7.03	2.17	5.15	-.54
8.21	1.98	6.32	-1.67
9.39	1.73	7.50	-1.71
10.57	2.10	8.68	-.46
11.75	2.13	9.86	.62
12.92	1.93	11.04	.87
14.09	1.80	12.22	-.08
15.26	1.80	13.39	-1.08
16.42	1.77	14.56	-1.45
17.57	1.81	15.72	-1.06
18.71	1.95	16.88	-.13
19.85	1.94	18.03	.53
20.97	1.74	19.17	.35
22.08	1.65	20.30	-.45
23.18	1.59	21.41	-1.25
24.26	1.60	22.52	-1.42
25.33	1.70	23.61	-.82
26.39	1.80	24.69	0.00
27.42	1.78	25.76	.26
28.44	1.68	26.80	-.05
29.44	1.68	27.83	-.67
		28.85	-1.25
		29.84	-1.49
		30.81	-1.26

APPENDIX J: REPRESENTATIVE DATA FOR BODY B AT 10 DEGREES

S/w	Cd	S/w	Cl
2.22	1.56	.02	.09
3.39	2.22	1.17	.68
4.56	2.40	2.34	1.62
5.74	3.00	3.50	1.17
6.91	2.67	4.68	-.04
8.09	1.77	5.85	-1.21
9.27	1.80	7.03	-1.67
10.45	2.17	8.21	-1.08
11.63	2.07	9.39	.33
12.81	2.08	10.57	.42
13.98	1.60	11.75	-.54
15.14	1.53	12.92	-1.50
16.30	1.82	14.08	-1.49
17.45	1.72	15.26	-.72
18.60	1.63	16.42	0.00
19.73	1.67	17.57	-.13
20.86	1.44	18.71	-.84
21.97	1.40	19.85	-1.36
23.07	1.59	20.97	-1.34
24.16	1.58	22.08	-.90
25.23	1.48	23.18	-.44
26.28	1.48	24.26	-.35
27.32	1.37	25.33	-.66
28.34	1.32	26.39	-1.06
29.34	1.42	27.42	-1.30
30.33	1.57	28.44	-1.31
31.29	1.60	29.44	-1.05
		30.42	-.73
		31.38	-.64

APPENDIX K: REPRESENTATIVE DATA FOR BODY B AT 20 DEGREES

S/w	Cd	S/w	Cl
2.34	1.91	.36	.48
3.50	2.12	1.52	1.66
4.68	2.12	2.69	2.68
5.85	2.67	3.86	1.75
7.03	3.12	5.03	-.12
8.21	2.96	6.21	-1.67
9.39	2.21	7.39	-1.50
10.57	2.58	8.57	-.04
11.75	2.71	9.75	1.25
12.92	3.08	10.93	.29
14.09	2.89	12.10	-1.12
15.26	2.21	13.28	-1.42
16.42	2.08	14.44	-.64
17.57	2.30	15.61	.81
18.71	2.44	16.76	1.04
19.85	2.67	17.91	0.00
20.97	2.50	19.05	-.93
22.08	2.03	20.18	-1.18
23.18	1.89	21.30	-.56
24.26	2.03	22.41	.47
25.33	2.02	23.51	.77
26.39	2.23	24.59	.30
27.42	2.12	25.65	-.67
28.44	1.99	26.70	-1.22
29.44	1.81	27.73	-1.06
30.42	1.96	28.75	-.40
		29.74	.48
		30.71	.38

APPENDIX L: REPRESENTATIVE DATA FOR BODY B AT 30 DEGREES

S/w	Cd	S/w	Cl
2.10	2.59	.13	.17
3.27	2.58	1.29	.81
4.44	2.37	2.45	1.70
5.62	2.62	3.62	1.92
6.80	3.25	4.79	1.46
7.98	3.29	5.97	.46
9.16	2.71	7.15	-.79
10.34	3.04	8.33	-.96
11.51	2.79	9.51	.25
12.69	2.83	10.69	1.62
13.86	3.15	11.87	1.08
15.03	2.81	13.04	-.29
16.19	2.43	14.21	-1.02
17.34	2.52	15.38	-.68
18.48	2.48	16.53	.22
19.62	2.40	17.68	.82
20.75	2.59	18.83	.71
21.86	2.60	19.96	.14
22.96	2.32	21.08	-.60
24.05	2.18	22.19	-.85
25.12	2.28	23.29	-.58
26.18	2.28	24.37	.15
27.22	2.28	25.44	.78
28.24	2.33	26.49	.64
29.24	2.45	27.53	0.00
30.23	2.27	28.54	-.74
31.19	2.13	29.54	-1.08
		30.52	-.73
		31.48	0.00

APPENDIX M: REPRESENTATIVE DATA FOR BODY B AT 40 DEGREES

S/w	Cd	S/w	Cl
2.34	2.55	.36	.09
3.50	2.29	1.52	.51
4.68	2.37	2.69	.72
5.85	2.42	3.86	1.00
7.03	2.48	5.03	1.29
8.21	2.54	6.21	1.12
9.39	2.71	7.38	.58
10.57	3.08	8.57	-.37
11.75	2.79	9.75	-1.08
12.92	2.58	10.83	-.71
14.09	3.02	12.10	.21
15.26	2.81	13.28	1.04
16.42	2.68	14.44	.94
17.57	2.78	15.61	.17
18.71	2.79	15.76	-.74
19.85	2.58	17.91	-.93
20.97	2.55	19.05	-.44
22.08	2.65	20.18	.09
23.18	2.56	21.30	.42
24.26	2.47	22.41	.33
25.33	2.48	23.51	-.19
26.39	2.54	24.59	-.64
27.42	2.49	25.65	-.83
28.44	2.45	26.70	-.53
29.44	2.45	27.73	-.22
30.42	2.45	28.75	-.06
31.38	2.45	29.74	-.12
		30.71	-.25

APPENDIX N: REPRESENTATIVE DATA FOR BODY B AT 45 DEGREES

S/w	Cd	S/w	Cl
2.34	2.93	.25	-.26
3.50	2.43	1.40	-.04
4.68	2.23	2.57	-.04
5.85	2.28	3.74	-.04
7.03	2.25	4.91	.04
8.21	2.20	6.09	.04
9.39	2.23	7.27	.08
10.57	2.18	8.45	.08
11.75	2.13	9.63	.04
12.92	2.03	10.81	-.12
14.09	2.01	11.98	-.21
15.26	1.97	13.16	0.00
16.42	1.95	14.33	.21
17.57	1.88	15.49	.17
18.71	1.88	16.65	-.17
19.85	1.87	17.80	-.43
20.97	1.83	18.94	-.44
22.08	1.84	20.07	-.41
23.18	1.78	21.19	-.23
24.26	1.78	22.30	-.09
25.33	1.74	23.40	-.10
26.39	1.78	24.48	-.20
27.42	1.78	25.55	-.31
28.44	1.80	26.60	-.53
29.44	1.79	27.63	-.65
30.42	1.84	28.65	-.68
31.38	1.88	29.64	-.60
		30.62	-.61

APPENDIX O: REPRESENTATIVE DATA FOR BODY C AT 0 DEGREES

S/w	Cd	S/w	Cl
2.19	1.79		
3.03	1.90		
3.88	2.08		
4.72	2.17		
5.57	2.23		
6.42	2.17		
7.27	2.11		
8.12	2.05		
8.97	2.02		
9.81	1.93		
10.65	1.91		
11.49	1.91		
12.32	1.89		
13.14	1.86	NEGLIGIBLE	
13.96	1.84		
14.78	1.77		
15.58	1.78		
16.37	1.75		
17.16	1.79		
17.93	1.80		
18.70	1.76		
19.45	1.81		
20.19	1.81		
20.91	1.86		
21.62	1.86		
22.32	1.86		

APPENDIX P: REPRESENTATIVE DATA FOR BODY C AT 10 DEGREES

S/w	Cd	S/w	Cl
2.27	2.16	.01	.20
3.11	2.05	.84	.97
3.96	2.23	1.68	1.26
4.81	2.29	2.52	.90
5.66	2.20	3.37	.38
6.51	2.35	4.21	-.24
7.36	2.56	5.06	-1.00
8.21	2.47	5.91	-1.66
9.05	2.38	6.76	-1.71
9.90	2.62	7.61	-1.14
10.74	2.59	8.46	-.14
11.57	2.30	9.31	.43
12.40	2.14	10.15	.24
13.23	2.28	10.99	-.58
14.05	2.17	11.82	-1.58
14.86	2.11	12.65	-2.17
15.66	2.36	13.47	-2.22
16.45	2.56	14.29	-1.75
17.24	2.62	15.10	-.84
18.01	2.27	15.90	.27
18.77	2.25	16.69	.55
19.52	2.36	17.47	-.06
20.26	2.33	18.24	-.98
20.98	2.28	19.00	-1.99
21.69	2.31	19.75	-2.47
22.39	2.36	20.48	-2.46
		21.20	-1.99
		21.90	-1.32
		22.59	-.59

APPENDIX Q: REPRESENTATIVE DATA FOR BODY C AT 20 DEGREES

S/w	Cd	S/w	Cl
2.27	2.09	.05	.10
3.11	2.02	.76	.87
3.96	2.11	1.60	1.31
4.81	2.23	2.44	1.09
5.66	2.59	3.28	.52
6.51	3.05	4.13	-.09
7.36	2.68	4.98	-1.09
8.21	2.02	5.83	-2.42
9.05	2.65	6.68	-3.03
9.90	2.77	7.53	-2.13
10.74	2.65	8.37	.24
11.57	2.89	9.22	.90
12.40	2.70	10.06	-.10
13.23	2.31	10.90	-1.50
14.05	1.87	11.74	-2.62
14.86	1.94	12.57	-2.77
15.66	2.06	13.39	-2.07
16.45	2.03	14.21	-.67
17.24	2.08	15.02	.37
18.01	2.20	15.82	.22
18.77	2.10	16.61	-.72
19.52	1.89	17.39	-1.75
20.26	1.73	18.16	-2.48
20.98	1.86	18.92	-2.53
21.69	2.00	19.67	-1.73
22.39	2.09	20.41	-.52
		21.13	.13
		21.83	-.42
		22.53	-1.17

APPENDIX R: REPRESENTATIVE DATA FOR BODY C AT 40 DEGREES

S/w	Cd	S/w	Cl
2.27	2.16	.26	-.25
3.11	2.08	1.10	-.73
3.96	2.29	1.93	-1.35
4.81	2.50	2.78	-1.90
5.66	2.47	3.62	-2.37
6.51	2.20	4.47	-2.65
7.36	2.65	5.32	-2.09
8.21	2.47	6.17	-.38
9.05	2.53	7.02	.76
9.90	3.05	7.87	.09
10.74	3.11	8.71	-1.42
11.57	2.74	9.56	-2.75
12.40	2.33	10.40	-2.85
13.23	2.57	11.24	-1.94
14.05	2.49	12.07	-.40
14.86	2.35	12.90	.56
15.66	2.36	13.72	.40
16.45	2.63	14.53	-.62
17.24	2.65	15.34	-1.74
18.01	2.53	16.14	-2.48
18.77	2.40	16.92	-2.42
19.52	2.36	17.70	-1.58
20.26	2.37	18.47	-.41
20.98	2.36	19.22	.48
21.69	2.31	19.97	.51
22.39	2.36	20.70	-.32
		21.41	-1.50
		22.11	-2.50

APPENDIX S: REPRESENTATIVE DATA FOR BODY D AT 0 DEGREES

S/w	Cd	S/w	Cl
3.70	1.21		
5.03	1.55		
6.36	1.73		
7.69	1.71		
9.02	1.80		
10.36	1.76		
11.69	1.71		
13.03	1.67		
14.36	1.65		
15.68	1.63		
17.00	1.49		
18.31	1.56		
19.62	1.46		
20.91	1.41	NEGLIGIBLE	
22.20	1.44		
23.47	1.48		
24.73	1.42		
25.98	1.37		
27.21	1.35		
28.42	1.29		
29.62	1.32		
30.80	1.36		
31.95	1.37		
33.09	1.41		
34.20	1.39		
35.29	1.43		

APPENDIX T: REPRESENTATIVE DATA FOR BODY D AT 10 DEGREES

S/w	Cd	S/w	Cl
3.44	2.13	.28	-.16
4.76	2.46	1.59	-.92
6.09	2.37	2.91	-1.39
7.42	2.09	4.23	-1.12
8.76	1.85	5.56	-.81
10.09	1.75	6.89	-.60
11.43	1.71	8.22	-.48
12.76	1.61	9.56	-.33
14.09	1.47	10.89	-.06
15.42	1.42	12.23	.27
16.74	1.40	13.56	.39
18.05	1.35	14.89	.30
19.36	1.28	16.21	.18
20.66	1.31	17.53	.31
21.94	1.24	18.84	.50
23.22	1.13	20.14	.60
24.48	1.16	21.43	.51
25.73	1.13	22.71	.26
26.96	1.18	23.98	.23
28.18	1.15	25.23	.38
29.38	1.12	26.47	.53
30.56	1.11	27.70	.57
31.72	1.14	28.90	.48
32.86	1.19	30.09	.31
33.98	1.16	31.26	.31
35.07	1.21	32.41	.41
		33.54	.61
		34.64	.58
		35.72	.47

APPENDIX U: REPRESENTATIVE DATA FOR BODY D AT 20 DEGREES

S/w	Cd	S/w	Cl
3.83	2.75	.41	-.38
5.16	3.18	1.72	-1.35
6.49	3.08	3.04	-1.82
7.82	3.27	4.36	-1.93
9.16	3.03	5.69	-1.75
10.49	2.51	7.02	-.66
11.83	2.27	8.36	.09
13.16	2.37	9.69	.18
14.49	2.42	11.03	-.42
15.81	2.61	12.36	-1.24
17.13	2.61	13.69	-1.21
18.44	2.32	15.02	-.36
19.75	2.08	16.34	.31
21.04	2.22	17.66	.18
22.33	2.22	18.97	-.50
23.60	2.21	20.27	-1.09
24.86	2.21	21.56	-1.08
26.10	2.15	22.84	-.46
27.33	2.03	24.10	.10
28.54	1.96	25.36	.14
29.74	2.05	26.60	-.28
30.91	2.10	27.82	-.79
32.07	2.14	29.02	-1.20
33.20	2.19	30.21	-1.11
34.31	2.09	31.38	-.72
35.40	1.98	32.52	-.45
		33.65	-.39
		34.75	-.41

APPENDIX V: REPRESENTATIVE DATA FOR BODY D AT 40 DEGREES

S/w	Cd	S/w	Cl
3.17	3.58	.41	-.38
4.50	3.65	1.72	-1.11
5.82	3.93	3.04	-1.76
7.16	3.60	4.36	-2.11
8.49	3.89	5.69	-2.11
9.83	4.36	7.02	-1.39
11.16	3.55	8.36	-.03
12.49	3.65	9.69	.51
13.83	4.17	11.03	-.03
15.15	4.17	12.36	-1.03
16.47	3.82	13.69	-1.75
17.79	3.82	15.02	-1.63
19.10	3.95	16.34	-.80
20.40	3.63	17.66	-.12
21.69	3.23	18.97	-.06
22.96	3.35	20.27	-.42
24.23	3.64	21.56	-.93
25.48	3.55	22.84	-1.28
26.72	3.41	24.10	-1.37
27.94	3.40	25.36	-.93
29.14	3.36	26.60	-.42
30.33	3.26	27.82	-.18
31.48	3.29	29.02	-.19
32.64	3.30	30.21	-.50
33.76	3.33	31.38	-1.05
34.86	3.29	32.52	-1.36
		33.65	-1.38
		34.75	-1.00

APPENDIX W: REPRESENTATIVE DATA FOR BODY E AT 0 DEGREES

S/w	Cd	S/w	Cl
2.69	1.65		
4.37	1.80		
6.06	1.76		
7.75	1.81		
9.45	1.83		
11.15	1.76		
12.85	1.69		
14.54	1.69		
16.24	1.59		
17.93	1.59		
19.62	1.54		
21.30	1.53		
22.98	1.48		
24.64	1.46		
26.29	1.46		
27.93	1.47		
29.55	1.42		
31.16	1.42	NEGLIGIBLE	
32.75	1.43		
34.32	1.46		
35.87	1.47		
37.39	1.56		
38.90	1.60		
40.38	1.71		
41.83	1.82		
43.25	1.83		
44.64	2.07		
46.00	1.95		
47.33	2.30		
48.62	2.22		
49.88	2.25		
51.10	2.43		
52.27	2.40		
53.41	2.60		
54.51	2.72		
55.56	2.61		

INITIAL DISTRIBUTION LIST

		No. Copies
1.	Defense Technical Information Center Cameron Station Alexandria, Virginia 22314	2
2.	Library, Code 0142 Naval Postgraduate School Monterey, California 93943	2
3.	Professor T. Sarpkaya, Code 69S1 Mechanical Engineering Department Naval Postgraduate School Monterey, California 93943	5
4.	Department Chairman, Code 69 Department of Mechanical Engineering Naval Postgraduate School Monterey, California 93943	1
5.	LCDR Clyde J. Ihrig Executive Officer USS SWORDFISH (SSN-579) FPO, San Francisco, California 96678	4

206628

Thesis
I188 Ihrig
c.1 Impulsively-started
flow about rectangular
cylinders.